Reference case 0

Length $b = 100$ km (exponential variation); Strickler coefficient $K = 45$ m$^{1/3}$s^{-1}; nonlinear friction.

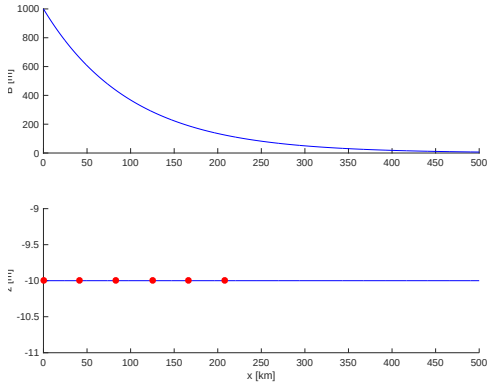

Figure 1: Longitudinal profiles of width and bottom. Dots indicates the locations where the temporal behaviour is shown in figure 3.

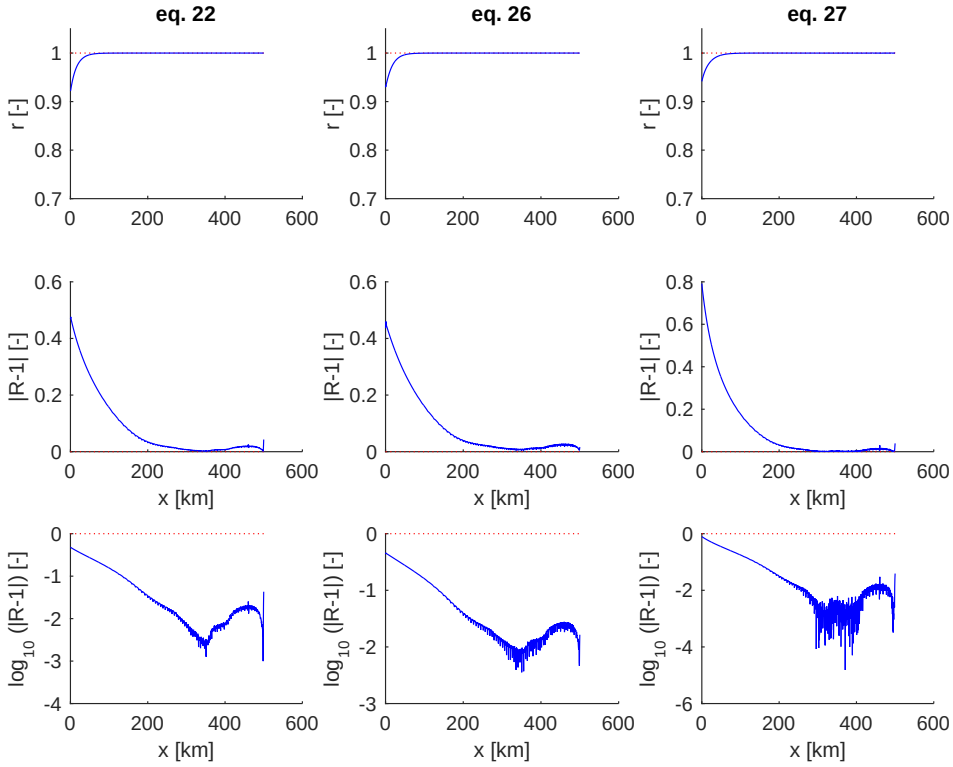

Figure 2: Longitudinal variation of the correlation coefficient r (first row) and of the two different functions of the ratio R between right hand side and left hand side of equations 22, 26 and 27 in the manuscript, respectively $|R-1|$ and $\log_{10}(|R-1|)$.

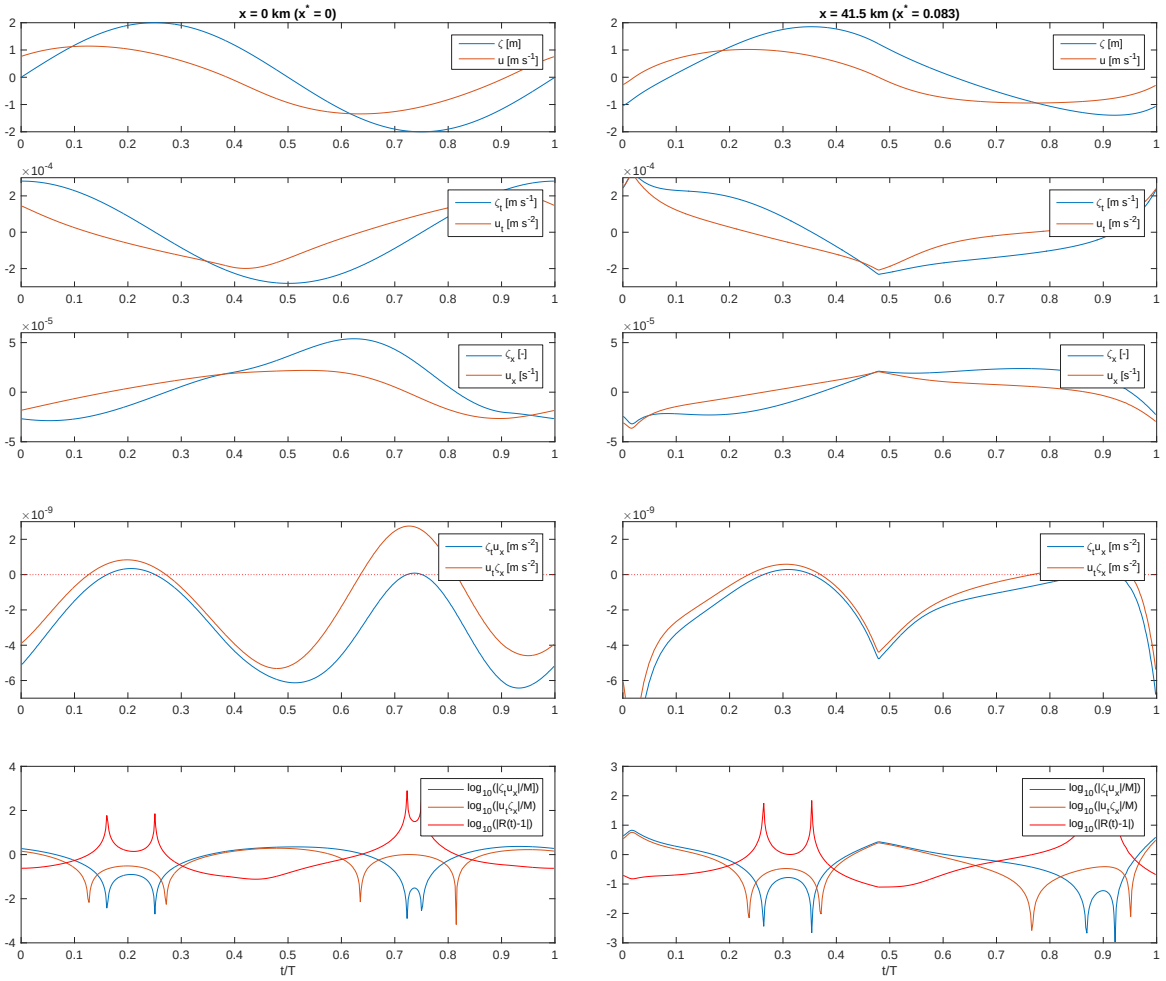

Figure 3: Temporal variation of ζ and u (first plot), ζ_t and u_t (second plot), ζ_x and u_x (third plot), $\zeta_t\, u_x$ and $u_t\, \zeta_x$ (fourth plot), and $\log_{10}(|\zeta_t u_x|/M])$, $\log_{10}(|u_t \zeta_x|/M)$, $\log_{10}(|R(t)-1|)$ (fifth plot, where $R(t) = (u_t\zeta_x)/(\zeta_t u_x)$ and M is the mean of the tidally averages of $|\zeta_t u_x|$ and $|u_t \zeta_x|$), in $x = 0$ km and $x = 41.5$ km.

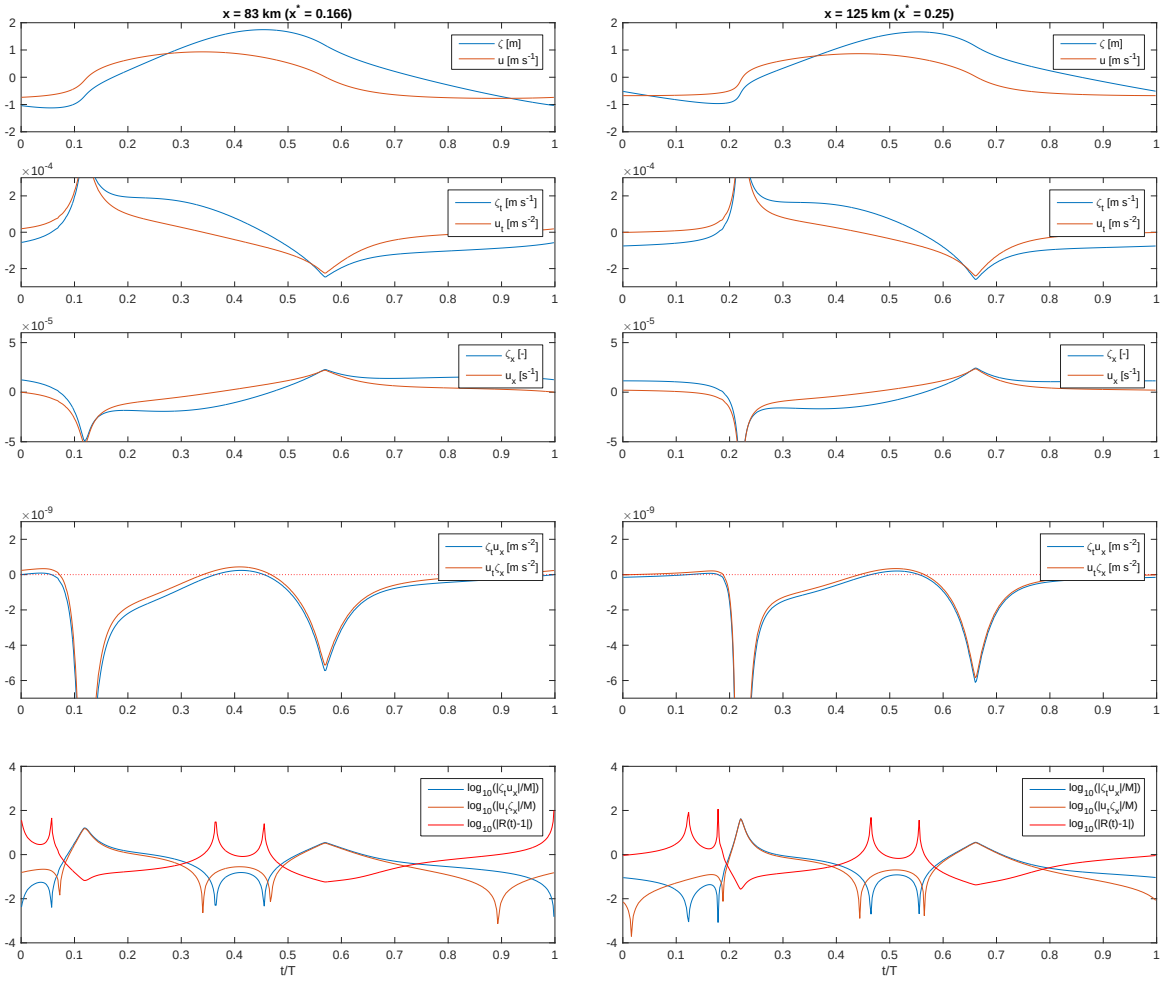

Figure 4: Temporal variation of ζ and u (first plot), ζ_t and u_t (second plot), ζ_x and u_x (third plot), $\zeta_t\, u_x$ and $u_t\, \zeta_x$ (fourth plot), and $\log_{10}(|\zeta_t u_x|/M])$, $\log_{10}(|u_t \zeta_x|/M)$, $\log_{10}(|R(t)-1|)$ (fifth plot, where $R(t) = (u_t \zeta_x)/(\zeta_t u_x)$ and M is the mean of the tidally averages of $|\zeta_t u_x|$ and $|u_t \zeta_x|$), in $x = 83$ km and $x = 125$ km.

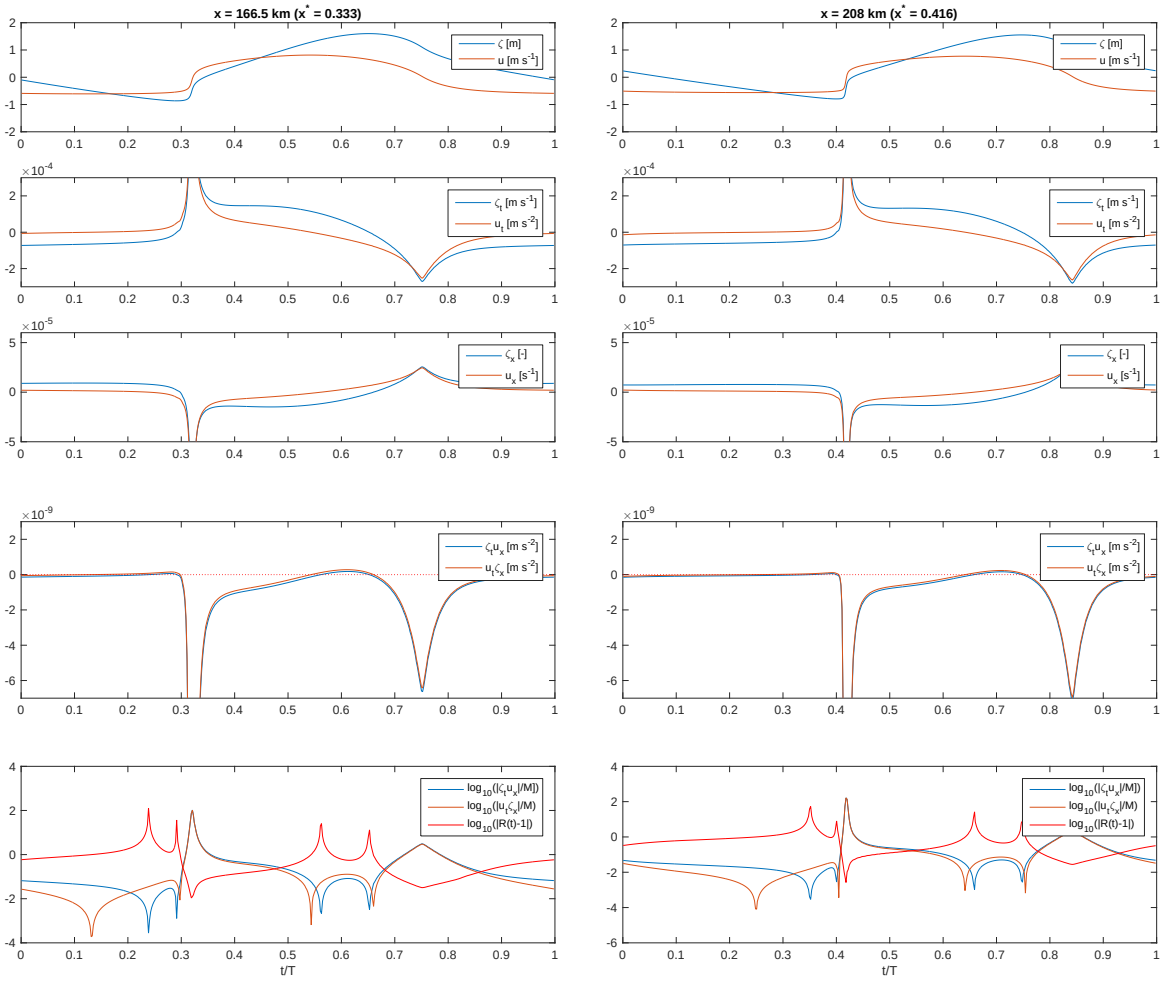

Figure 5: Temporal variation of ζ and u (first plot), ζ_t and u_t (second plot), ζ_x and u_x (third plot), $\zeta_t\, u_x$ and $u_t\, \zeta_x$ (fourth plot), and $\log_{10}(|\zeta_t u_x|/M])$, $\log_{10}(|u_t \zeta_x|/M)$, $\log_{10}(|R(t)-1|)$ (fifth plot, where $R(t) = (u_t\zeta_x)/(\zeta_t u_x)$ and M is the mean of the tidally averages of $|\zeta_t u_x|$ and $|u_t \zeta_x|$), in $x = 166.5$ km and $x = 208$ km.

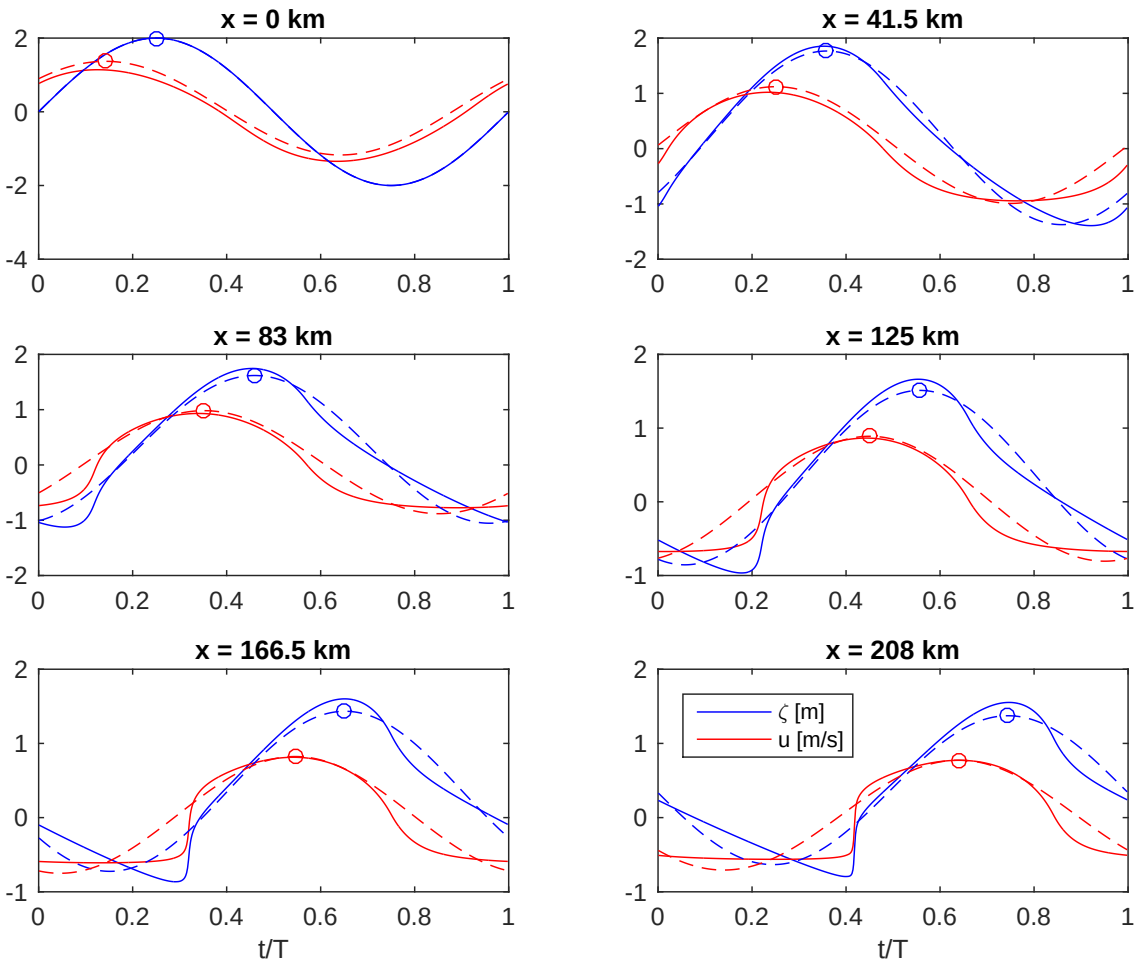

Figure 6: Tidal waves and Fourier series truncated at the first harmonic. Circles indicate the maxima of the dominant tidal component, from which it is possible to detect the phase lag u-ζ.

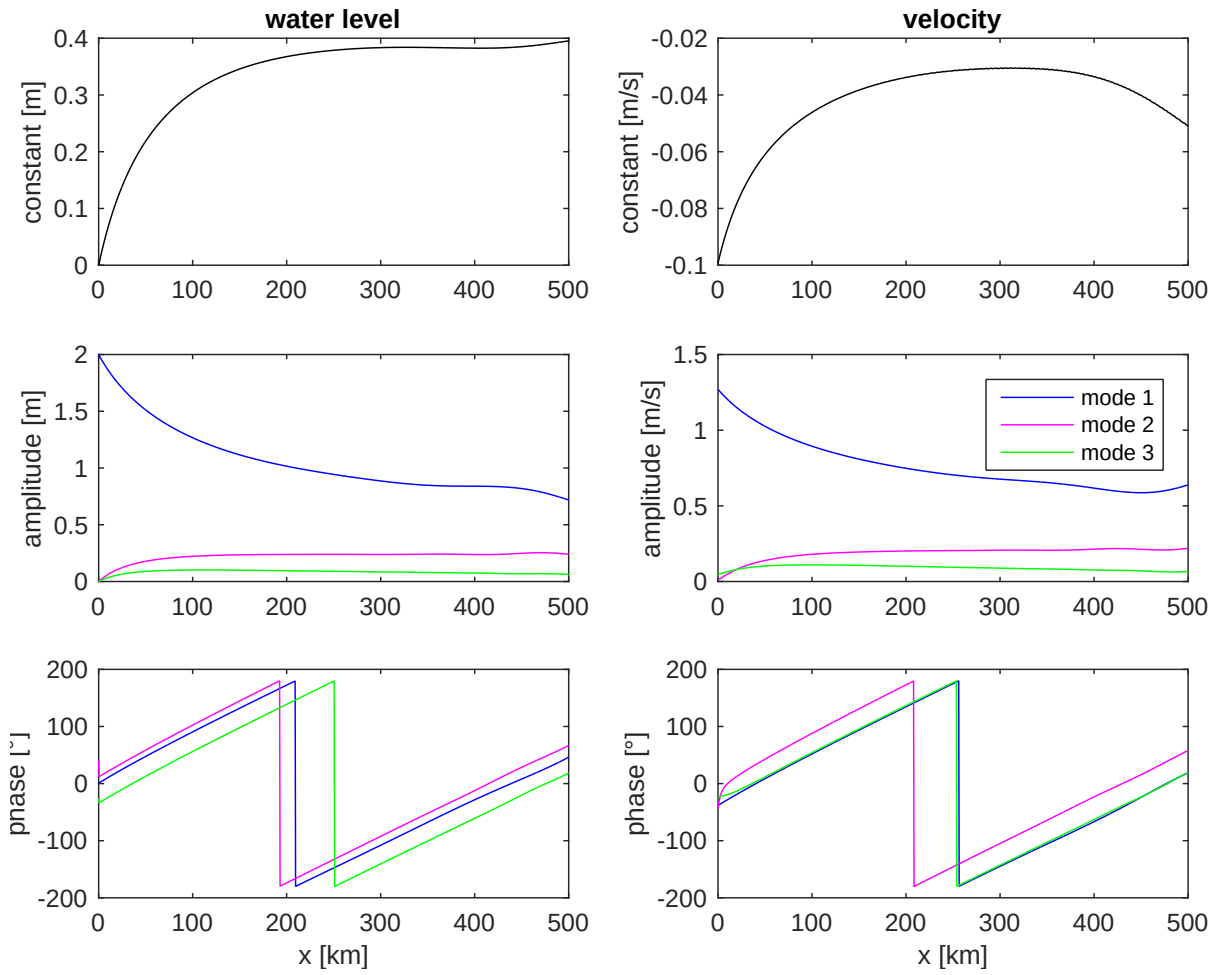

Figure 7: Fourier analysis of tidal wave. From top to bottom: constant term, amplitudes, phases of first three modes. Left column: water level ζ; right column: velocity u.

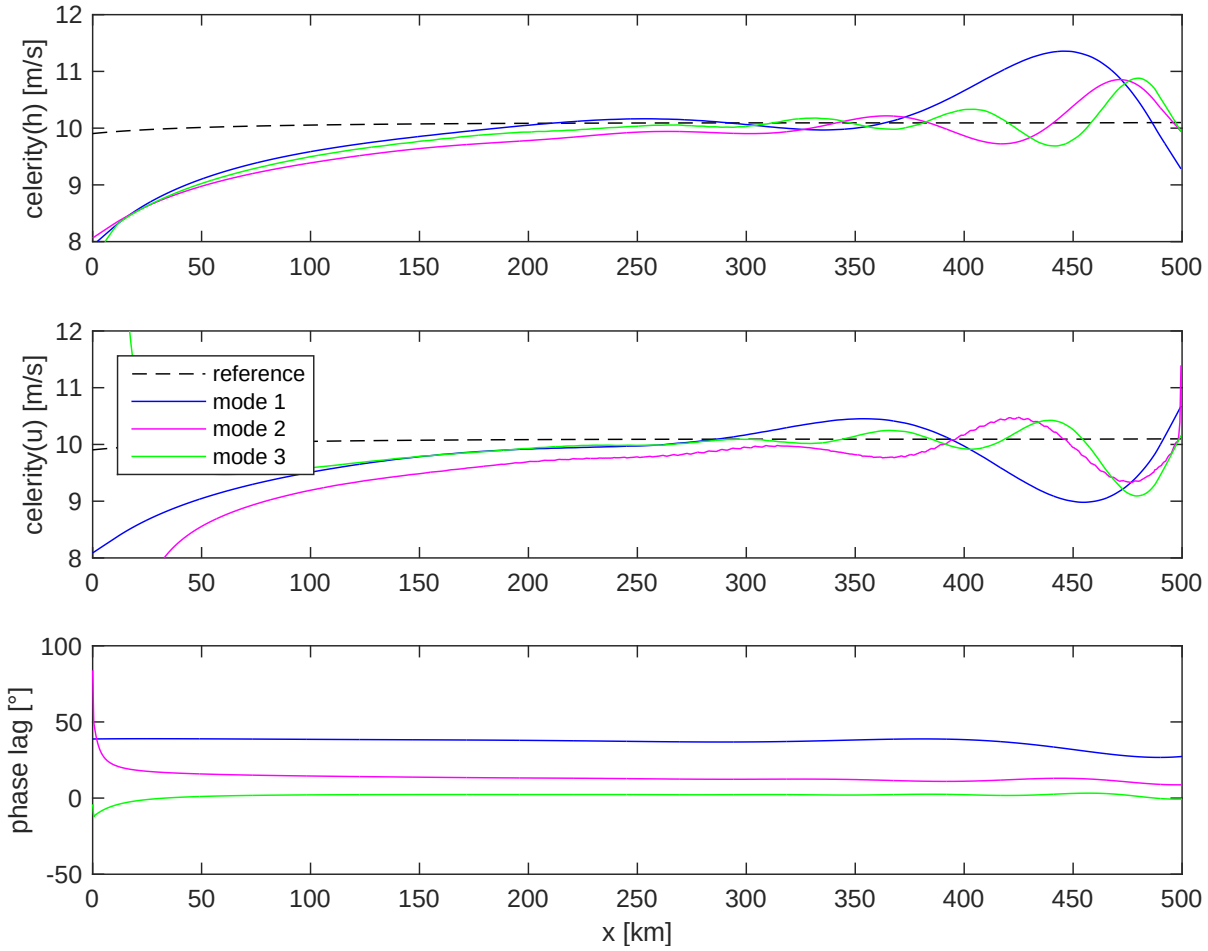

Figure 8: Wave celerity for water level ζ, for velocity u, phase lag u-ζ. Colors refer to the first three modes; black dashed line to wave celerity in a frictionless prismatic channel.

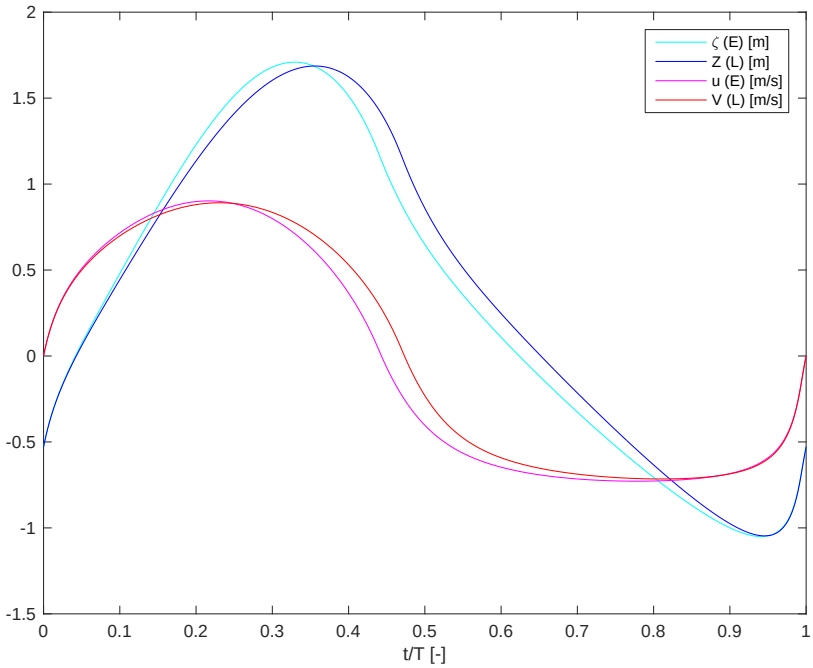

Figure 9: Lagrangean water level Z and velocity V compared with Eulerian values ζ and u in $x = 100$ km.

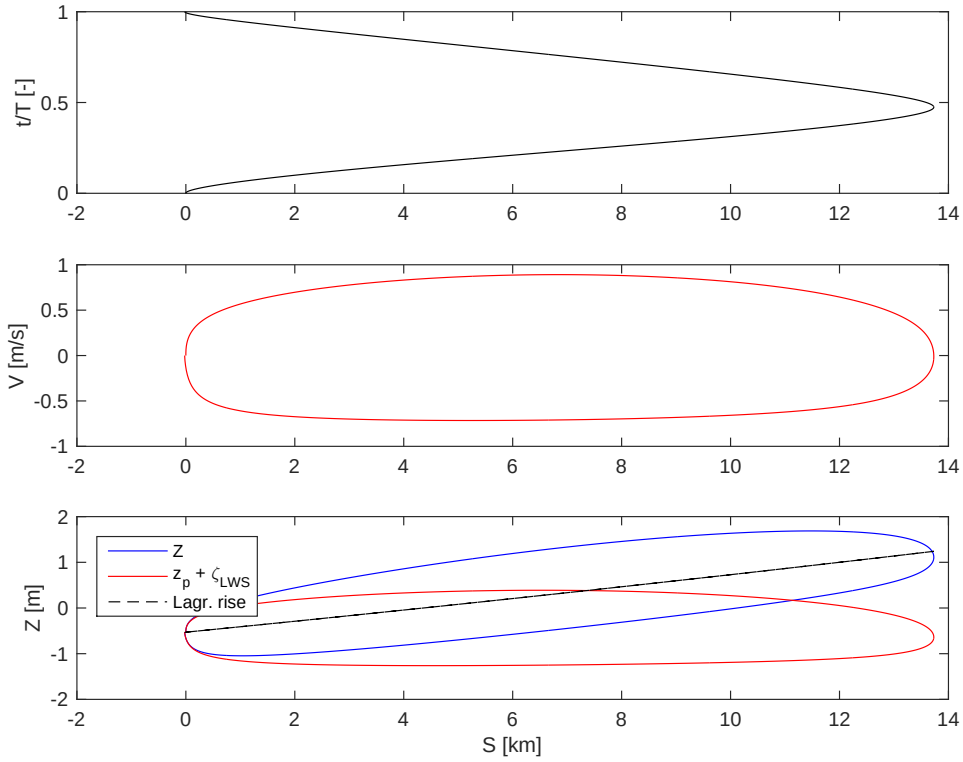

Figure 10: Lagrangean displacement S in time (first plot) and ellipses V-S (second plot) and Z-S (third plot).

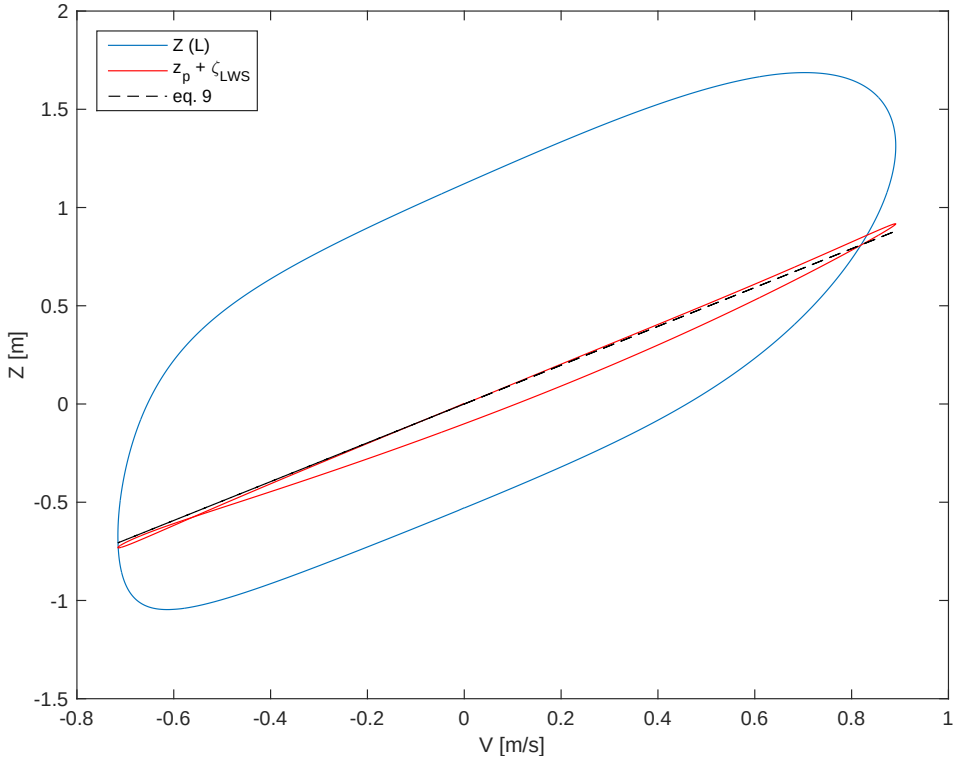

Figure 11: Lagrangean water level against velocity V: Z is the actual value, $z_p + \zeta_{LWS}$ is the transformed water level. Black dashed lines: equation (9).

Variant 1

Length $b = 25$ km (exponential variation); Strickler coefficient $K = 45$ m$^{1/3}$s^{-1}; nonlinear friction.

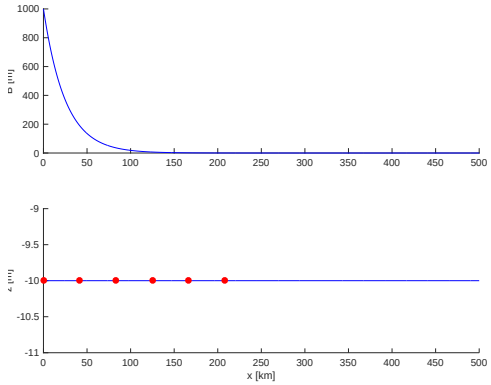

Figure 1: Longitudinal profiles of width and bottom. Dots indicates the locations where the temporal behaviour is shown in figure 3.

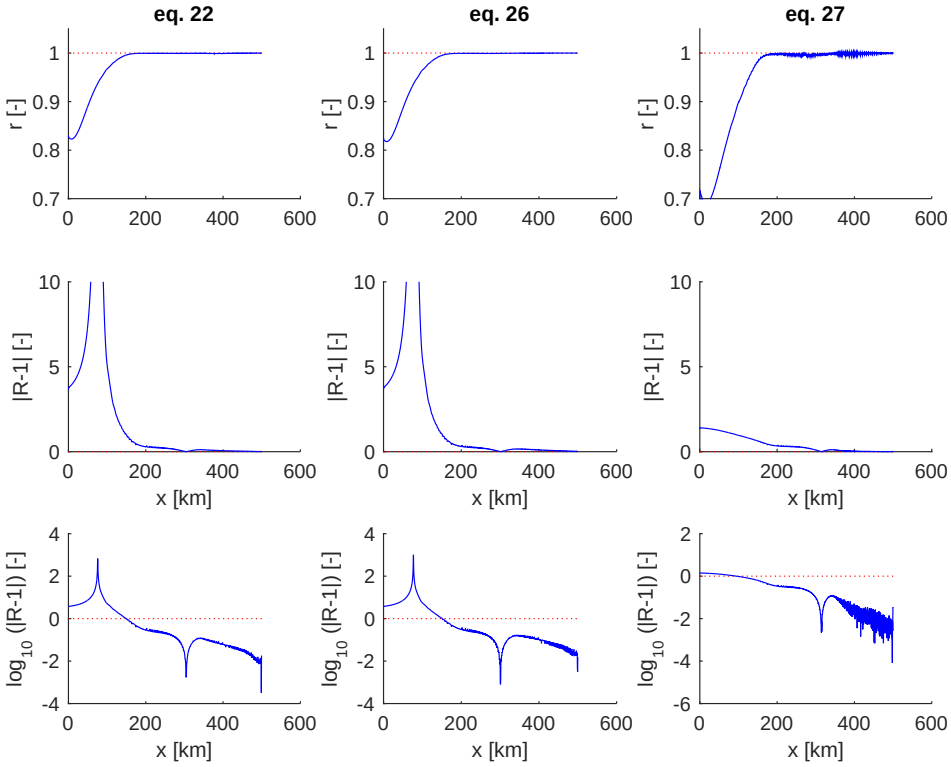

Figure 2: Longitudinal variation of the correlation coefficient r (first row) and of the two different functions of the ratio R between right hand side and left hand side of equations 22, 26 and 27 in the manuscript, respectively $|R-1|$ and $\log_{10}(|R-1|)$.

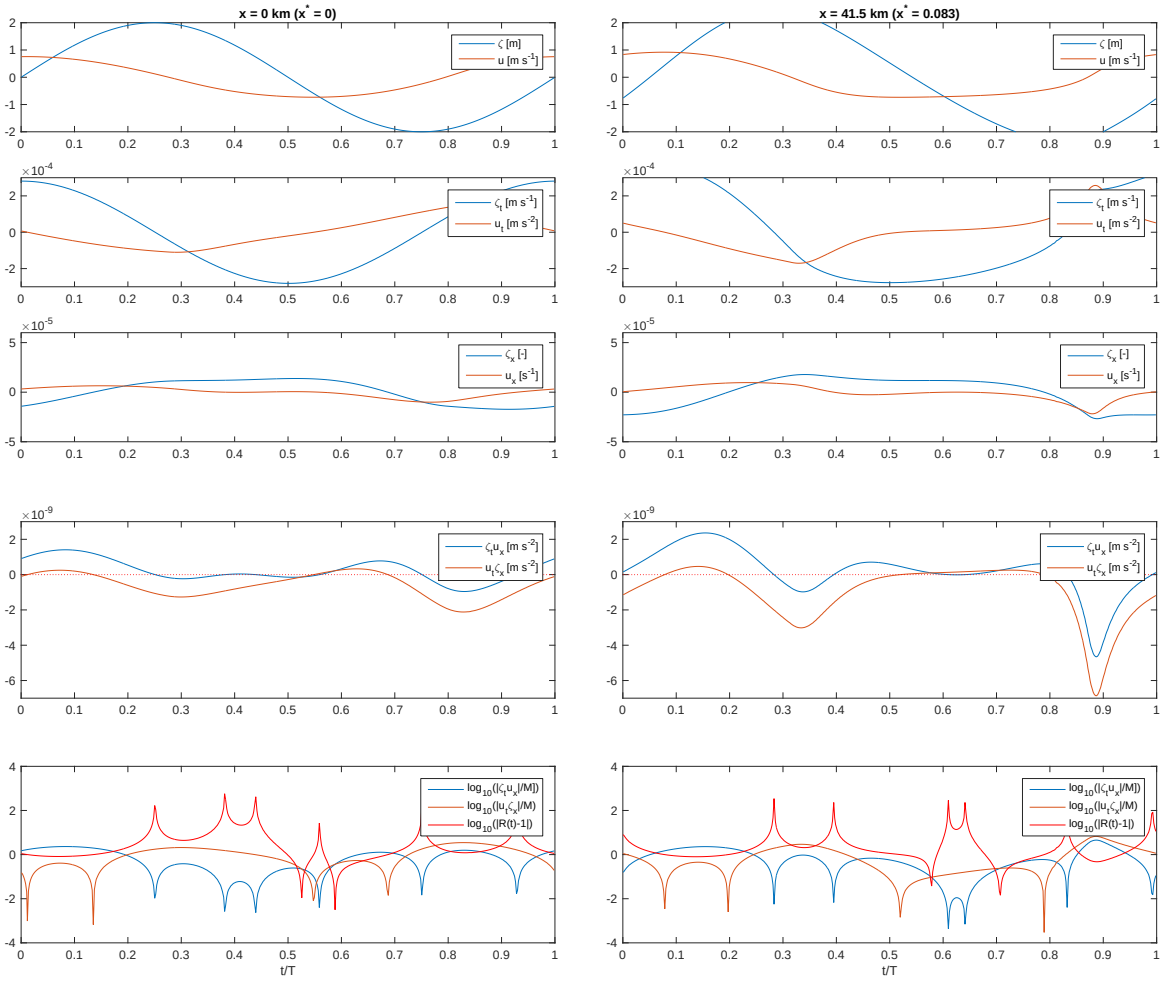

Figure 3: Temporal variation of ζ and u (first plot), ζ_t and u_t (second plot), ζ_x and u_x (third plot), $\zeta_t\, u_x$ and $u_t\, \zeta_x$ (fourth plot), and $\log_{10}(|\zeta_t u_x|/M])$, $\log_{10}(|u_t \zeta_x|/M)$, $\log_{10}(|R(t)-1|)$ (fifth plot, where $R(t) = (u_t \zeta_x)/(\zeta_t u_x)$ and M is the mean of the tidally averages of $|\zeta_t u_x|$ and $|u_t \zeta_x|$), in $x = 0$ km and $x = 41.5$ km.

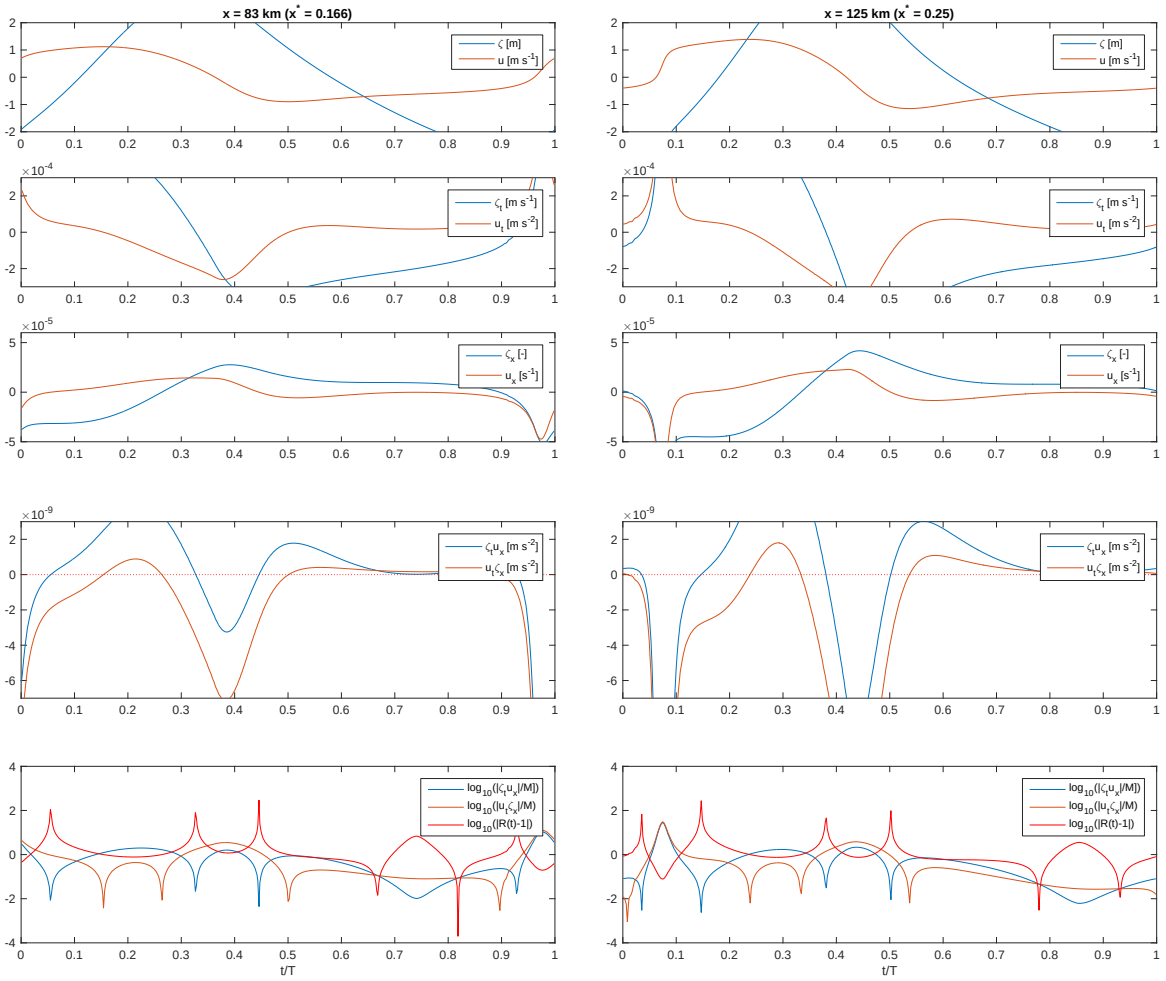

Figure 4: Temporal variation of ζ and u (first plot), ζ_t and u_t (second plot), ζ_x and u_x (third plot), $\zeta_t\, u_x$ and $u_t\, \zeta_x$ (fourth plot), and $\log_{10}(|\zeta_t u_x|/M])$, $\log_{10}(|u_t \zeta_x|/M)$, $\log_{10}(|R(t)-1|)$ (fifth plot, where $R(t) = (u_t\zeta_x)/(\zeta_t u_x)$ and M is the mean of the tidally averages of $|\zeta_t u_x|$ and $|u_t \zeta_x|$), in $x = 83$ km and $x = 125$ km.

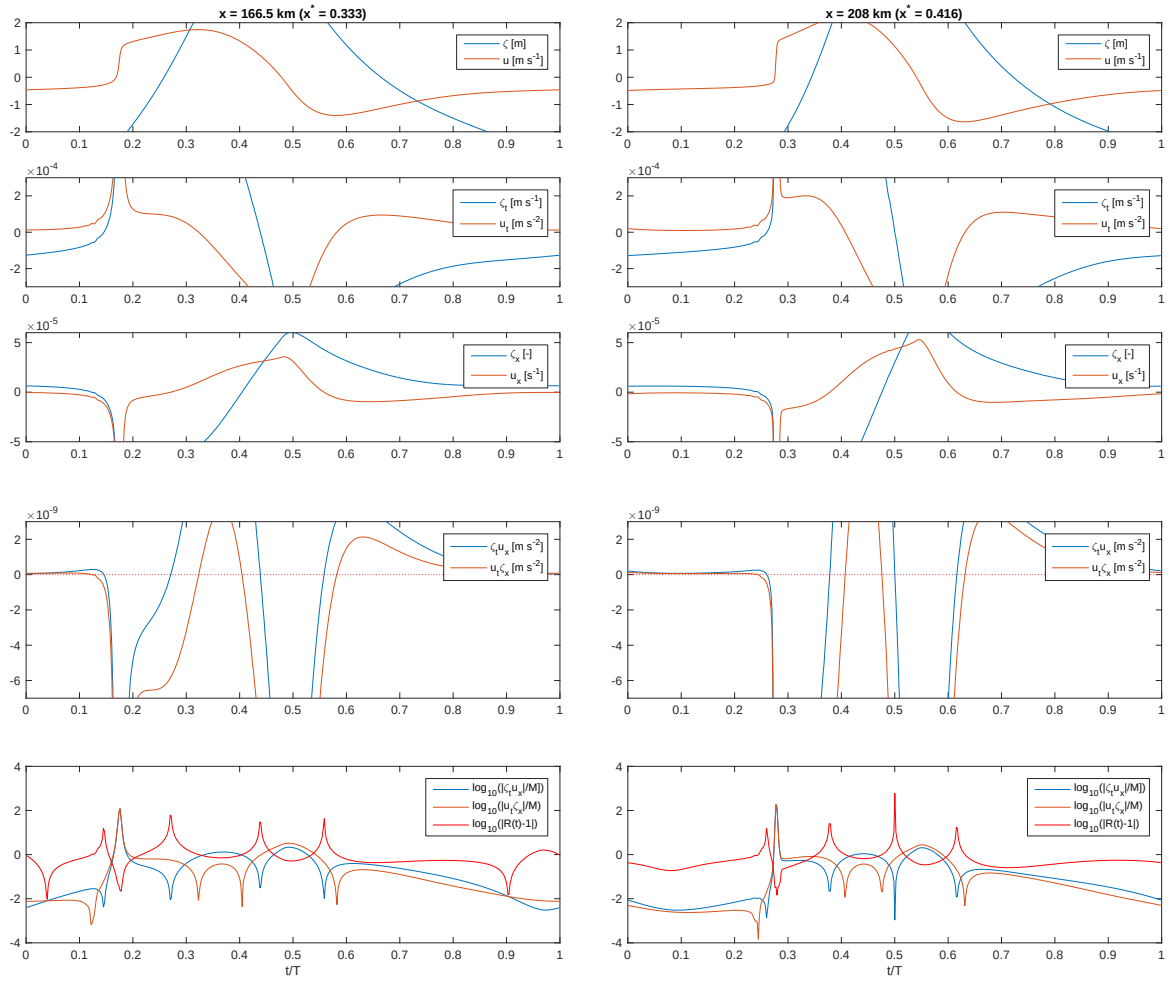

Figure 5: Temporal variation of ζ and u (first plot), ζ_t and u_t (second plot), ζ_x and u_x (third plot), $\zeta_t\, u_x$ and $u_t\, \zeta_x$ (fourth plot), and $\log_{10}(|\zeta_t u_x|/M])$, $\log_{10}(|u_t \zeta_x|/M)$, $\log_{10}(|R(t)-1|)$ (fifth plot, where $R(t) = (u_t\zeta_x)/(\zeta_t u_x)$ and M is the mean of the tidally averages of $|\zeta_t u_x|$ and $|u_t \zeta_x|$), in $x = 166.5$ km and $x = 208$ km.

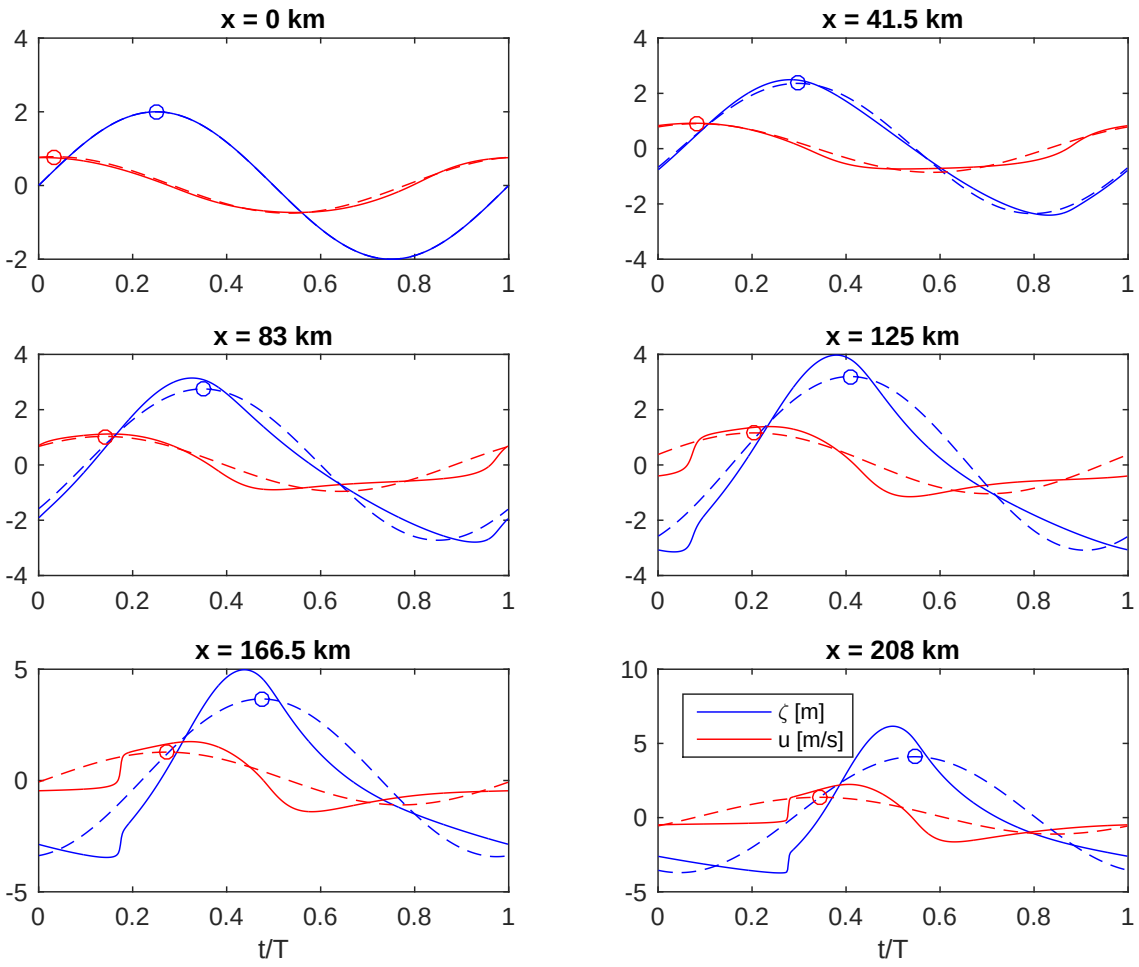

Figure 6: Tidal waves and Fourier series truncated at the first harmonic. Circles indicate the maxima of the dominant tidal component, from which it is possible to detect the phase lag u-ζ.

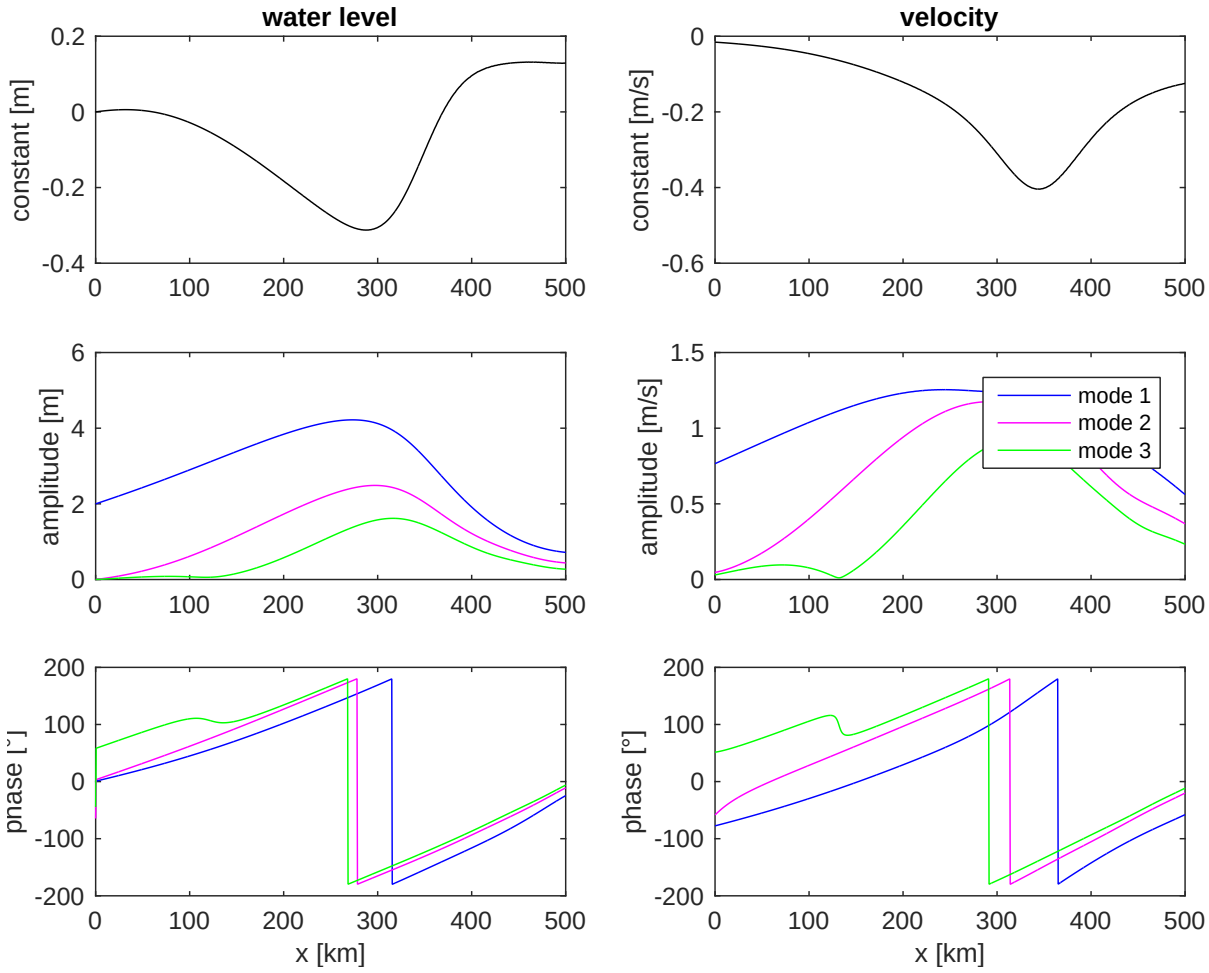

Figure 7: Fourier analysis of tidal wave. From top to bottom: constant term, amplitudes, phases of first three modes. Left column: water level ζ; right column: velocity u.

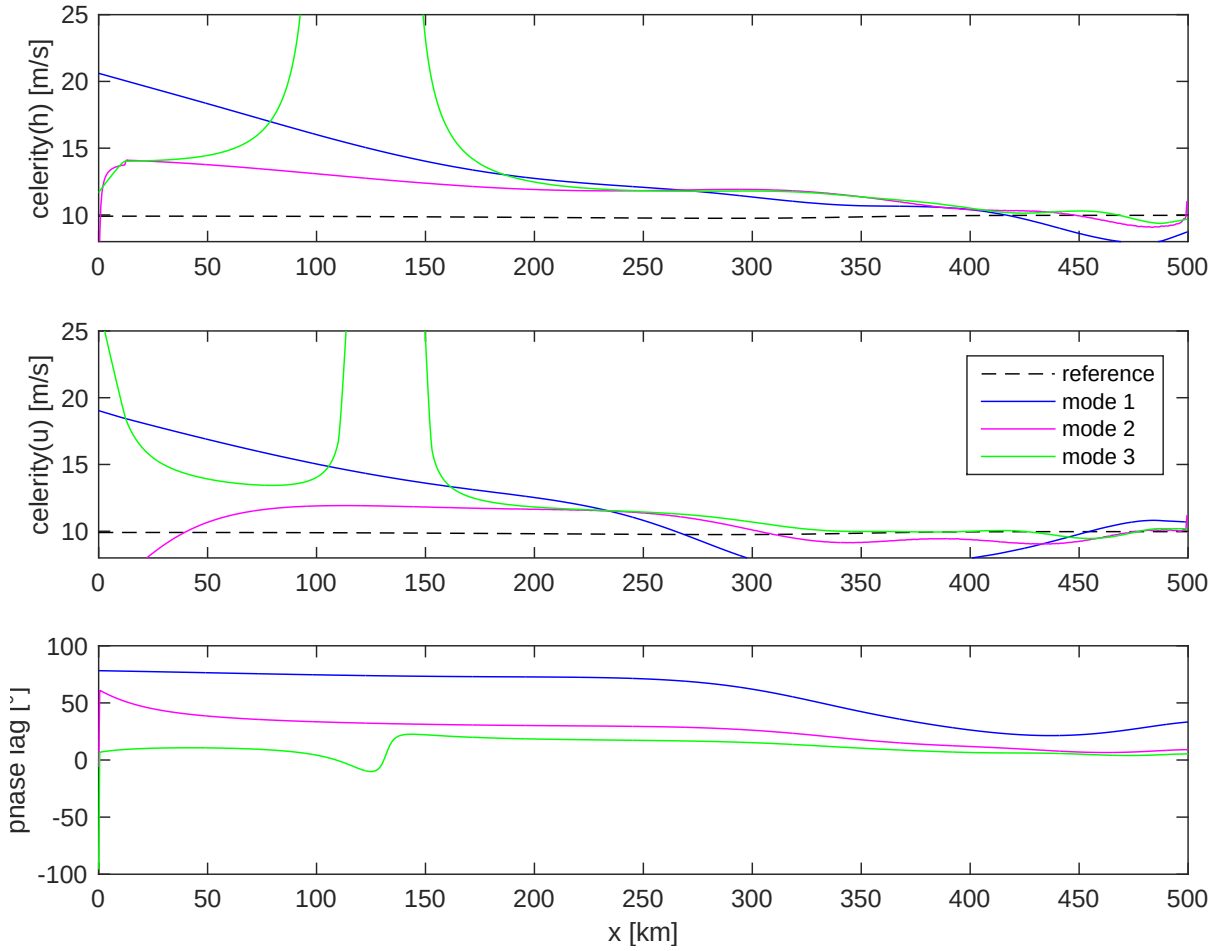

Figure 8: Wave celerity for water level ζ, for velocity u, phase lag u-ζ. Colors refer to the first three modes; black dashed line to wave celerity in a frictionless prismatic channel.

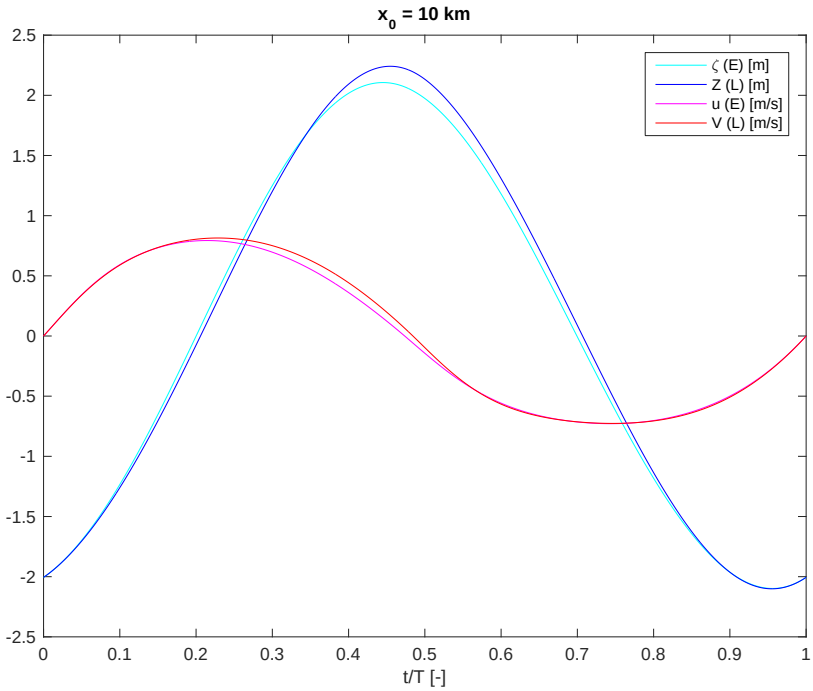

Figure 9: Lagrangean water level Z and velocity V compared with Eulerian values ζ and u, for $x_0 = 10$ km.

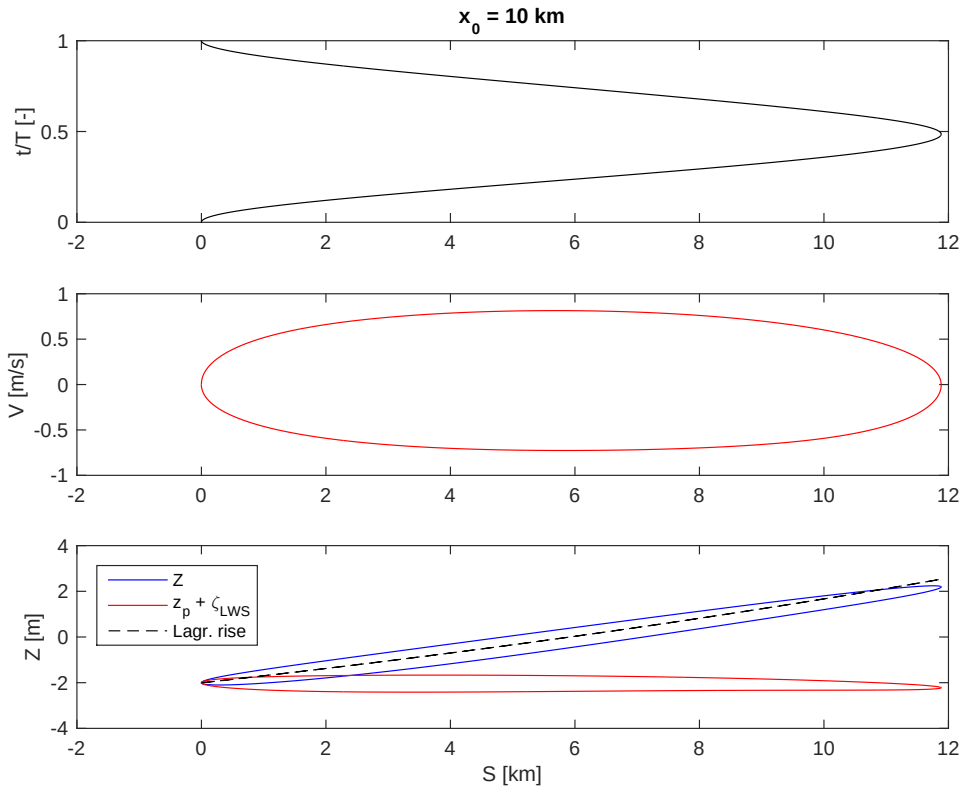

Figure 10: Lagrangean displacement S in time (first plot) and ellipses V-S (second plot) and Z-S (third plot), for $x_0 = 10$ km.

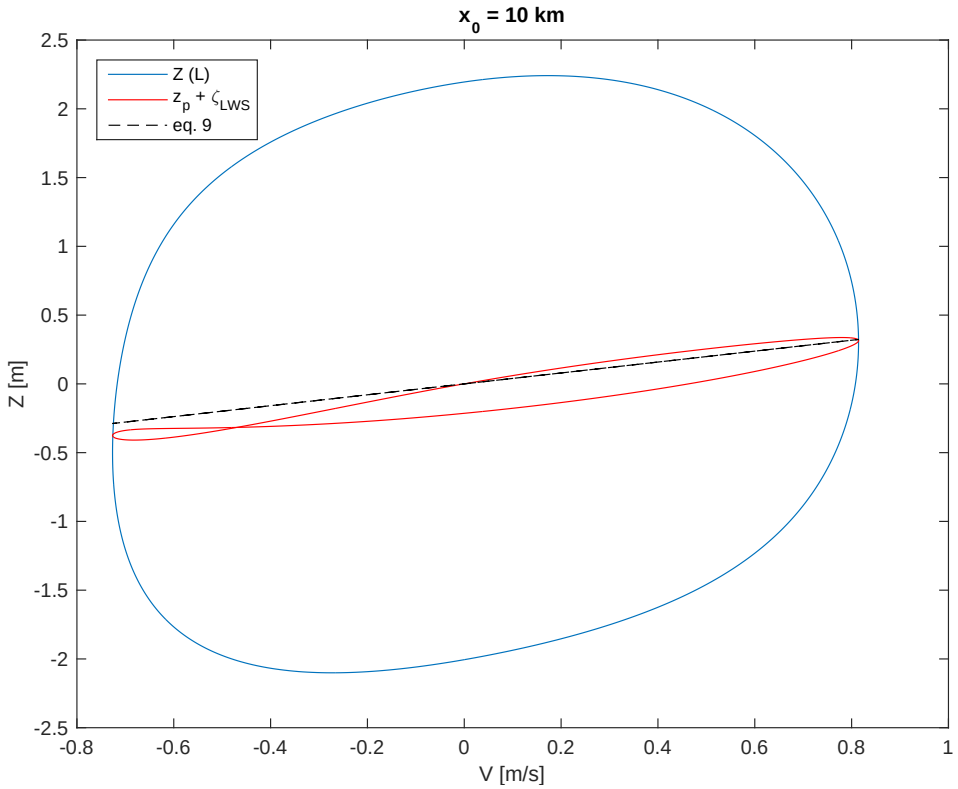

Figure 11: Lagrangean water level against velocity V: Z is the actual value, $z_p + \zeta_{LWS}$ is the transformed water level, for $x_0 = 10$ km. Black dashed lines: equation (9).

Variant 2

Length $b = 300$ km (exponential variation); Strickler coefficient $K = 45$ m$^{1/3}$s^{-1}; nonlinear friction.

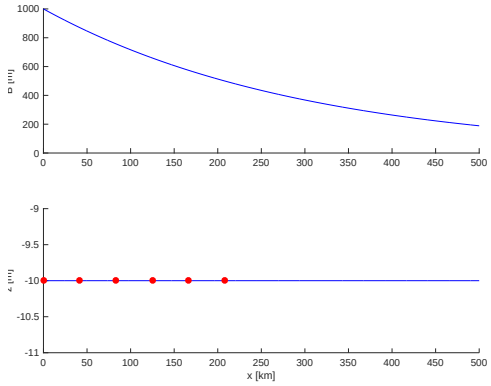

Figure 1: Longitudinal profiles of width and bottom. Dots indicates the locations where the temporal behaviour is shown in figure 3.

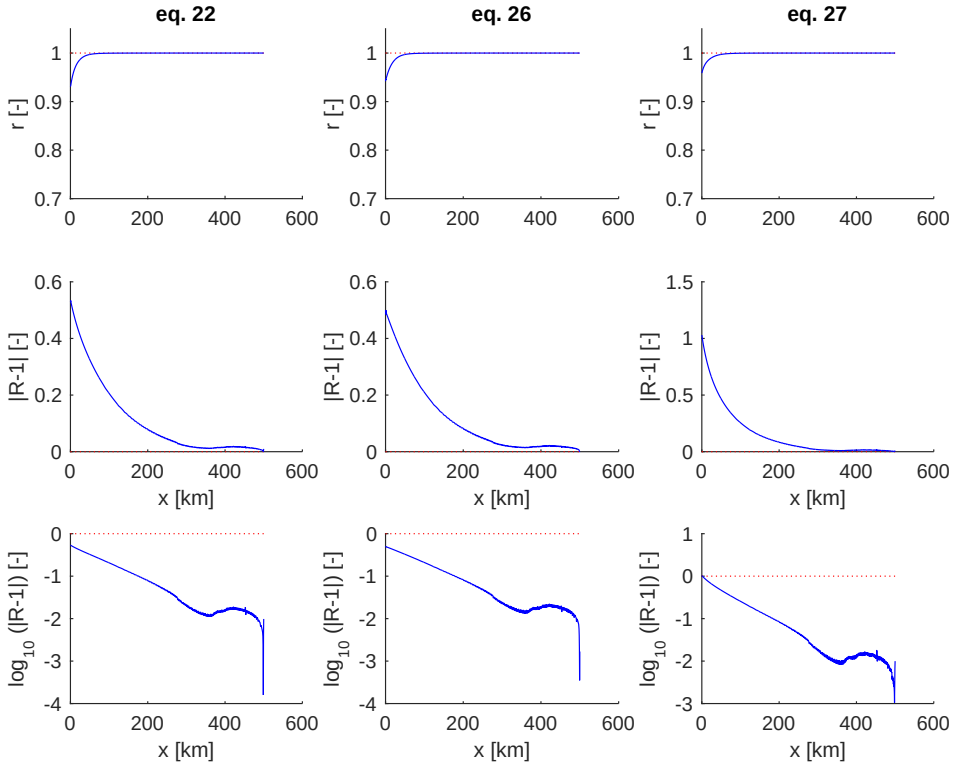

Figure 2: Longitudinal variation of the correlation coefficient r (first row) and of the two different functions of the ratio R between right hand side and left hand side of equations 22, 26 and 27 in the manuscript, respectively $|R-1|$ and $\log_{10}(|R-1|)$.

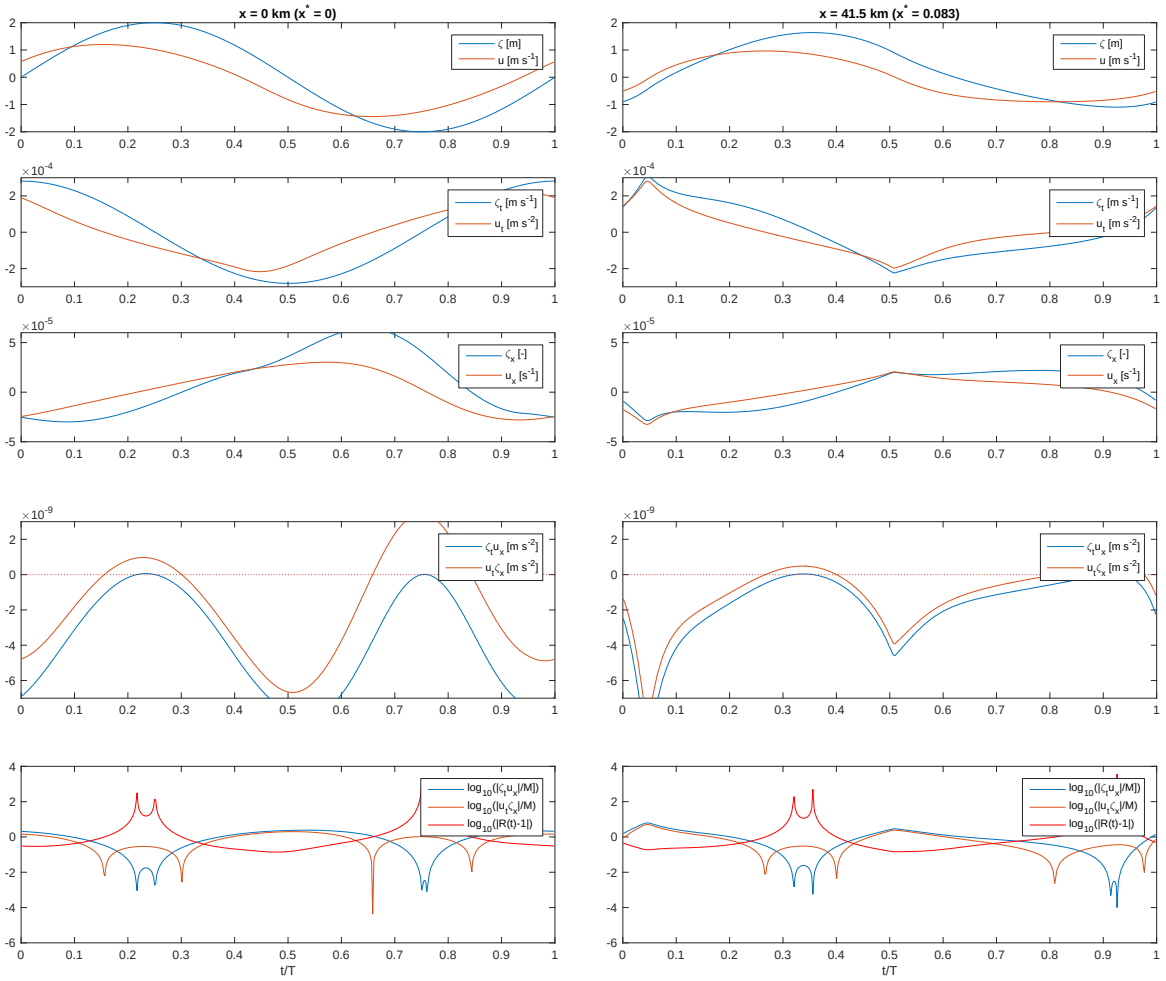

Figure 3: Temporal variation of ζ and u (first plot), ζ_t and u_t (second plot), ζ_x and u_x (third plot), $\zeta_t\, u_x$ and $u_t\, \zeta_x$ (fourth plot), and $\log_{10}(|\zeta_t u_x|/M])$, $\log_{10}(|u_t \zeta_x|/M)$, $\log_{10}(|R(t)-1|)$ (fifth plot, where $R(t) = (u_t \zeta_x)/(\zeta_t u_x)$ and M is the mean of the tidally averages of $|\zeta_t u_x|$ and $|u_t \zeta_x|$), in $x = 0$ km and $x = 41.5$ km.

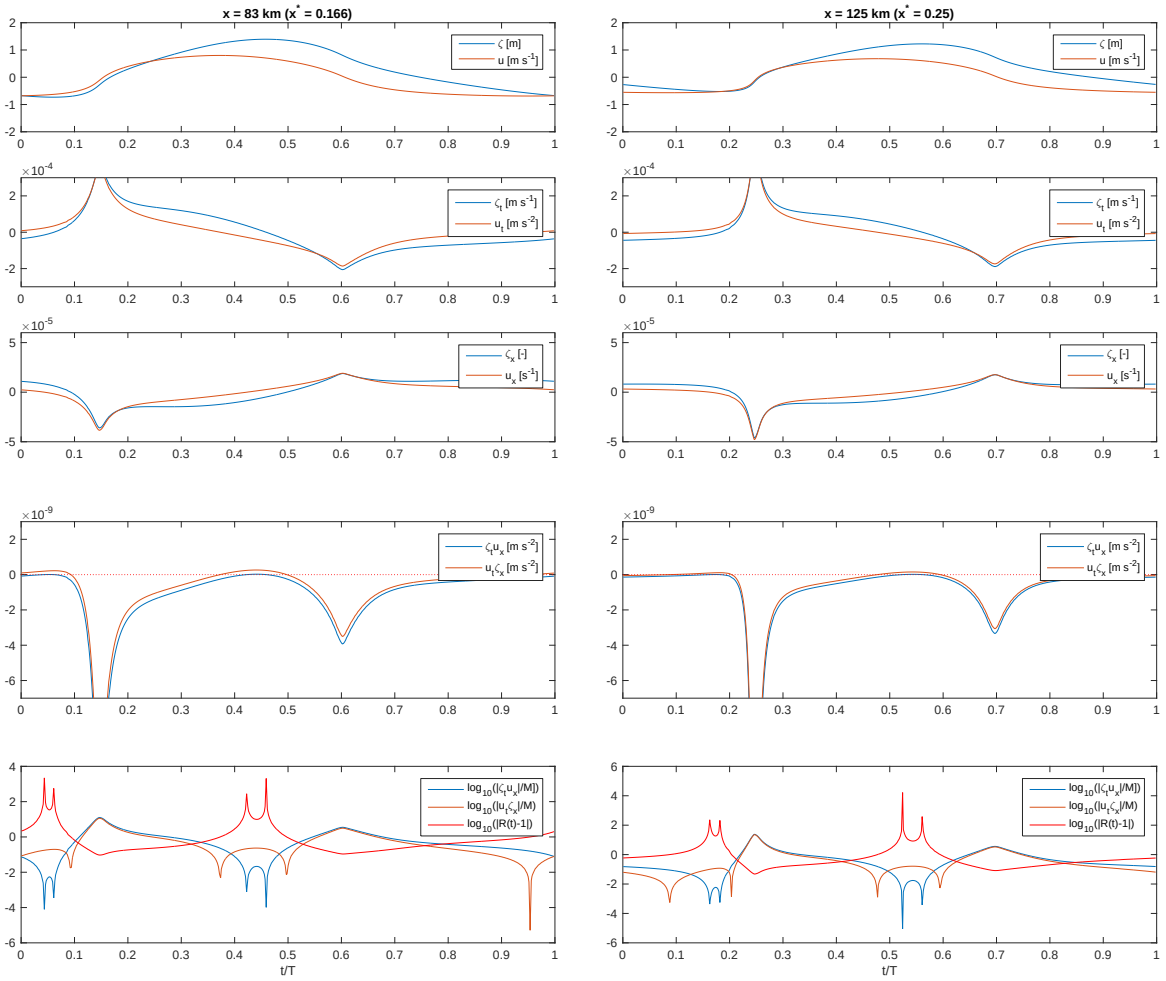

Figure 4: Temporal variation of ζ and u (first plot), ζ_t and u_t (second plot), ζ_x and u_x (third plot), $\zeta_t\, u_x$ and $u_t\, \zeta_x$ (fourth plot), and $\log_{10}(|\zeta_t u_x|/M])$, $\log_{10}(|u_t \zeta_x|/M)$, $\log_{10}(|R(t)-1|)$ (fifth plot, where $R(t) = (u_t \zeta_x)/(\zeta_t u_x)$ and M is the mean of the tidally averages of $|\zeta_t u_x|$ and $|u_t \zeta_x|$), in $x = 83$ km and $x = 125$ km.

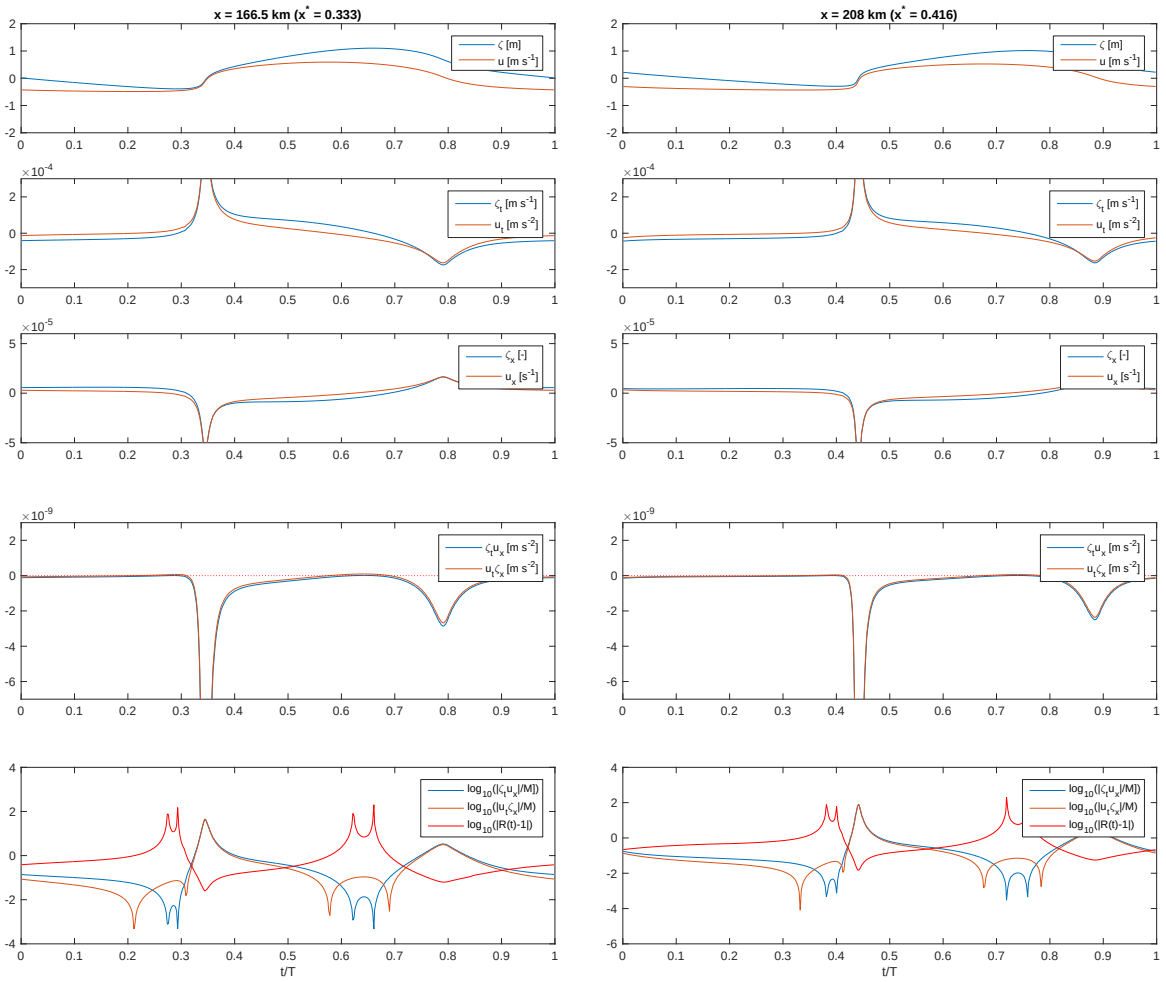

Figure 5: Temporal variation of ζ and u (first plot), ζ_t and u_t (second plot), ζ_x and u_x (third plot), $\zeta_t\, u_x$ and $u_t\, \zeta_x$ (fourth plot), and $\log_{10}(|\zeta_t u_x|/M])$, $\log_{10}(|u_t \zeta_x|/M)$, $\log_{10}(|R(t)-1|)$ (fifth plot, where $R(t) = (u_t \zeta_x)/(\zeta_t u_x)$ and M is the mean of the tidally averages of $|\zeta_t u_x|$ and $|u_t \zeta_x|$), in $x = 166.5$ km and $x = 208$ km.

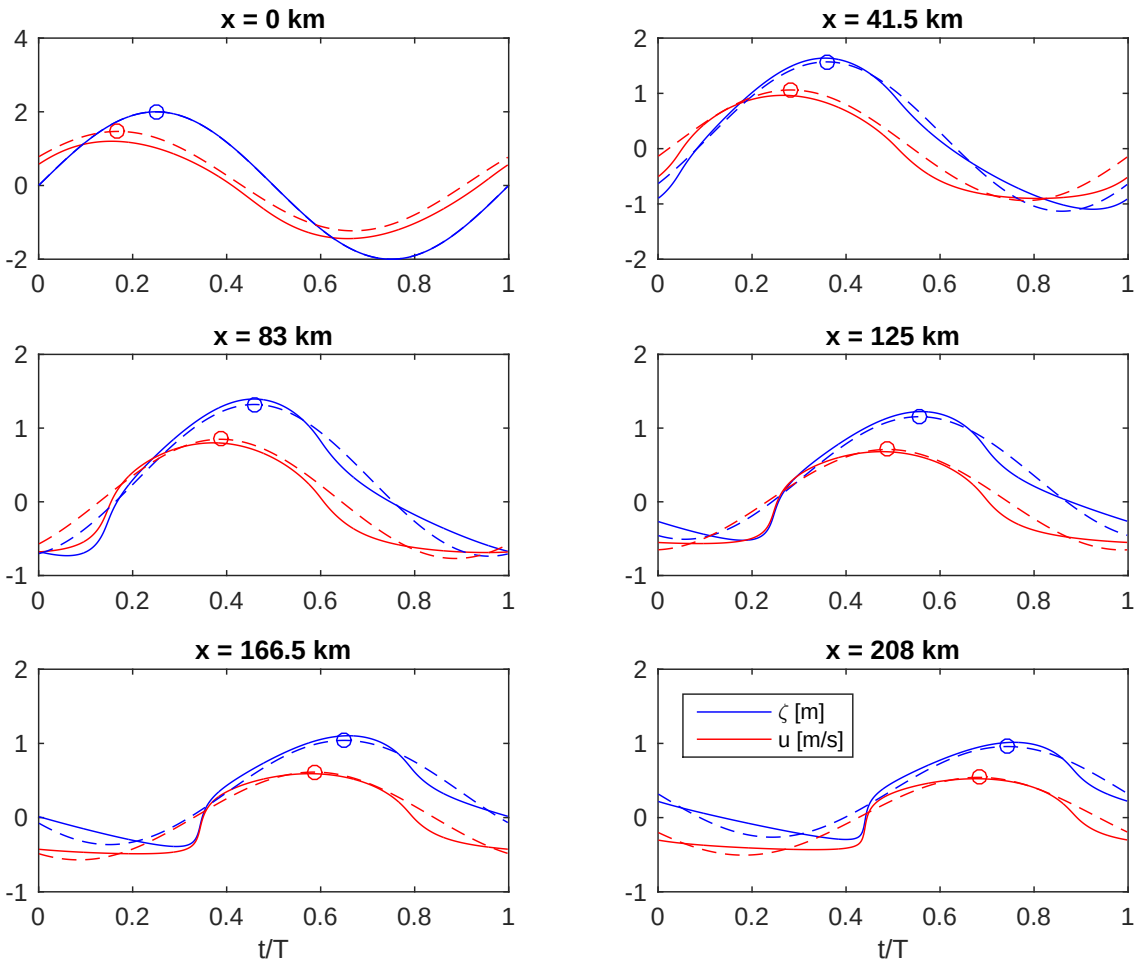

Figure 6: Tidal waves and Fourier series truncated at the first harmonic. Circles indicate the maxima of the dominant tidal component, from which it is possible to detect the phase lag u-ζ.

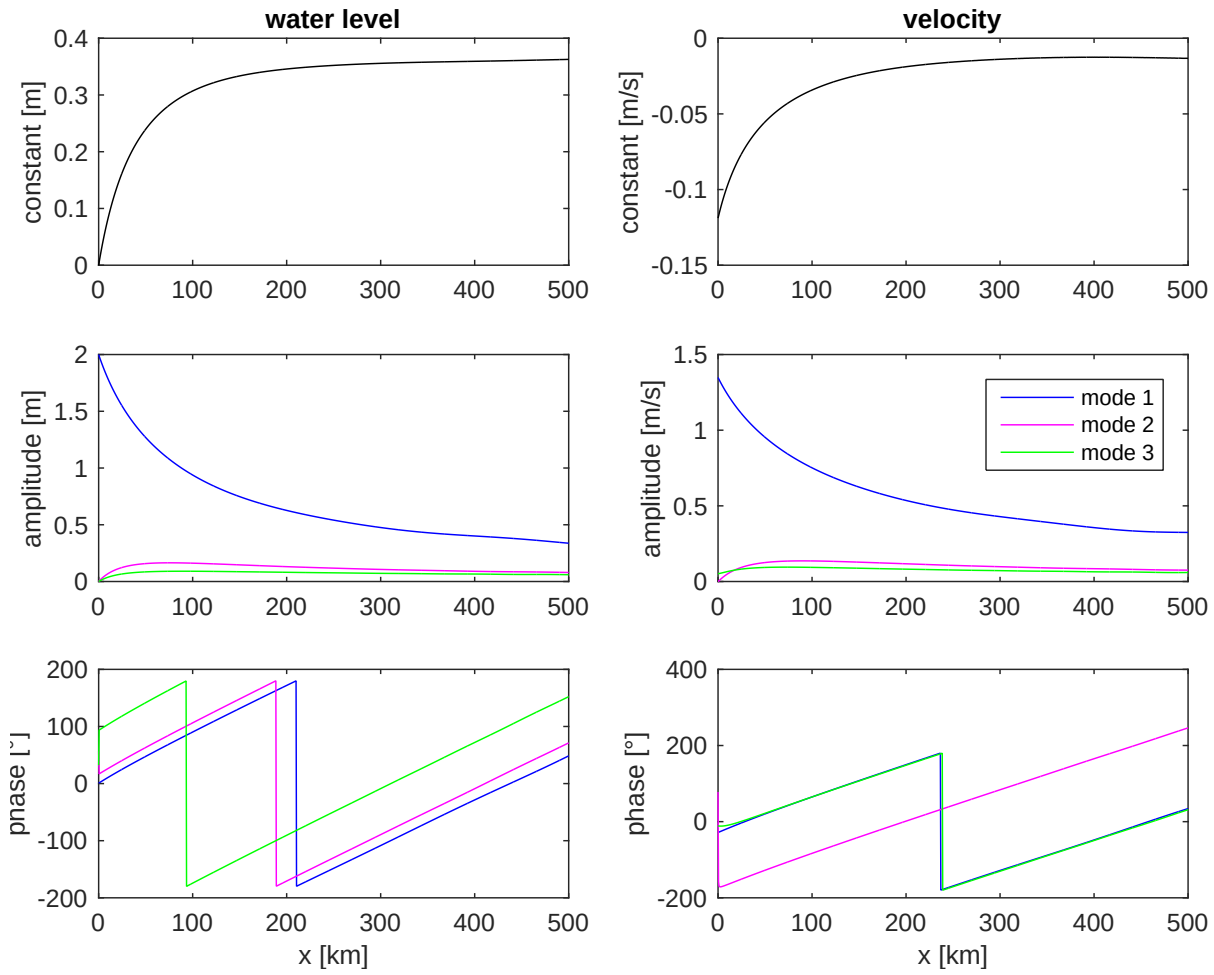

Figure 7: Fourier analysis of tidal wave. From top to bottom: constant term, amplitudes, phases of first three modes. Left column: water level ζ; right column: velocity u.

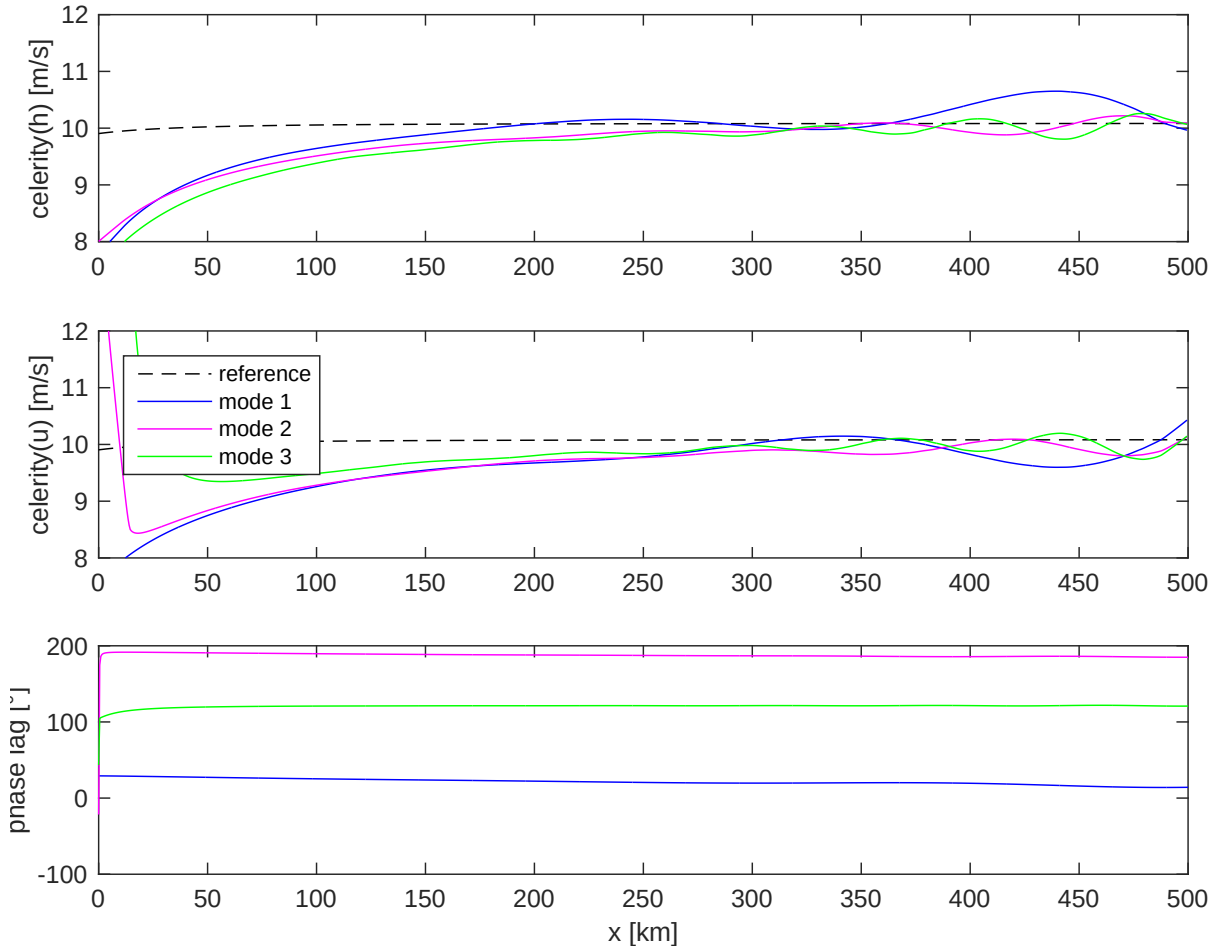

Figure 8: Wave celerity for water level ζ, for velocity u, phase lag u-ζ. Colors refer to the first three modes; black dashed line to wave celerity in a frictionless prismatic channel.

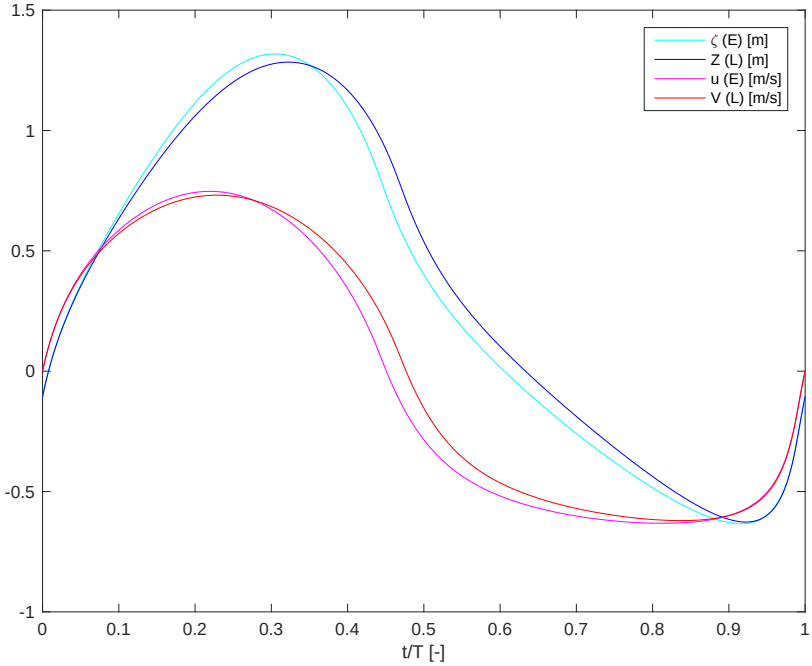

Figure 9: Lagrangean water level Z and velocity V compared with Eulerian values ζ and u in $x = 100$ km.

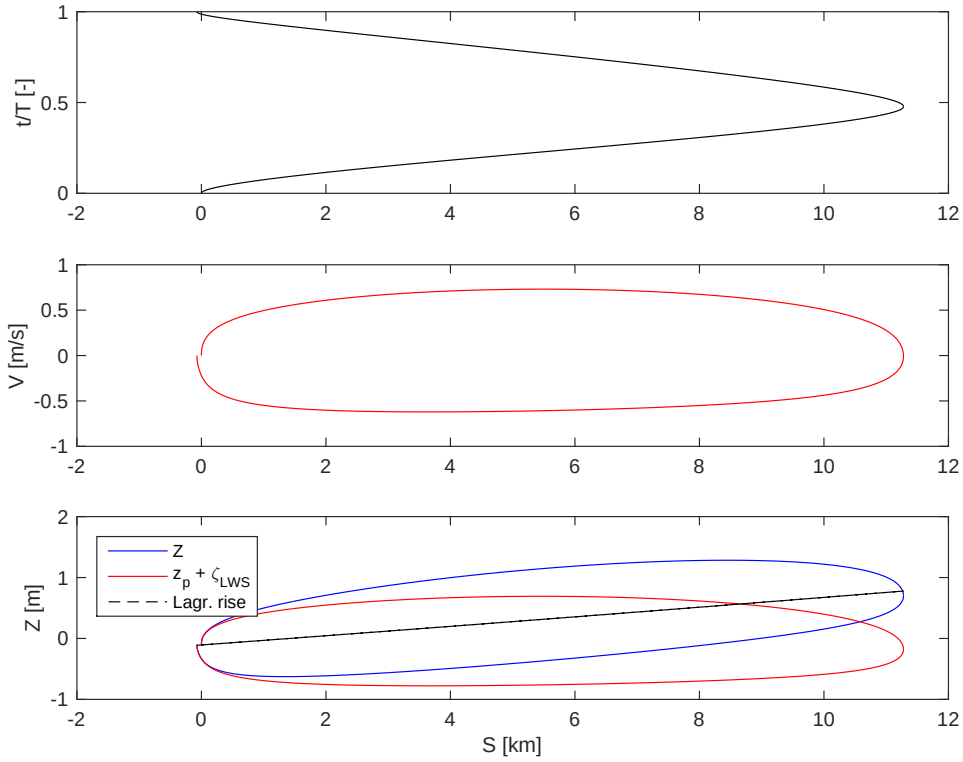

Figure 10: Lagrangean displacement S in time (first plot) and ellipses V-S (second plot) and Z-S (third plot).

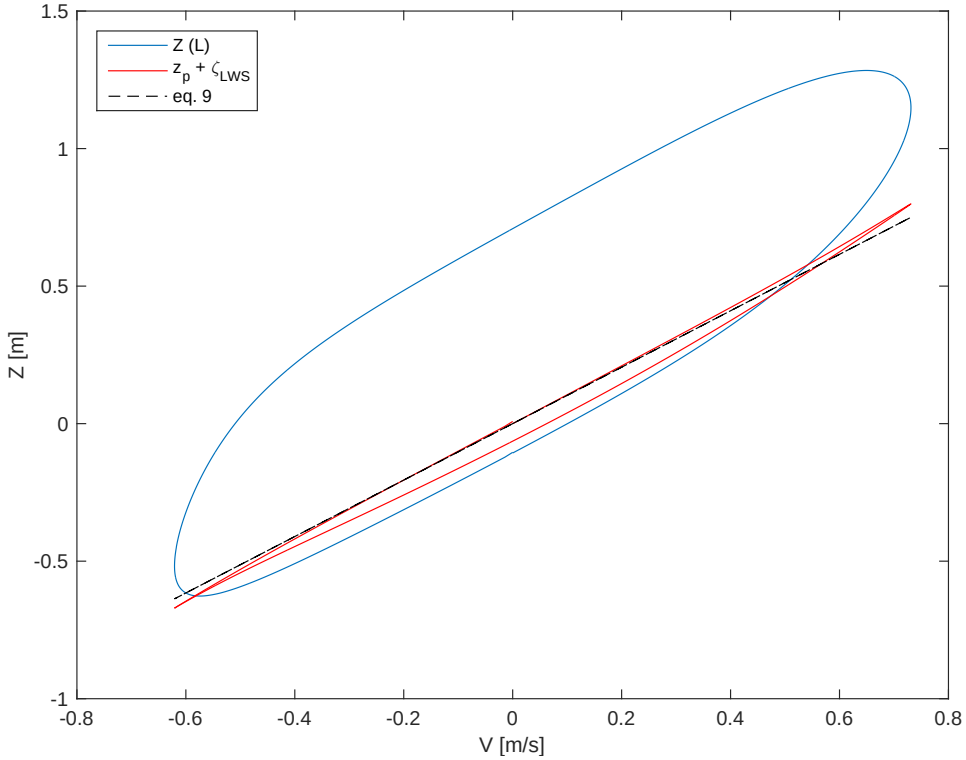

Figure 11: Lagrangean water level against velocity V: Z is the actual value, $z_p + \zeta_{LWS}$ is the transformed water level. Black dashed lines: equation (9).

Variant 3

Length $b = 100$ km (exponential variation); Strickler coefficient $K = 20$ m$^{1/3}$s^{-1}; nonlinear friction.

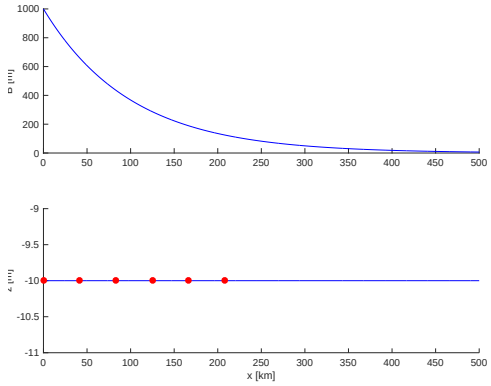

Figure 1: Longitudinal profiles of width and bottom. Dots indicates the locations where the temporal behaviour is shown in figure 3.

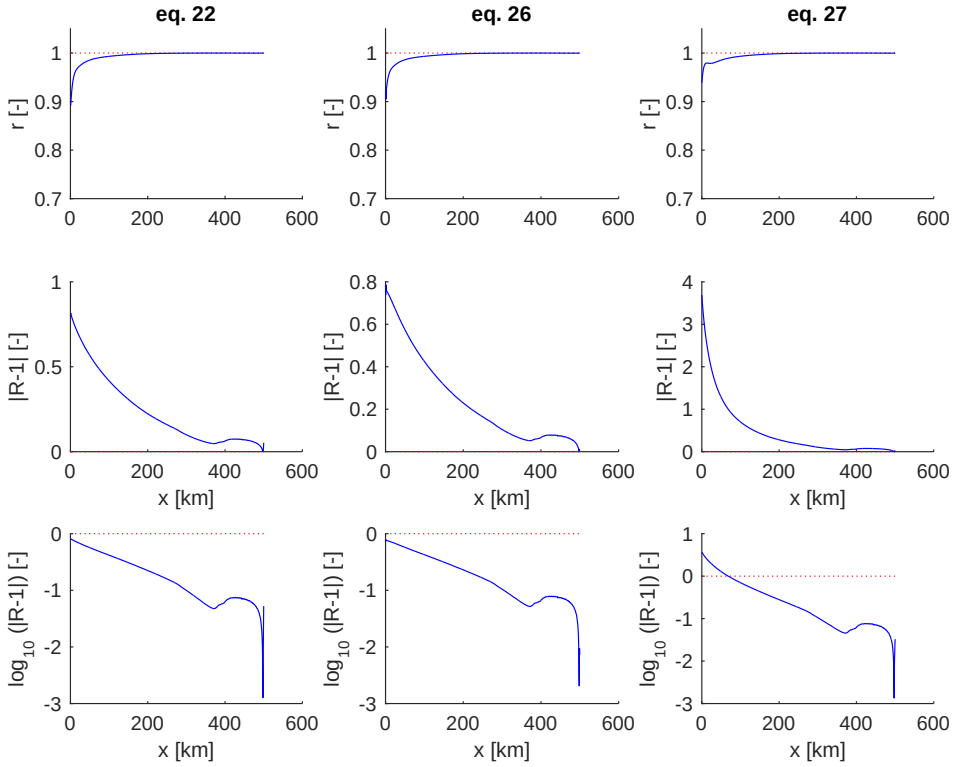

Figure 2: Longitudinal variation of the correlation coefficient r (first row) and of the two different functions of the ratio R between right hand side and left hand side of equations 22, 26 and 27 in the manuscript, respectively $|R-1|$ and $\log_{10}(|R-1|)$.

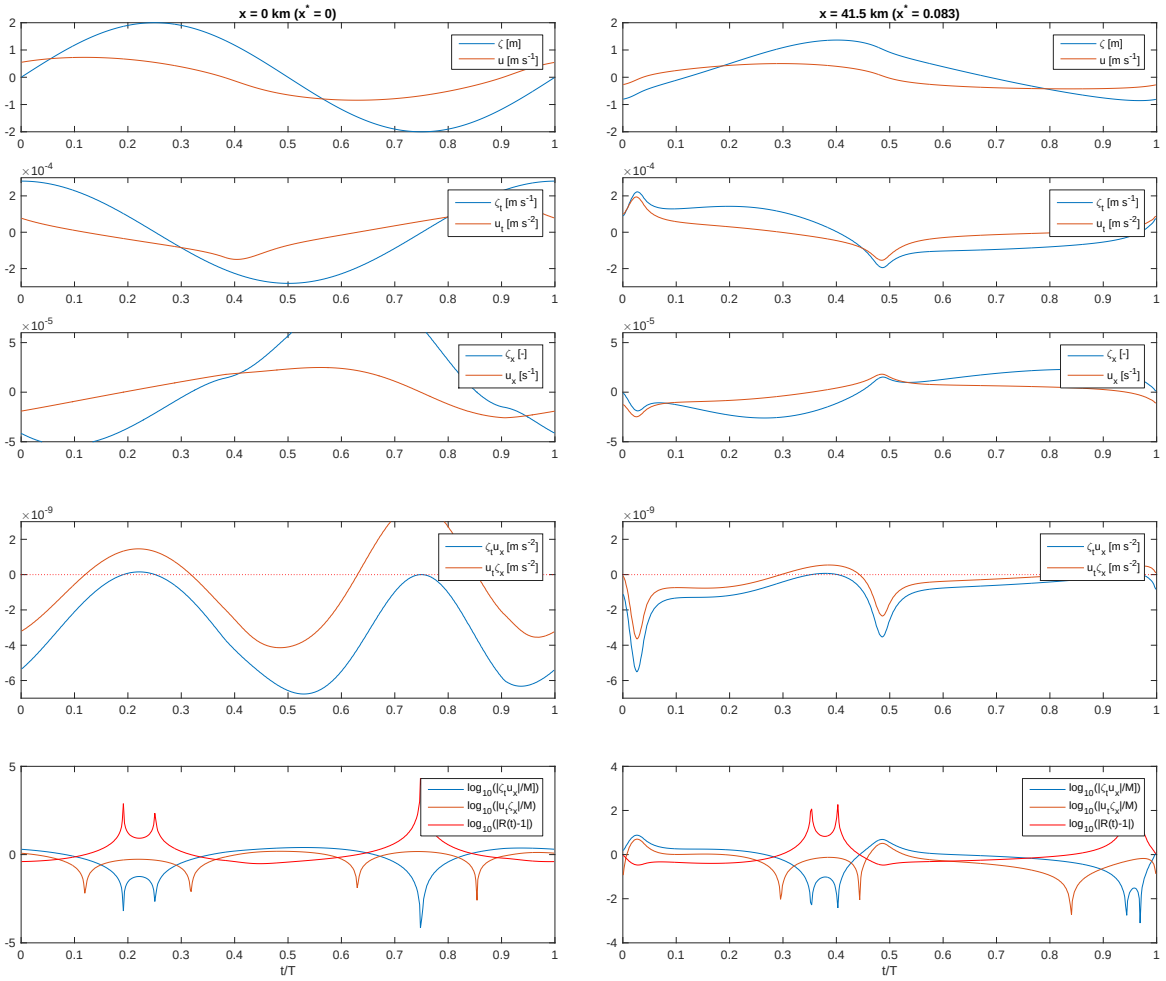

Figure 3: Temporal variation of ζ and u (first plot), ζ_t and u_t (second plot), ζ_x and u_x (third plot), $\zeta_t\, u_x$ and $u_t\, \zeta_x$ (fourth plot), and $\log_{10}(|\zeta_t u_x|/M])$, $\log_{10}(|u_t \zeta_x|/M)$, $\log_{10}(|R(t)-1|)$ (fifth plot, where $R(t) = (u_t \zeta_x)/(\zeta_t u_x)$ and M is the mean of the tidally averages of $|\zeta_t u_x|$ and $|u_t \zeta_x|$), in $x = 0$ km and $x = 41.5$ km.

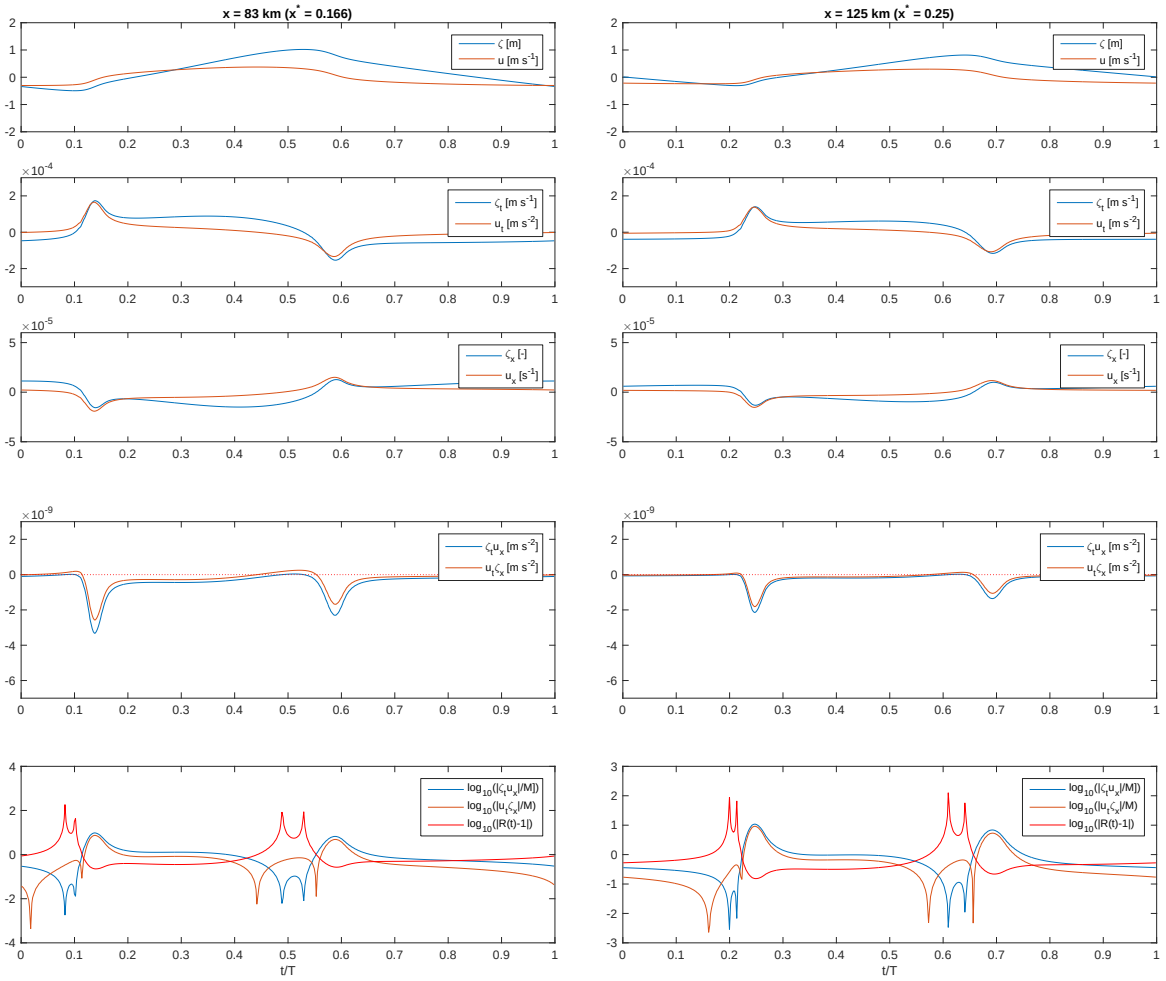

Figure 4: Temporal variation of ζ and u (first plot), ζ_t and u_t (second plot), ζ_x and u_x (third plot), $\zeta_t\, u_x$ and $u_t\, \zeta_x$ (fourth plot), and $\log_{10}(|\zeta_t u_x|/M])$, $\log_{10}(|u_t \zeta_x|/M)$, $\log_{10}(|R(t)-1|)$ (fifth plot, where $R(t) = (u_t \zeta_x)/(\zeta_t u_x)$ and M is the mean of the tidally averages of $|\zeta_t u_x|$ and $|u_t \zeta_x|$), in $x = 83$ km and $x = 125$ km.

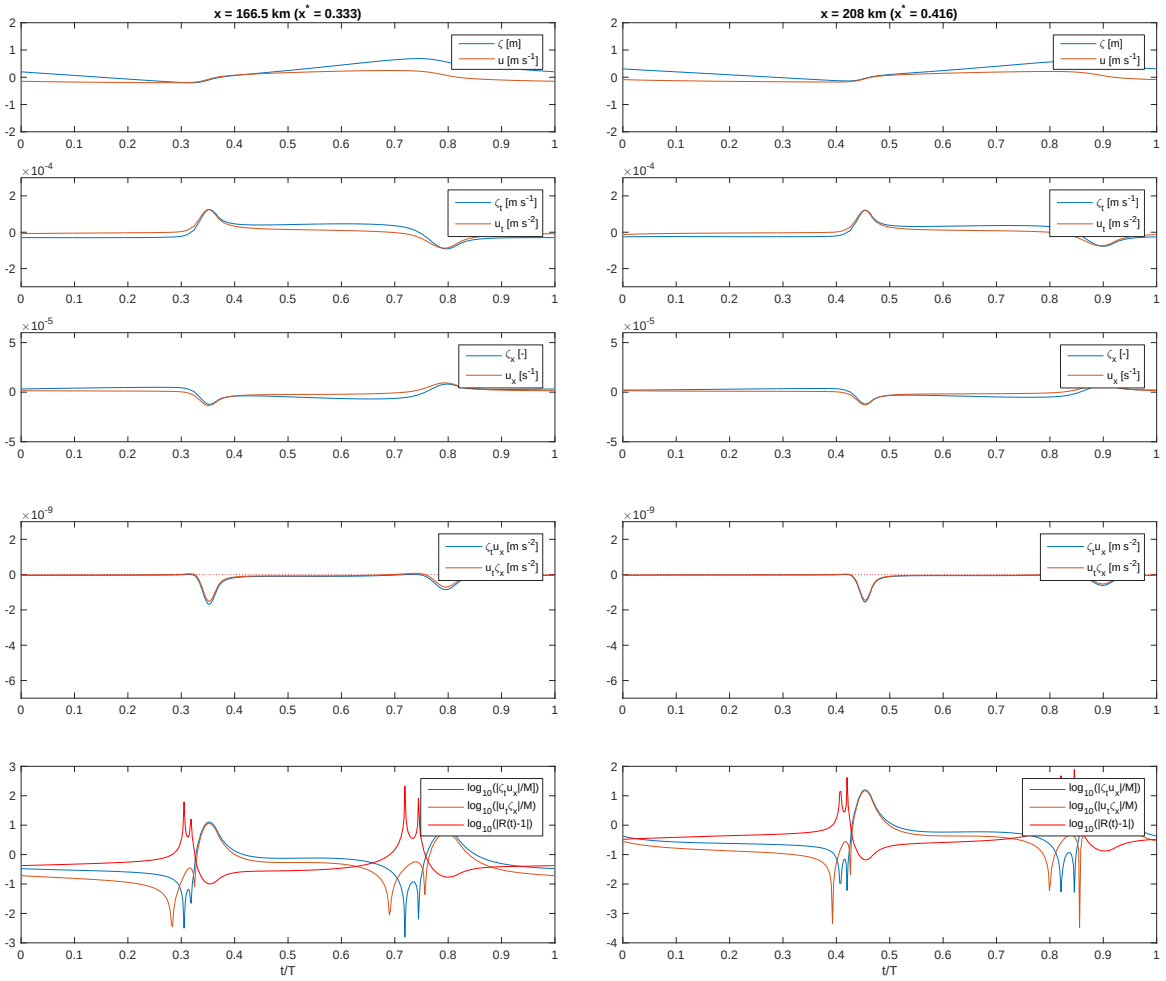

Figure 5: Temporal variation of ζ and u (first plot), ζ_t and u_t (second plot), ζ_x and u_x (third plot), $\zeta_t\, u_x$ and $u_t\, \zeta_x$ (fourth plot), and $\log_{10}(|\zeta_t u_x|/M])$, $\log_{10}(|u_t \zeta_x|/M)$, $\log_{10}(|R(t)-1|)$ (fifth plot, where $R(t) = (u_t\zeta_x)/(\zeta_t u_x)$ and M is the mean of the tidally averages of $|\zeta_t u_x|$ and $|u_t \zeta_x|$), in $x = 166.5$ km and $x = 208$ km.

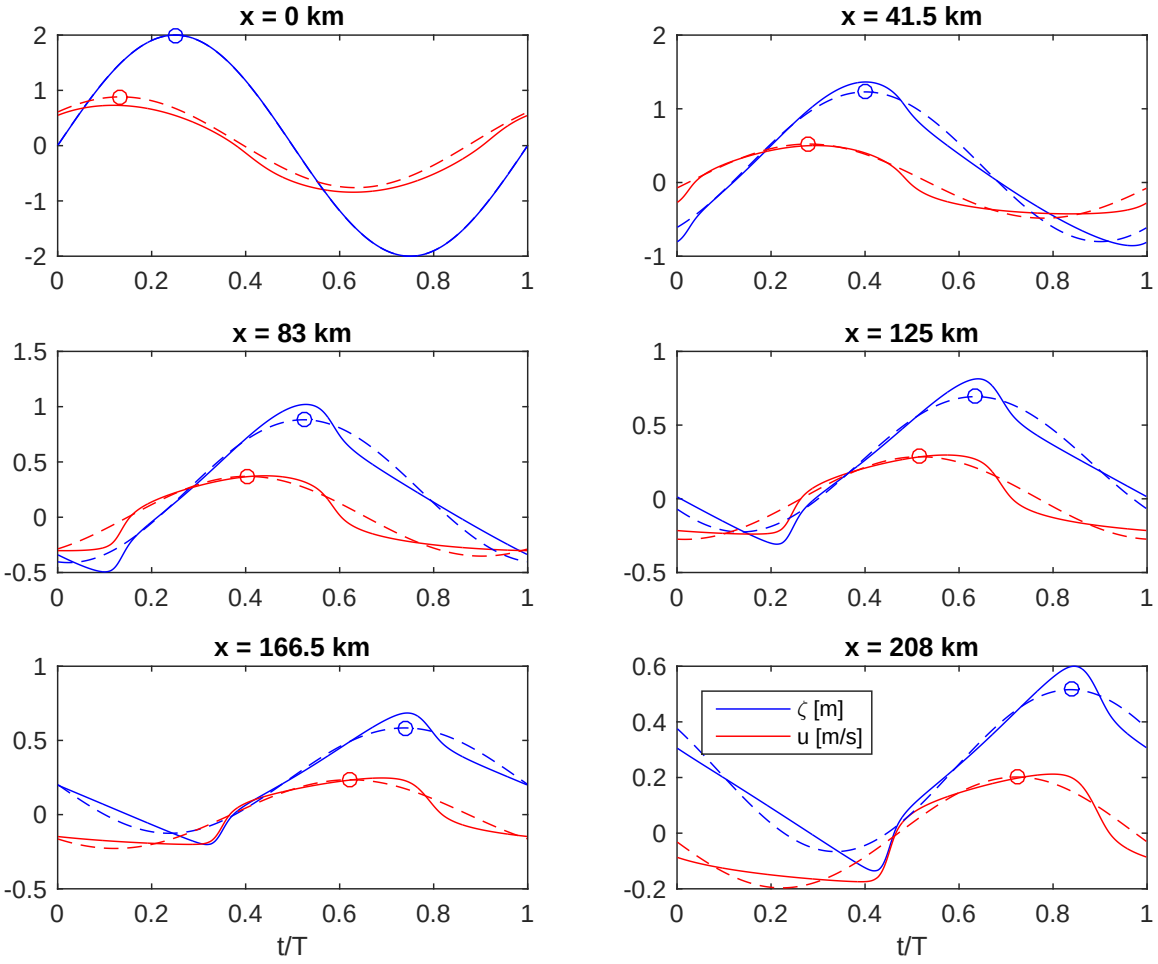

Figure 6: Tidal waves and Fourier series truncated at the first harmonic. Circles indicate the maxima of the dominant tidal component, from which it is possible to detect the phase lag u-ζ.

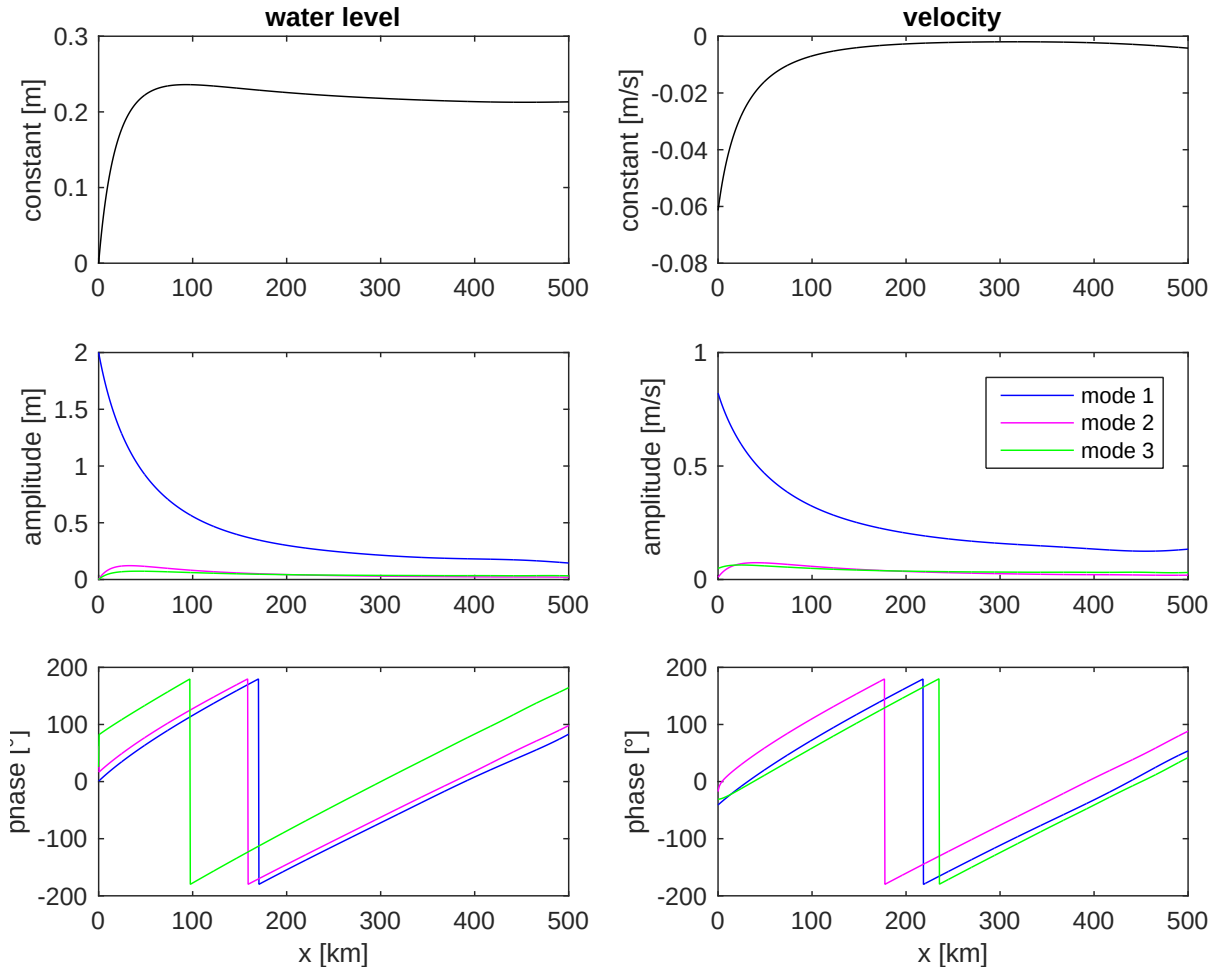

Figure 7: Fourier analysis of tidal wave. From top to bottom: constant term, amplitudes, phases of first three modes. Left column: water level ζ; right column: velocity u.

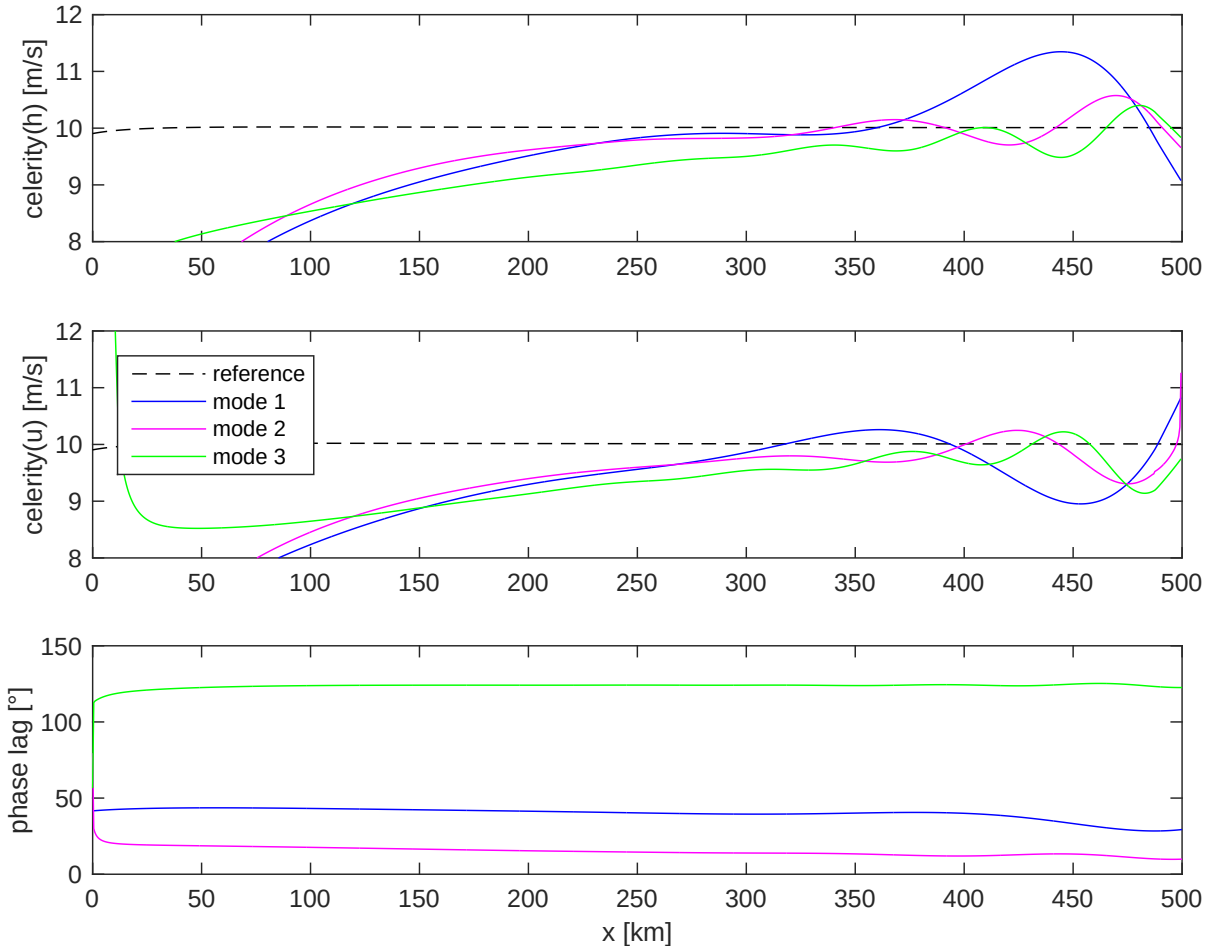

Figure 8: Wave celerity for water level ζ, for velocity u, phase lag u-ζ. Colors refer to the first three modes; black dashed line to wave celerity in a frictionless prismatic channel.

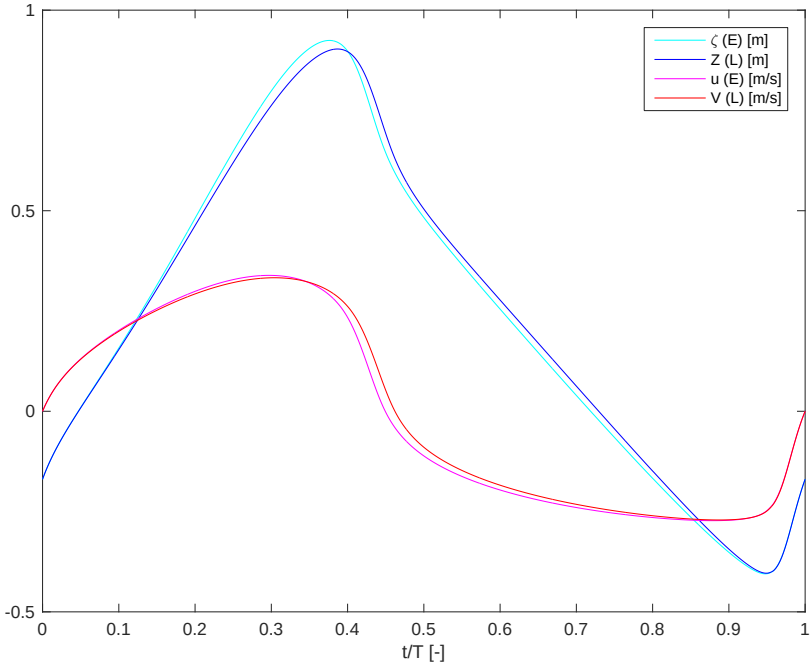

Figure 9: Lagrangean water level Z and velocity V compared with Eulerian values ζ and u in $x = 100$ km.

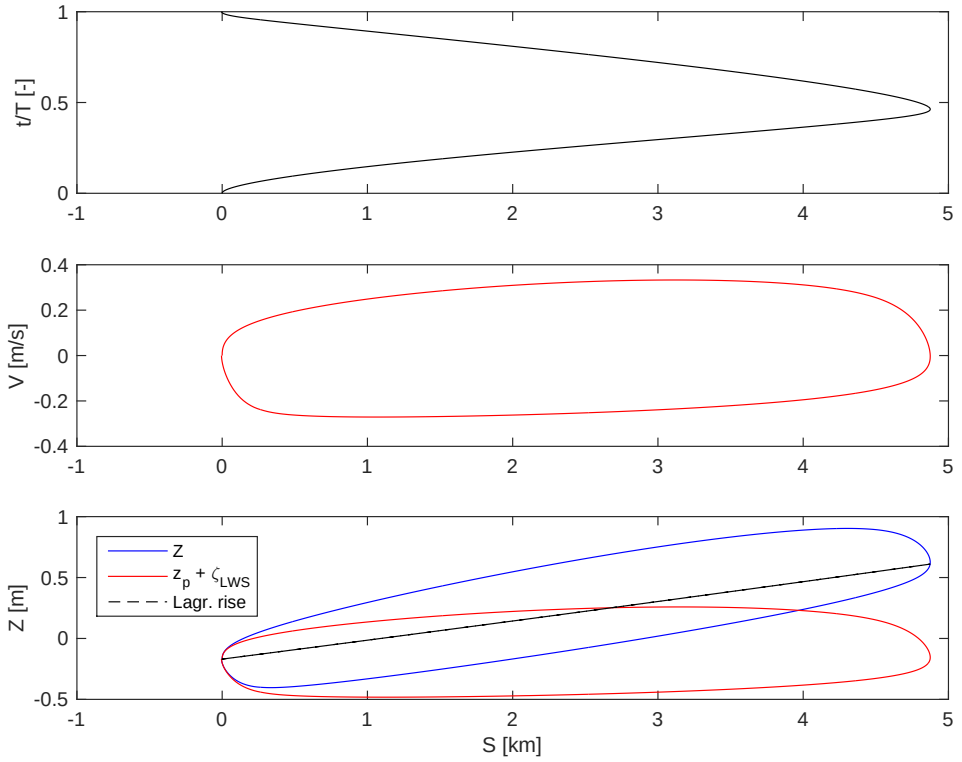

Figure 10: Lagrangean displacement S in time (first plot) and ellipses V-S (second plot) and Z-S (third plot).

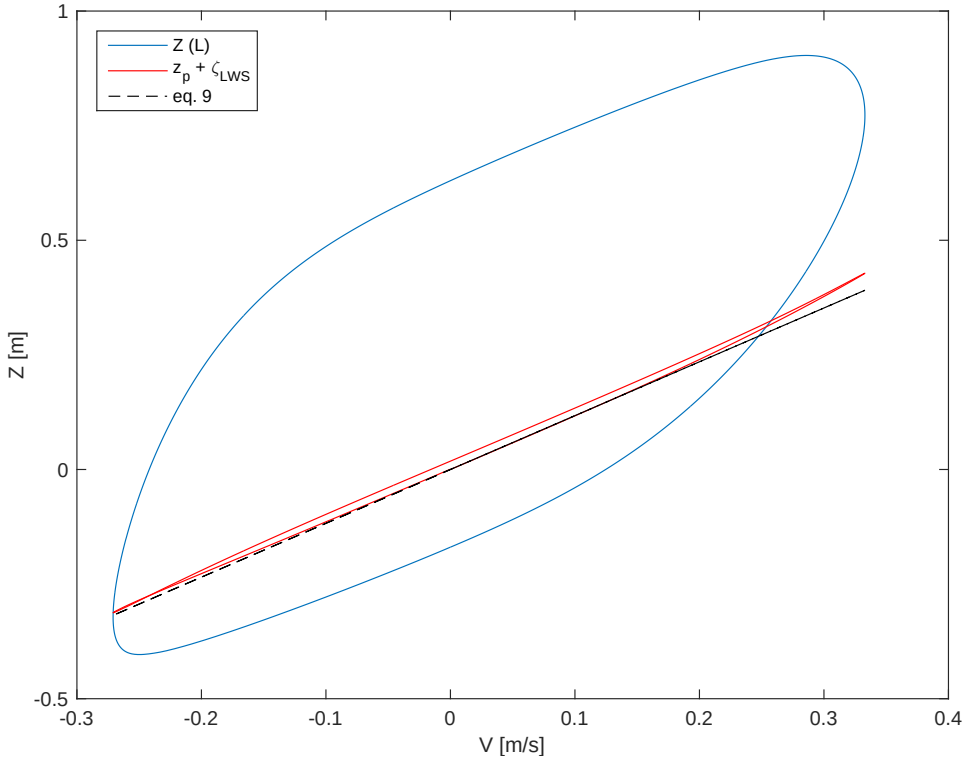

Figure 11: Lagrangean water level against velocity V: Z is the actual value, $z_p + \zeta_{LWS}$ is the transformed water level. Black dashed lines: equation (9).

Variant 4

Length $b = 100$ km (exponential variation); Strickler coefficient $K = 80$ m$^{1/3}$s^{-1}; nonlinear friction.

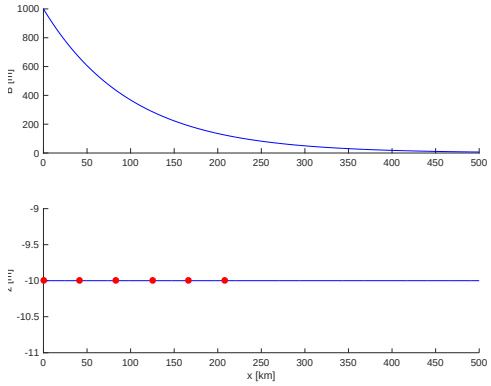

Figure 1: Longitudinal profiles of width and bottom. Dots indicates the locations where the temporal behaviour is shown in figure 3.

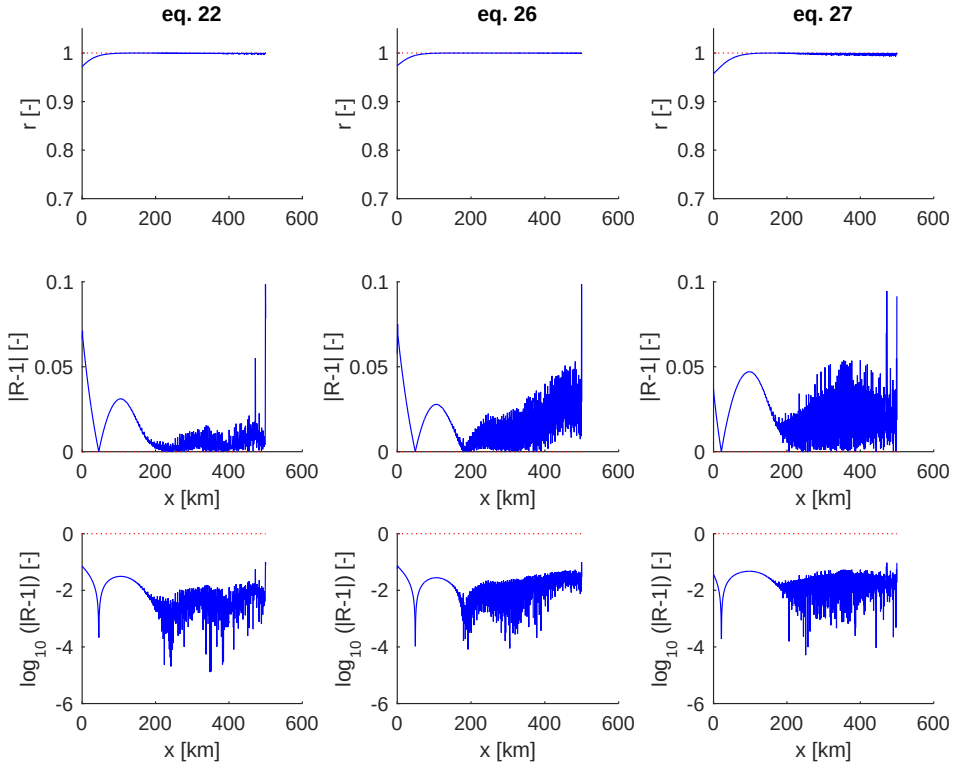

Figure 2: Longitudinal variation of the correlation coefficient r (first row) and of the two different functions of the ratio R between right hand side and left hand side of equations 22, 26 and 27 in the manuscript, respectively $|R-1|$ and $\log_{10}(|R-1|)$.

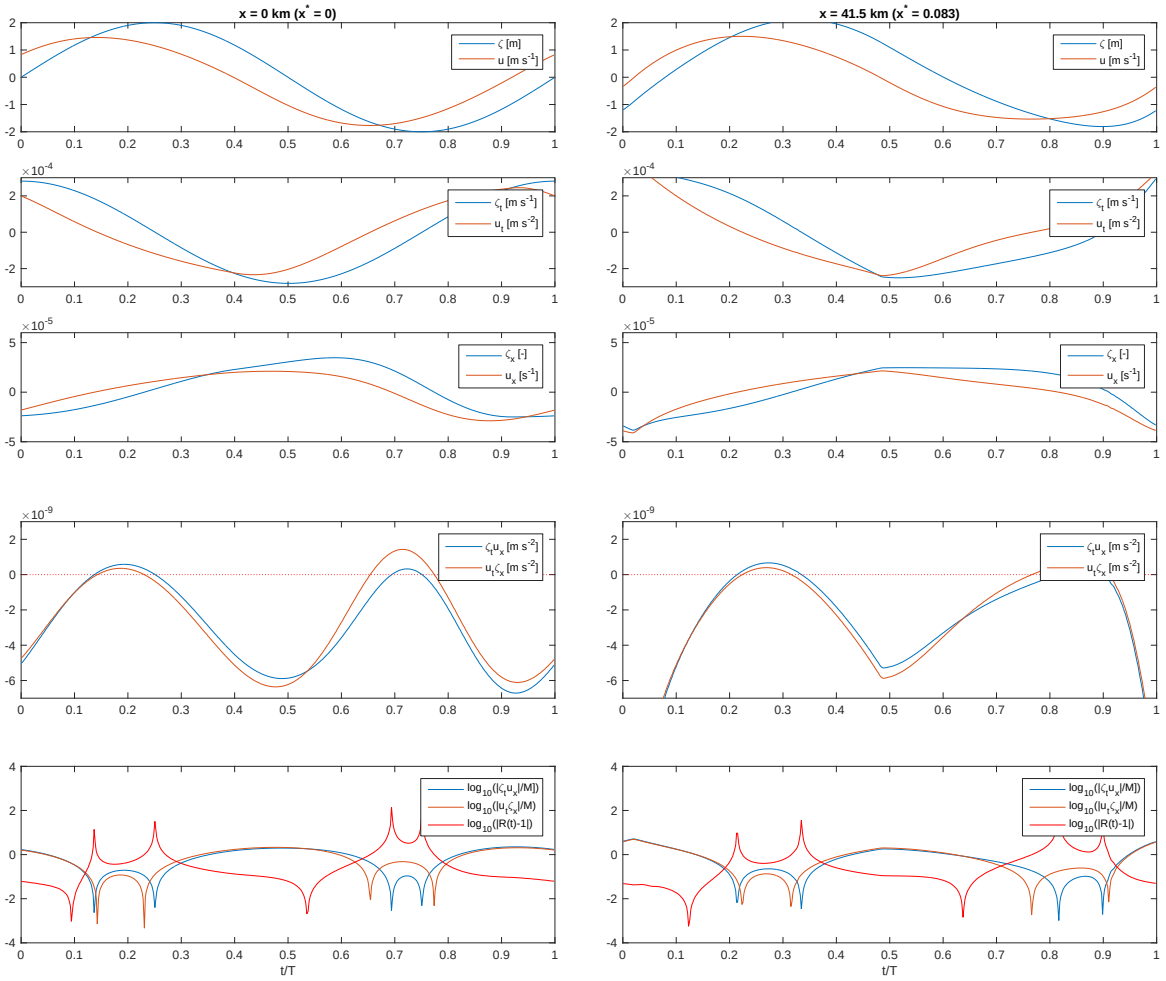

Figure 3: Temporal variation of ζ and u (first plot), ζ_t and u_t (second plot), ζ_x and u_x (third plot), $\zeta_t\, u_x$ and $u_t\, \zeta_x$ (fourth plot), and $\log_{10}(|\zeta_t u_x|/M])$, $\log_{10}(|u_t \zeta_x|/M)$, $\log_{10}(|R(t)-1|)$ (fifth plot, where $R(t) = (u_t \zeta_x)/(\zeta_t u_x)$ and M is the mean of the tidally averages of $|\zeta_t u_x|$ and $|u_t \zeta_x|$), in $x = 0$ km and $x = 41.5$ km.

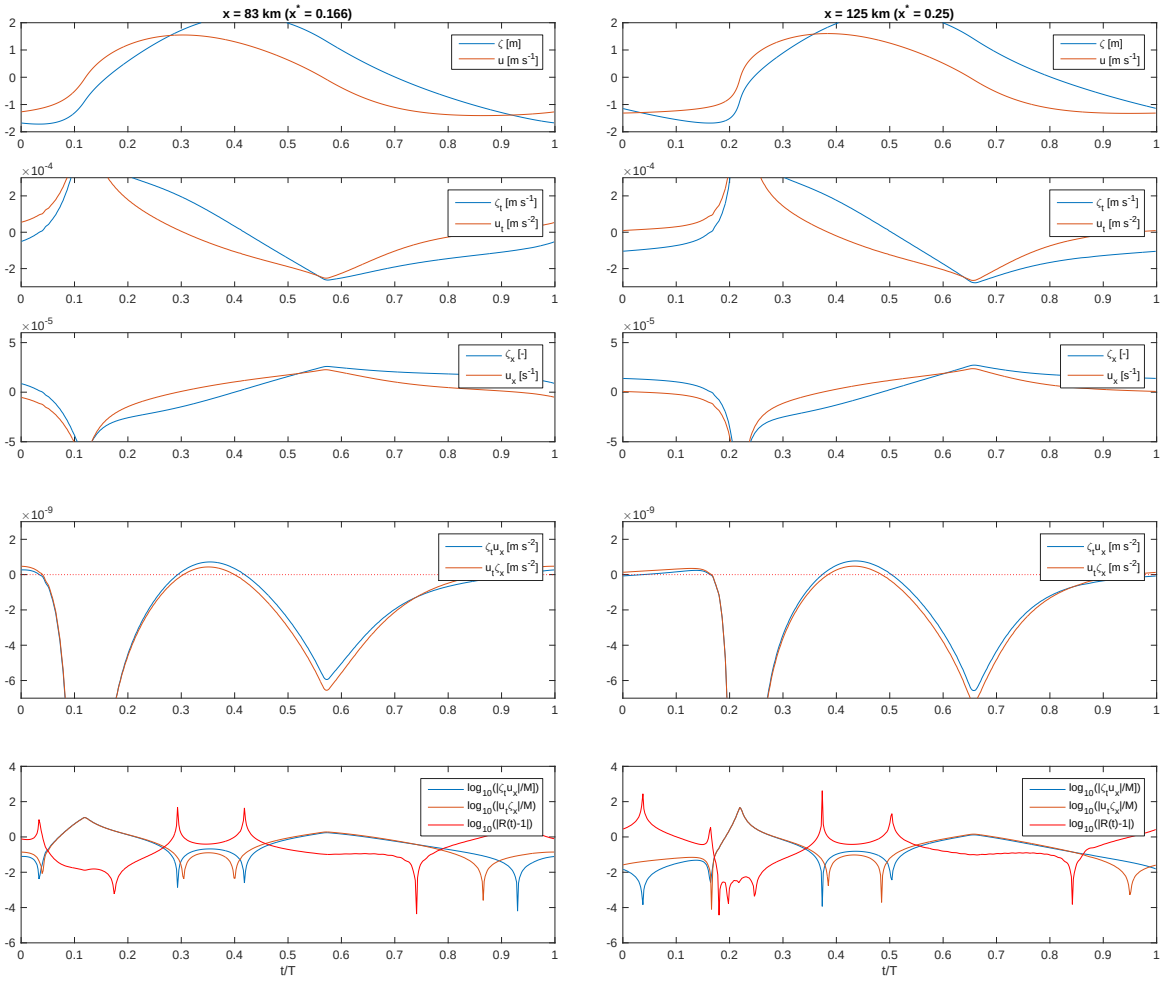

Figure 4: Temporal variation of ζ and u (first plot), ζ_t and u_t (second plot), ζ_x and u_x (third plot), $\zeta_t\, u_x$ and $u_t\, \zeta_x$ (fourth plot), and $\log_{10}(|\zeta_t u_x|/M])$, $\log_{10}(|u_t \zeta_x|/M)$, $\log_{10}(|R(t)-1|)$ (fifth plot, where $R(t) = (u_t \zeta_x)/(\zeta_t u_x)$ and M is the mean of the tidally averages of $|\zeta_t u_x|$ and $|u_t \zeta_x|$), in $x = 83$ km and $x = 125$ km.

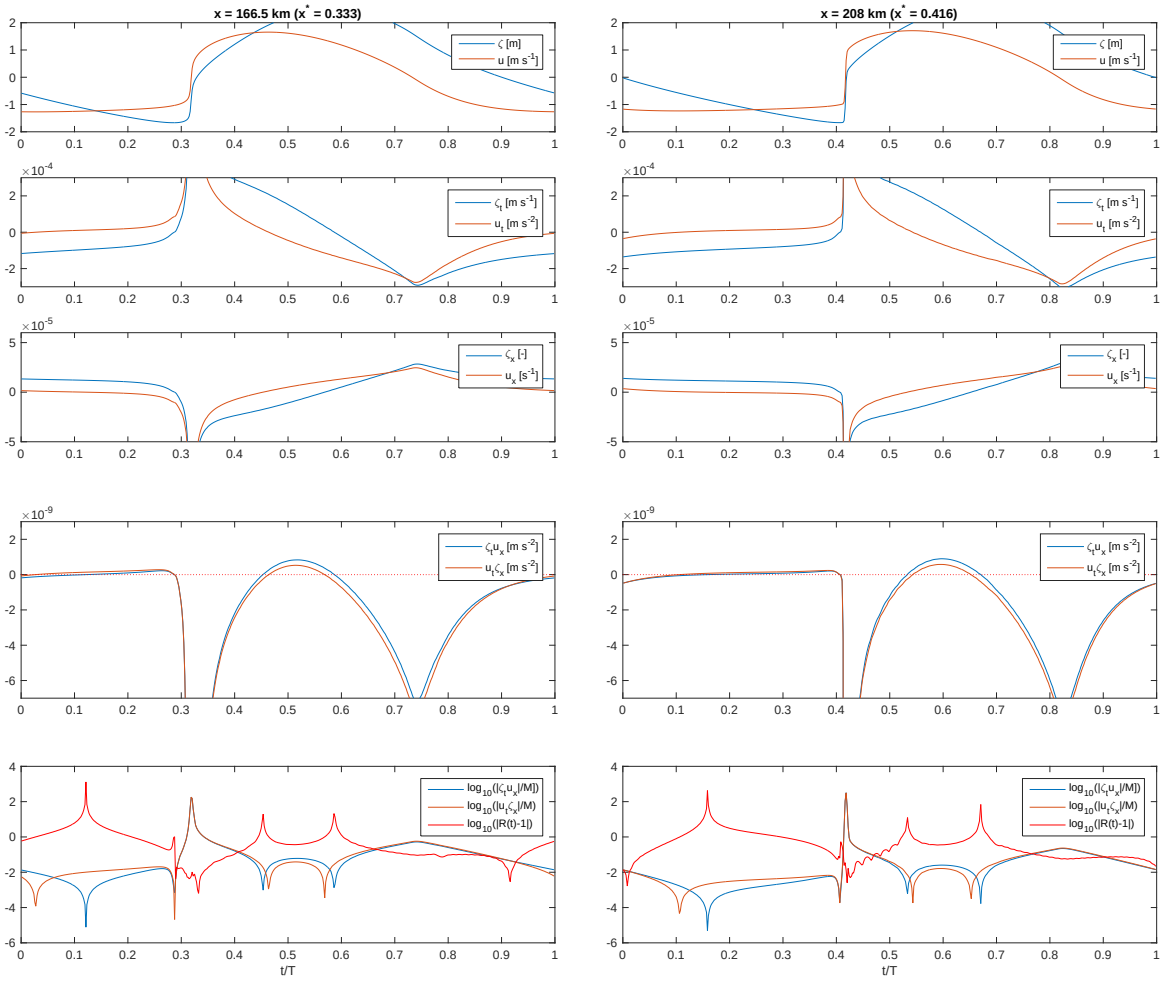

Figure 5: Temporal variation of ζ and u (first plot), ζ_t and u_t (second plot), ζ_x and u_x (third plot), $\zeta_t\, u_x$ and $u_t\, \zeta_x$ (fourth plot), and $\log_{10}(|\zeta_t u_x|/M])$, $\log_{10}(|u_t \zeta_x|/M)$, $\log_{10}(|R(t)-1|)$ (fifth plot, where $R(t) = (u_t \zeta_x)/(\zeta_t u_x)$ and M is the mean of the tidally averages of $|\zeta_t u_x|$ and $|u_t \zeta_x|$), in $x = 166.5$ km and $x = 208$ km.

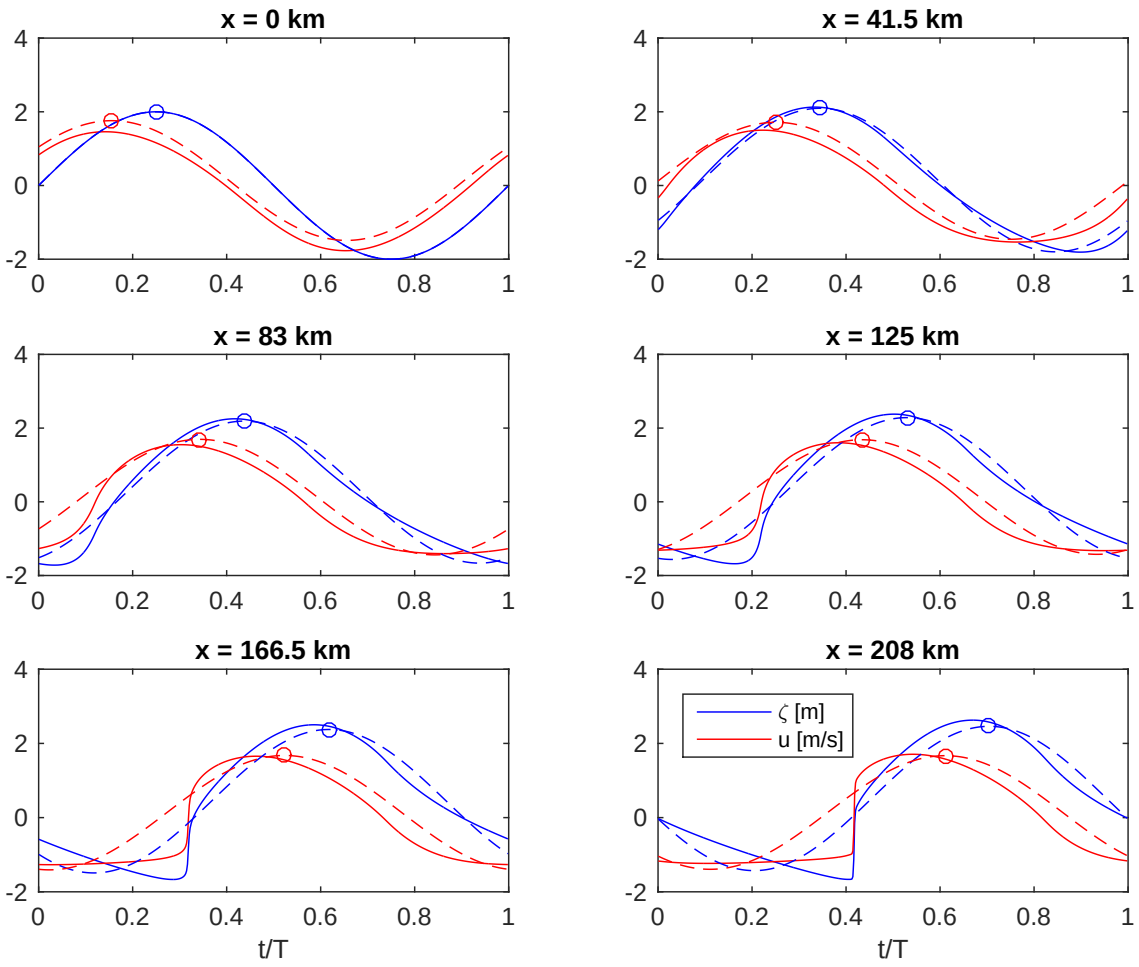

Figure 6: Tidal waves and Fourier series truncated at the first harmonic. Circles indicate the maxima of the dominant tidal component, from which it is possible to detect the phase lag u-ζ.

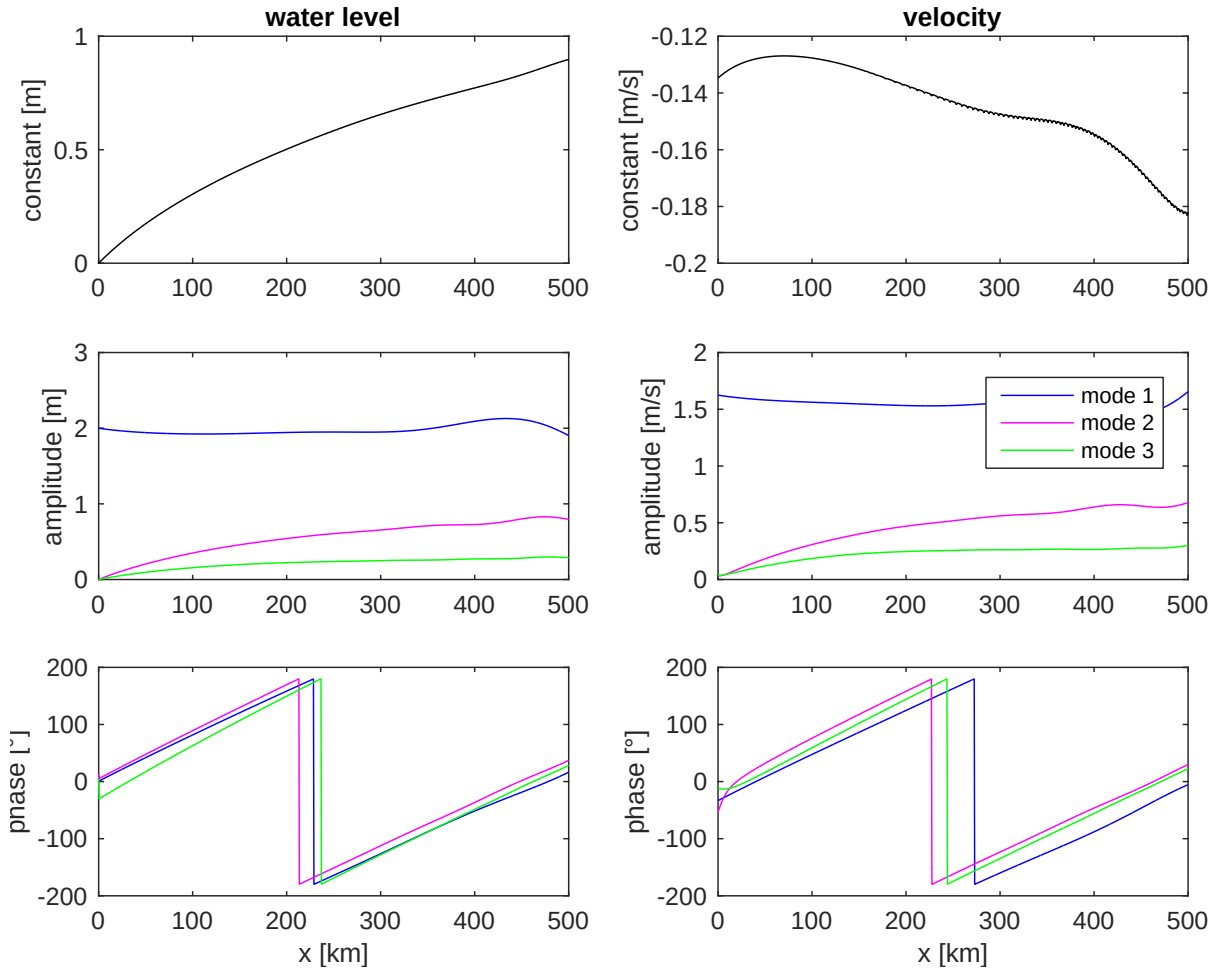

Figure 7: Fourier analysis of tidal wave. From top to bottom: constant term, amplitudes, phases of first three modes. Left column: water level ζ; right column: velocity u.

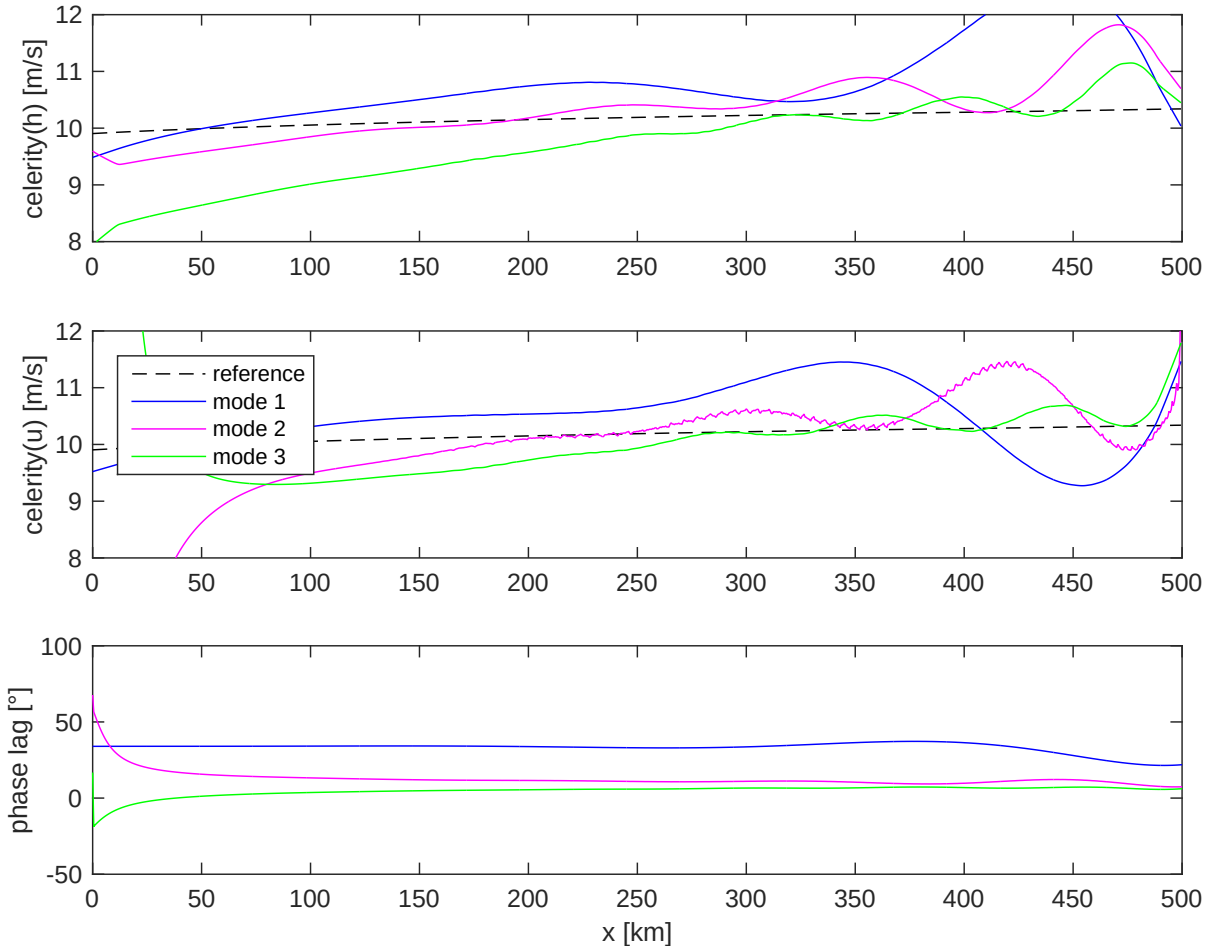

Figure 8: Wave celerity for water level ζ, for velocity u, phase lag u-ζ. Colors refer to the first three modes; black dashed line to wave celerity in a frictionless prismatic channel.

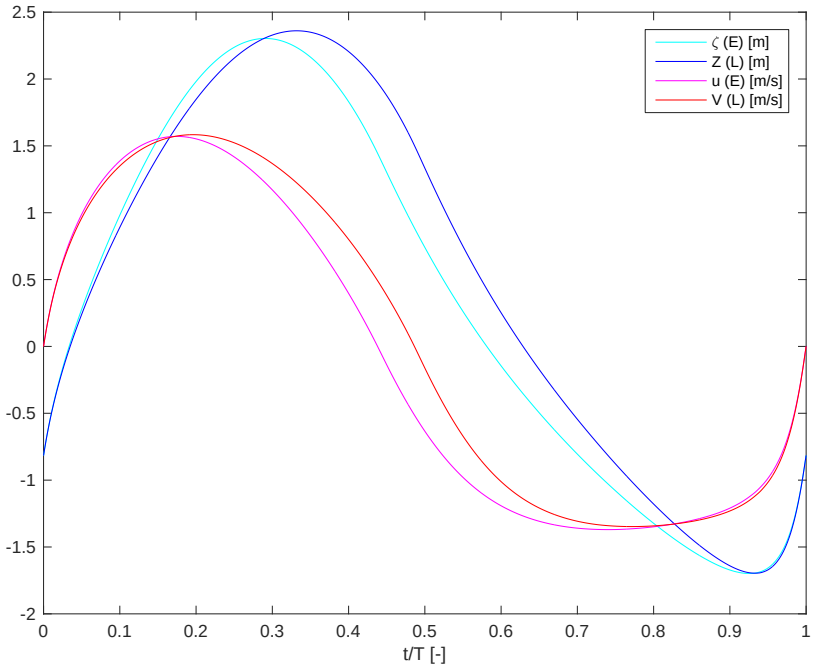

Figure 9: Lagrangean water level Z and velocity V compared with Eulerian values ζ and u in $x = 100$ km.

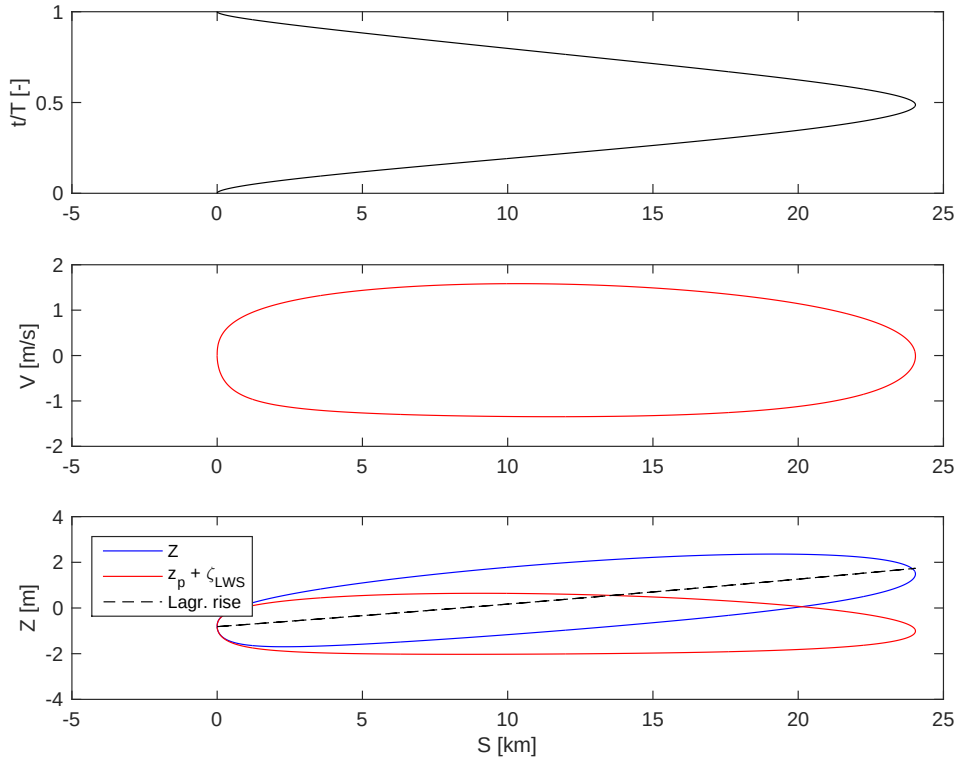

Figure 10: Lagrangean displacement S in time (first plot) and ellipses V-S (second plot) and Z-S (third plot).

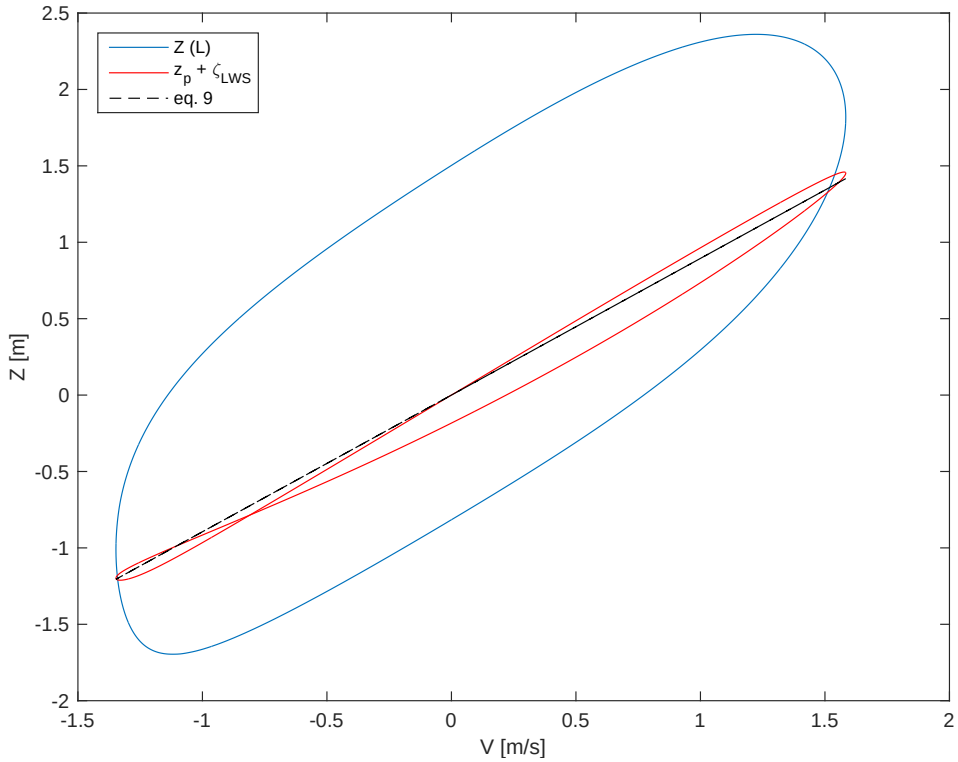

Figure 11: Lagrangean water level against velocity V: Z is the actual value, $z_p + \zeta_{LWS}$ is the transformed water level. Black dashed lines: equation (9).

Variant 5

Length $b = 100$ km (exponential variation); Strickler coefficient $K = 45$ m$^{1/3}$s^{-1}; linear friction.

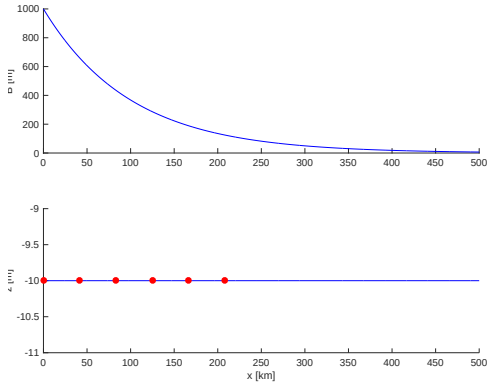

Figure 1: Longitudinal profiles of width and bottom. Dots indicates the locations where the temporal behaviour is shown in figure 3.

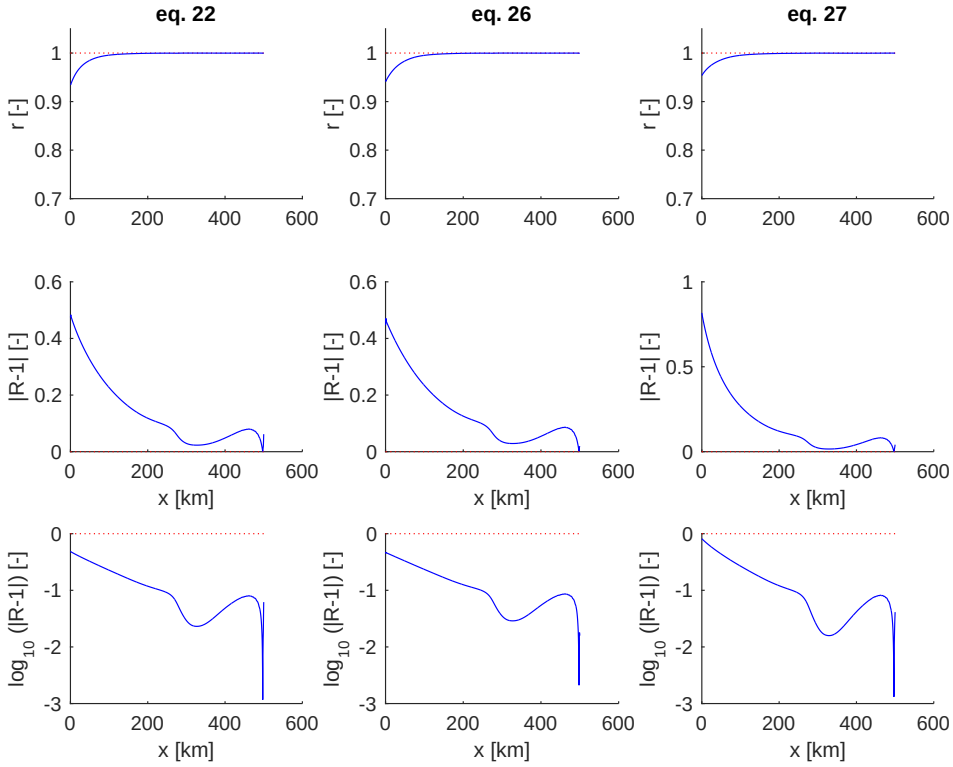

Figure 2: Longitudinal variation of the correlation coefficient r (first row) and of the two different functions of the ratio R between right hand side and left hand side of equations 22, 26 and 27 in the manuscript, respectively $|R-1|$ and $\log_{10}(|R-1|)$.

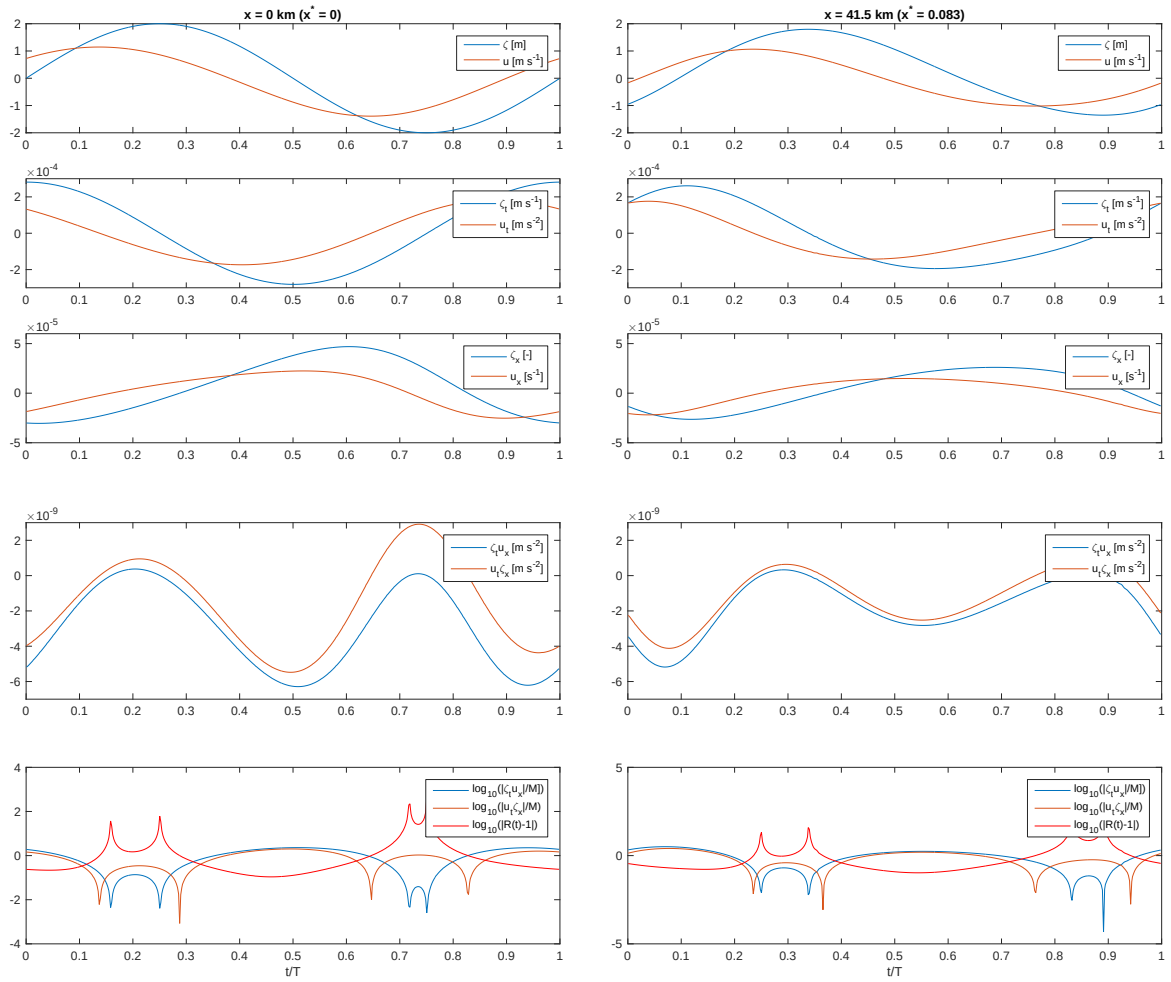

Figure 3: Temporal variation of ζ and u (first plot), ζ_t and u_t (second plot), ζ_x and u_x (third plot), $\zeta_t\, u_x$ and $u_t\, \zeta_x$ (fourth plot), and $\log_{10}(|\zeta_t u_x|/M])$, $\log_{10}(|u_t \zeta_x|/M)$, $\log_{10}(|R(t)-1|)$ (fifth plot, where $R(t) = (u_t \zeta_x)/(\zeta_t u_x)$ and M is the mean of the tidally averages of $|\zeta_t u_x|$ and $|u_t \zeta_x|$), in $x = 0$ km and $x = 41.5$ km.

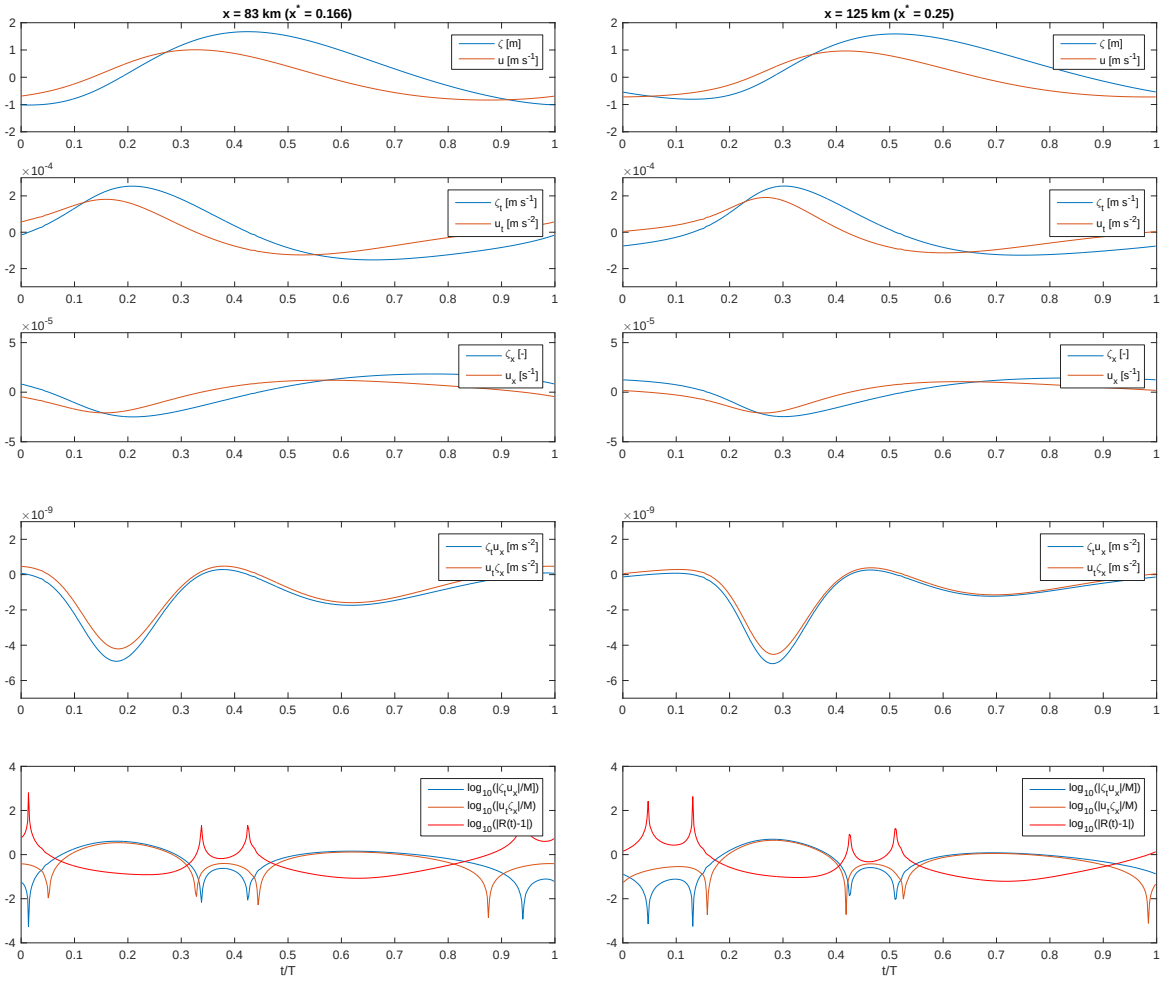

Figure 4: Temporal variation of ζ and u (first plot), ζ_t and u_t (second plot), ζ_x and u_x (third plot), $\zeta_t\, u_x$ and $u_t\, \zeta_x$ (fourth plot), and $\log_{10}(|\zeta_t u_x|/M])$, $\log_{10}(|u_t \zeta_x|/M)$, $\log_{10}(|R(t)-1|)$ (fifth plot, where $R(t) = (u_t \zeta_x)/(\zeta_t u_x)$ and M is the mean of the tidally averages of $|\zeta_t u_x|$ and $|u_t \zeta_x|$), in $x = 83$ km and $x = 125$ km.

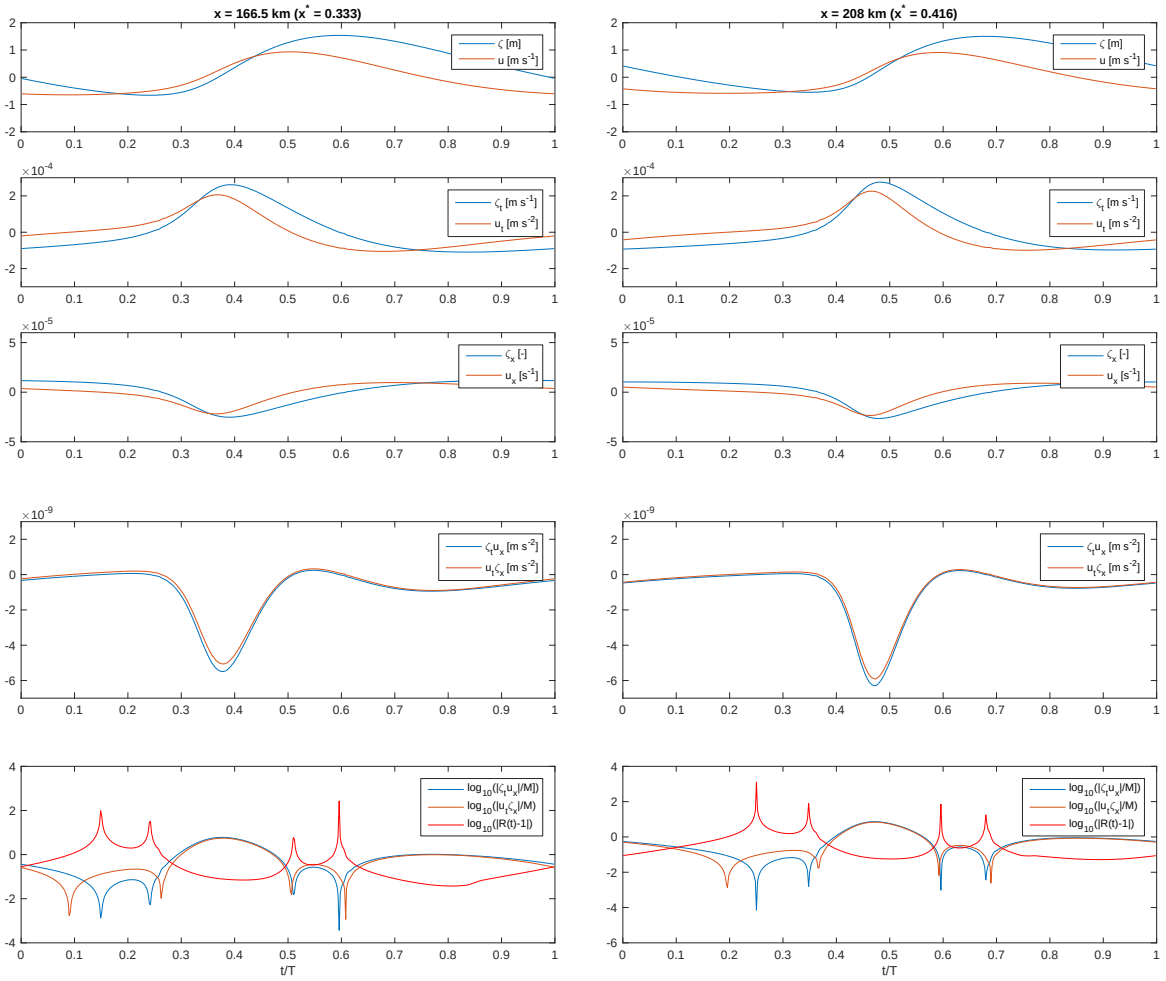

Figure 5: Temporal variation of ζ and u (first plot), ζ_t and u_t (second plot), ζ_x and u_x (third plot), $\zeta_t\, u_x$ and $u_t\, \zeta_x$ (fourth plot), and $\log_{10}(|\zeta_t u_x|/M])$, $\log_{10}(|u_t \zeta_x|/M)$, $\log_{10}(|R(t)-1|)$ (fifth plot, where $R(t) = (u_t\zeta_x)/(\zeta_t u_x)$ and M is the mean of the tidally averages of $|\zeta_t u_x|$ and $|u_t \zeta_x|$), in $x = 166.5$ km and $x = 208$ km.

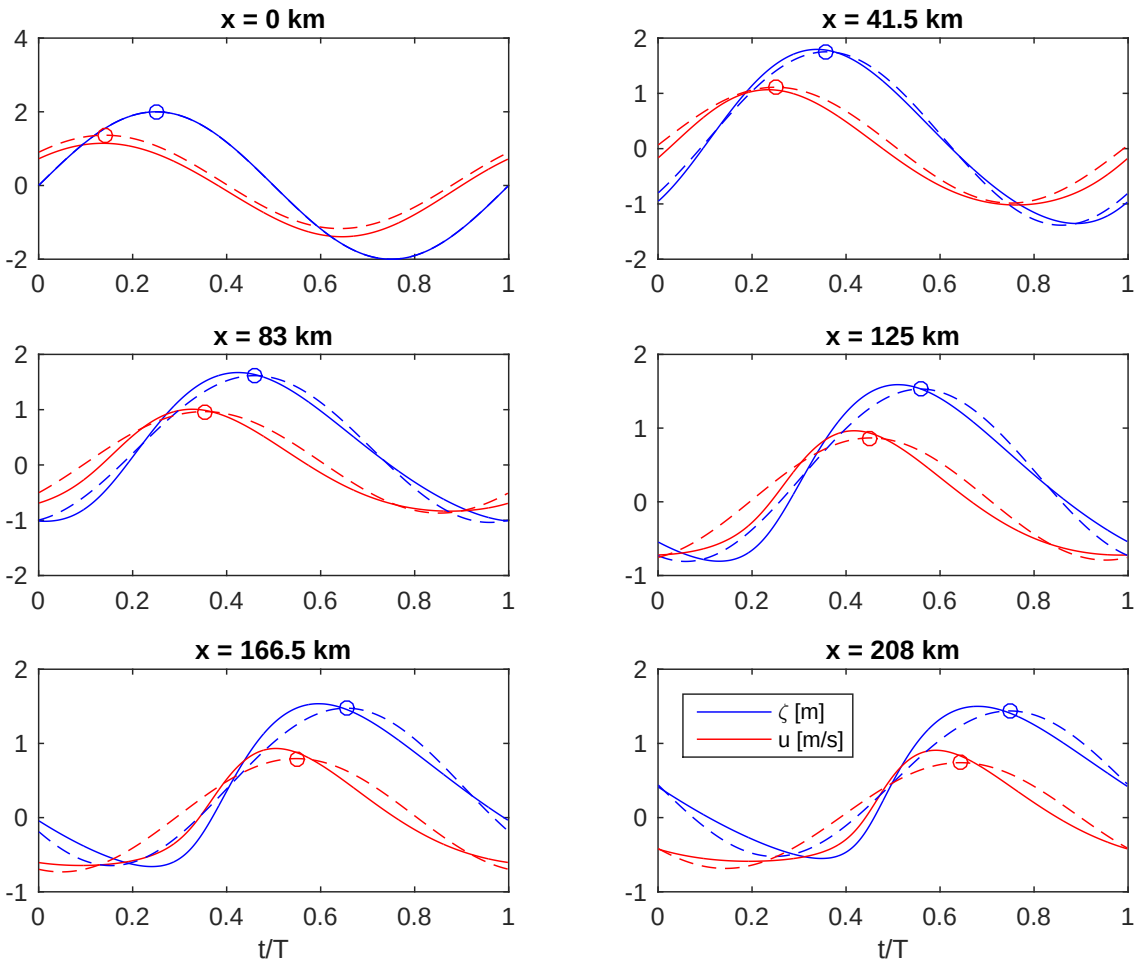

Figure 6: Tidal waves and Fourier series truncated at the first harmonic. Circles indicate the maxima of the dominant tidal component, from which it is possible to detect the phase lag u-ζ.

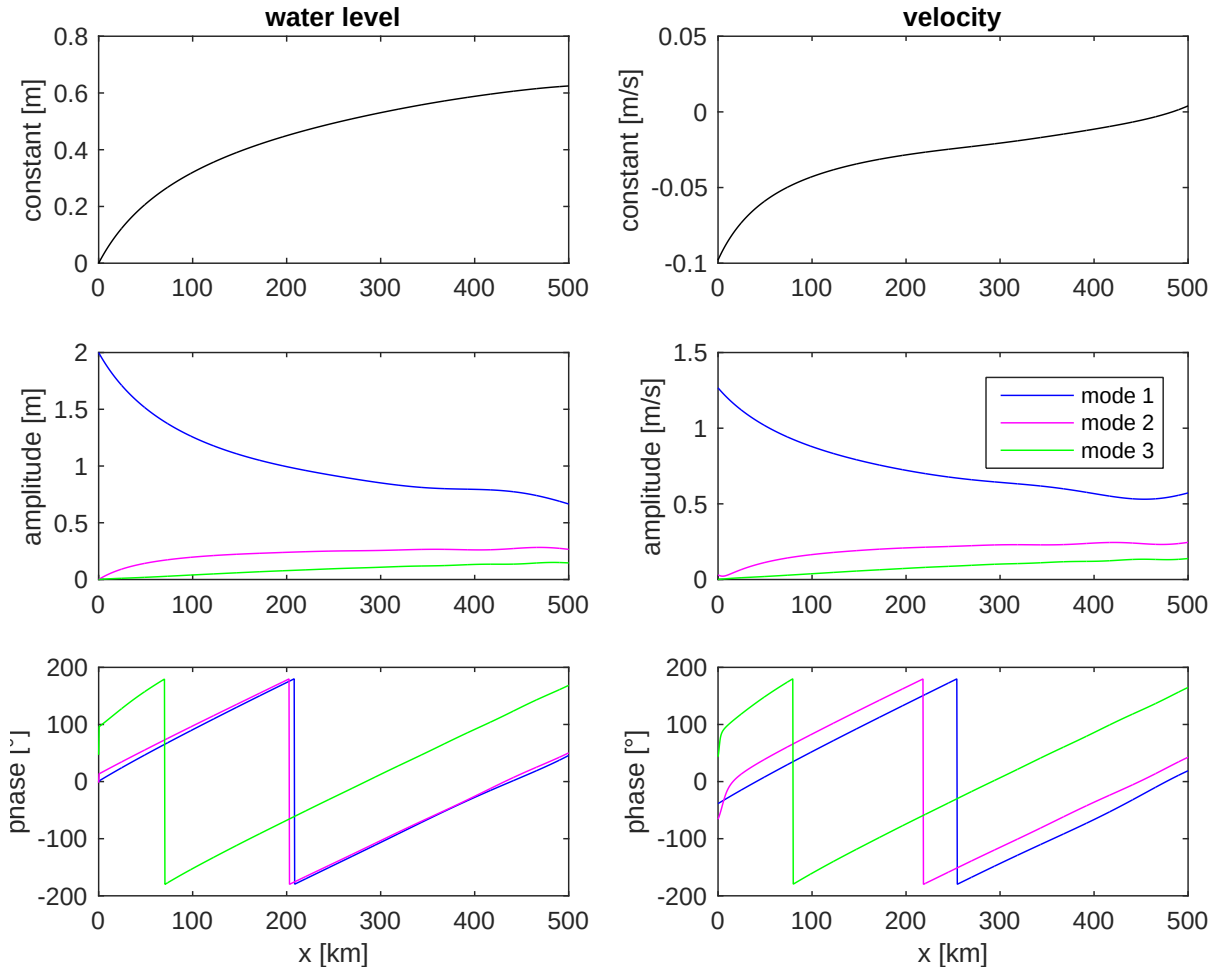

Figure 7: Fourier analysis of tidal wave. From top to bottom: constant term, amplitudes, phases of first three modes. Left column: water level ζ; right column: velocity u.

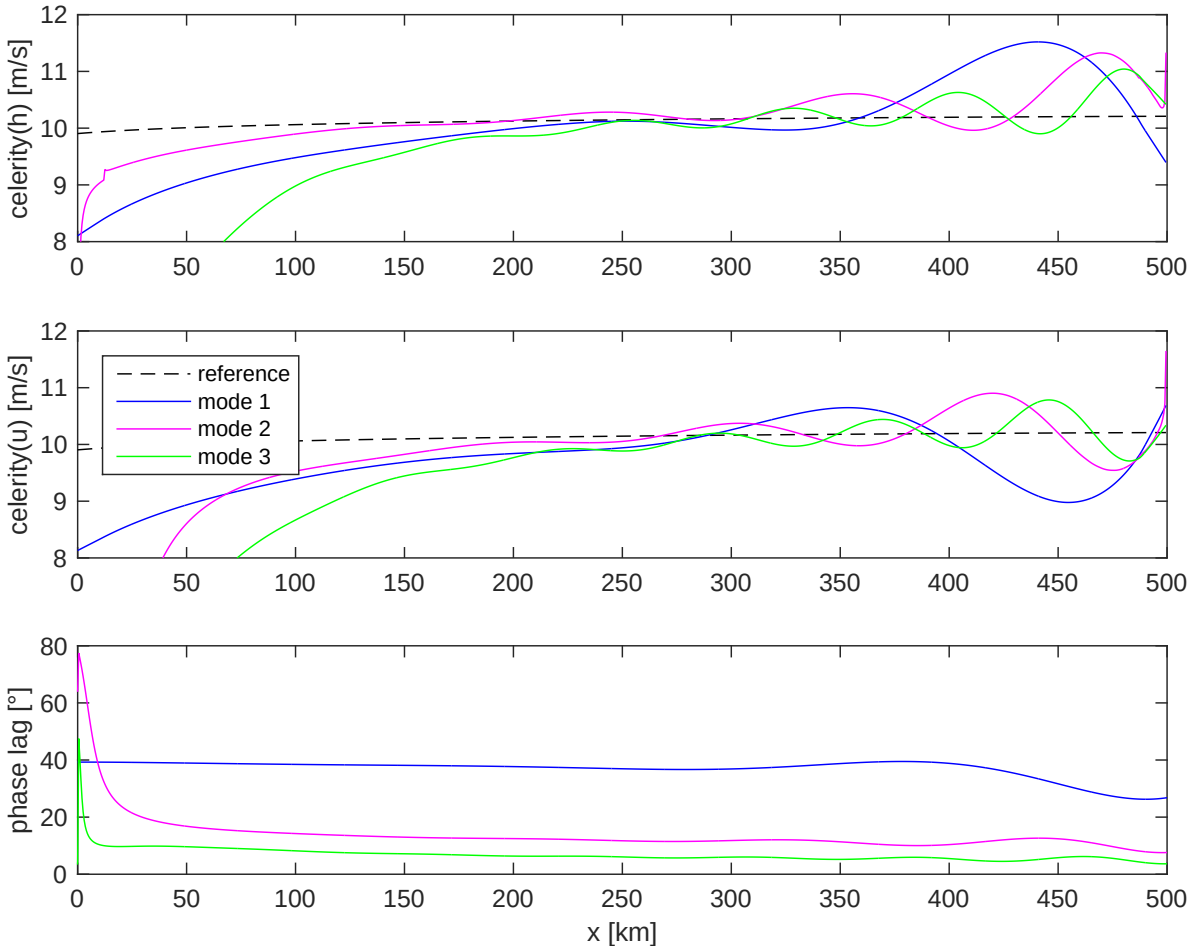

Figure 8: Wave celerity for water level ζ, for velocity u, phase lag u-ζ. Colors refer to the first three modes; black dashed line to wave celerity in a frictionless prismatic channel.

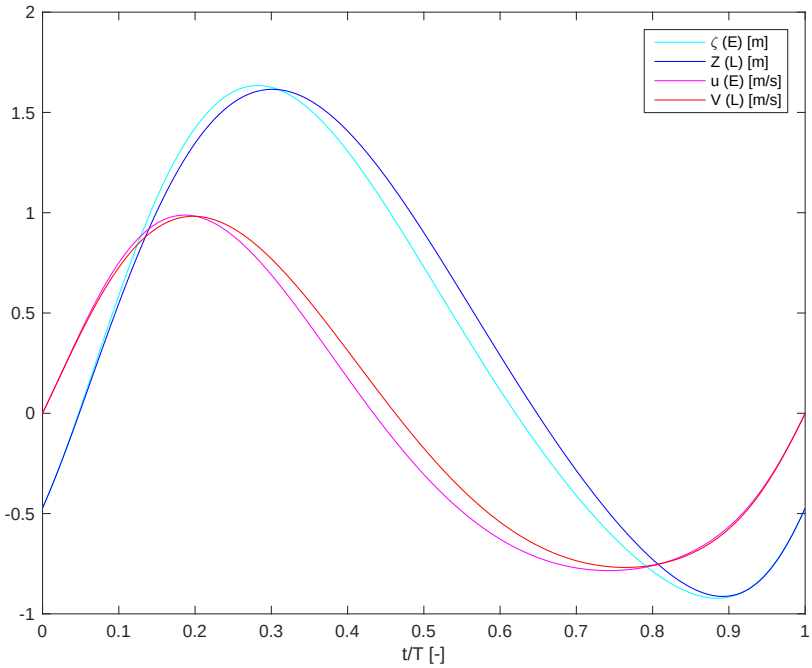

Figure 9: Lagrangean water level Z and velocity V compared with Eulerian values ζ and u in $x = 100$ km.

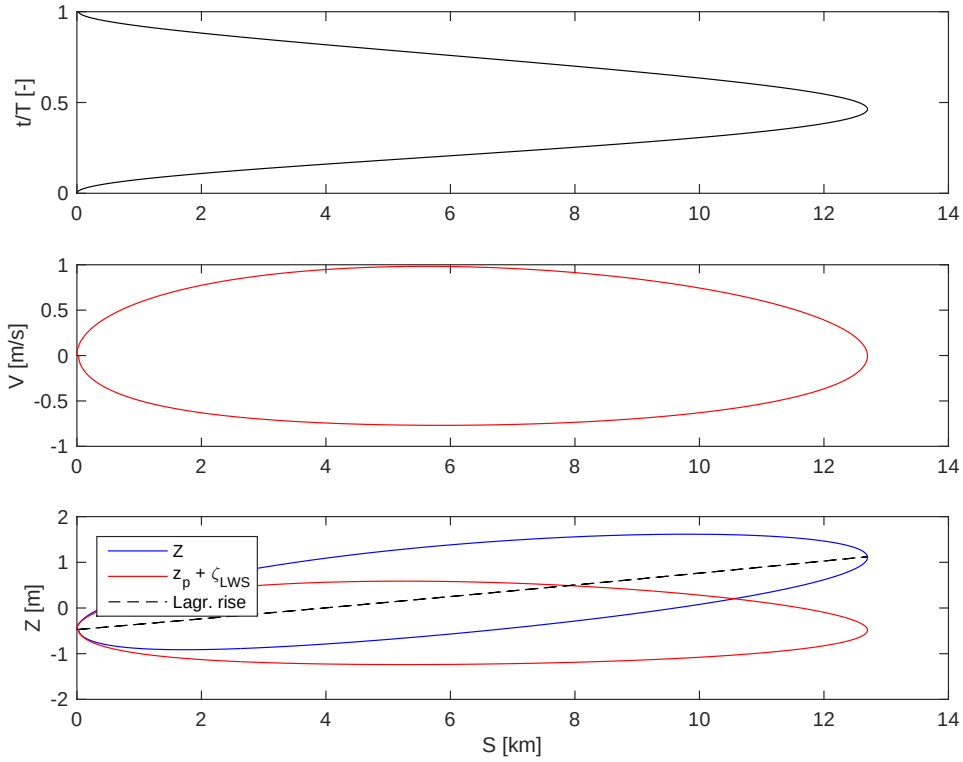

Figure 10: Lagrangean displacement S in time (first plot) and ellipses V-S (second plot) and Z-S (third plot).

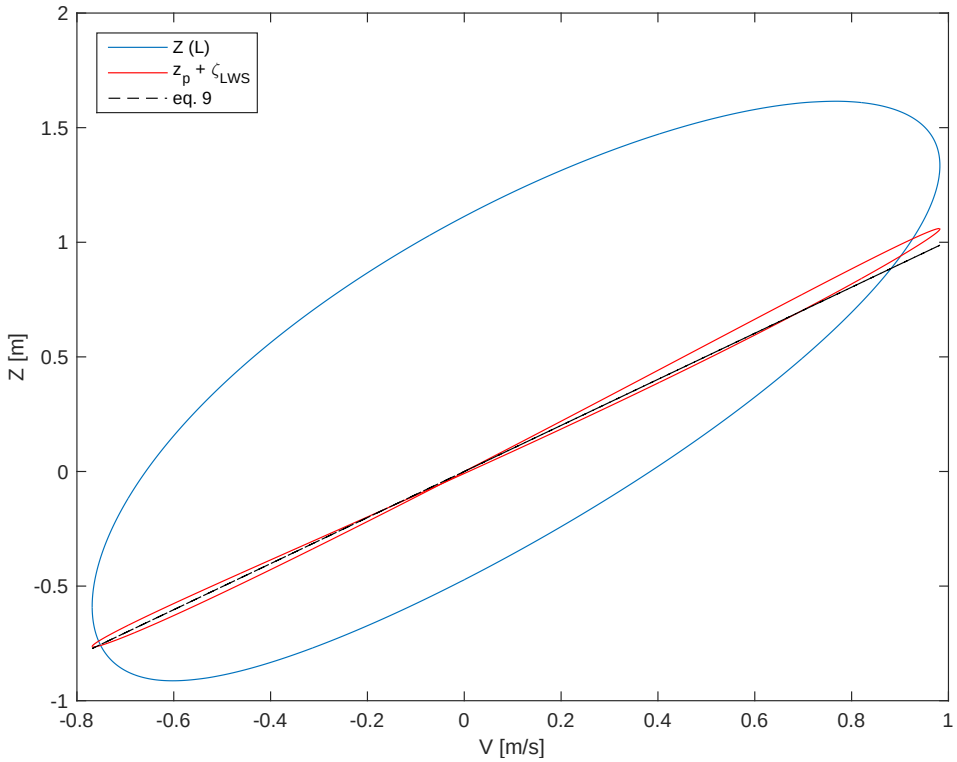

Figure 11: Lagrangean water level against velocity V: Z is the actual value, $z_p + \zeta_{LWS}$ is the transformed water level. Black dashed lines: equation (9).

Variant 6

Length $b = 25$ km (exponential variation); Strickler coefficient $K = 45$ m$^{1/3}$s^{-1}; nonlinear friction; asymptotic width $B_\infty = 10$ m.

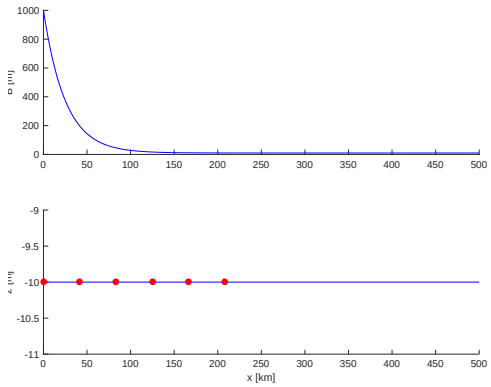

Figure 1: Longitudinal profiles of width and bottom. Dots indicates the locations where the temporal behaviour is shown in figure 3.

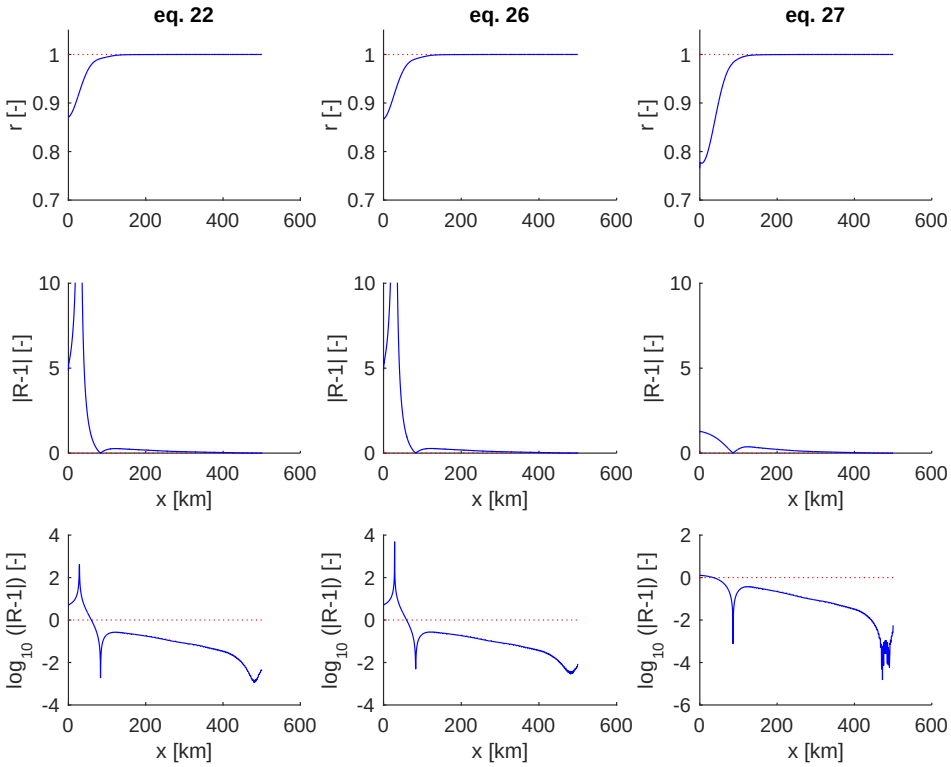

Figure 2: Longitudinal variation of the correlation coefficient r (first row) and of the two different functions of the ratio R between right hand side and left hand side of equations 22, 26 and 27 in the manuscript, respectively $|R-1|$ and $\log_{10}(|R-1|)$.

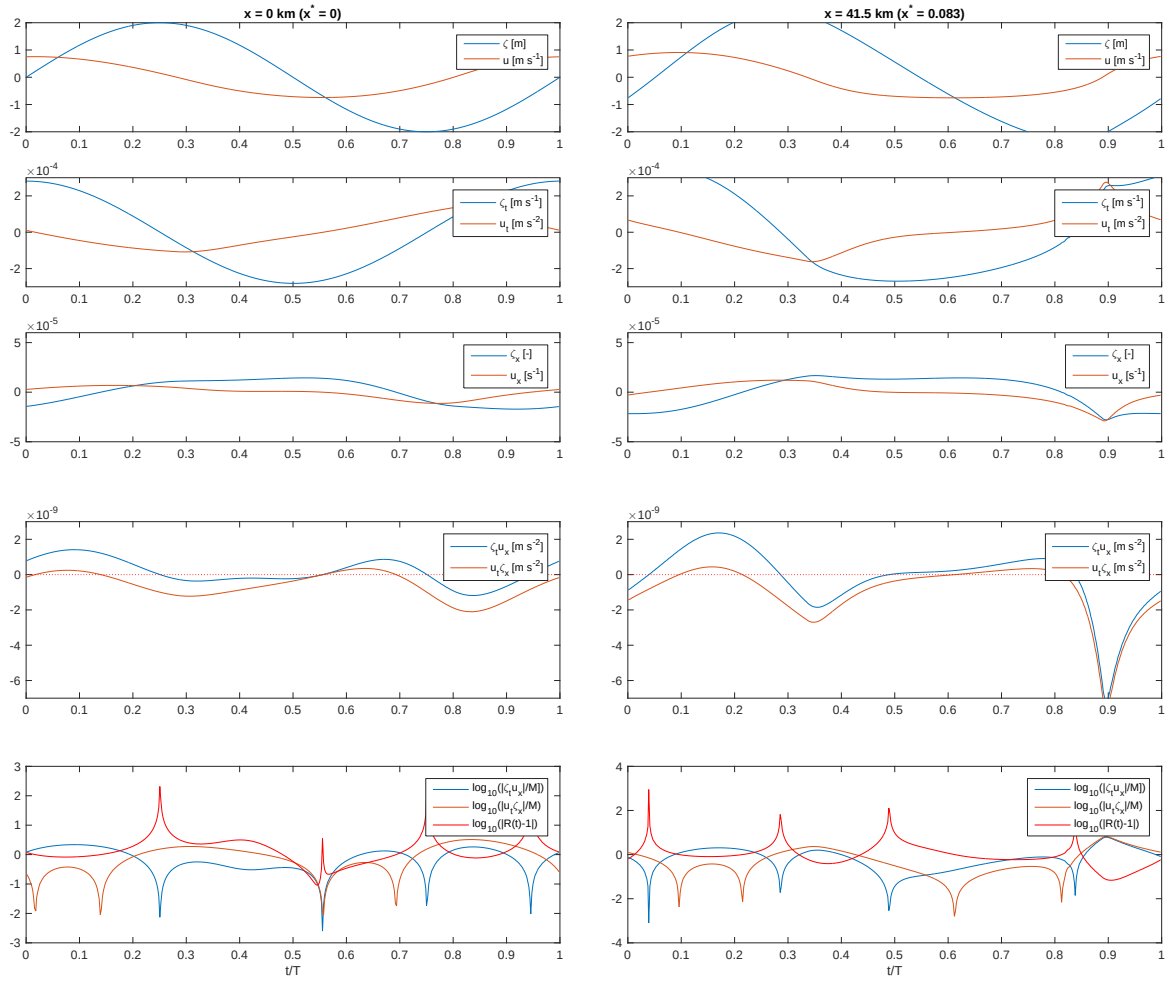

Figure 3: Temporal variation of ζ and u (first plot), ζ_t and u_t (second plot), ζ_x and u_x (third plot), $\zeta_t\, u_x$ and $u_t\, \zeta_x$ (fourth plot), and $\log_{10}(|\zeta_t u_x|/M])$, $\log_{10}(|u_t \zeta_x|/M)$, $\log_{10}(|R(t)-1|)$ (fifth plot, where $R(t) = (u_t \zeta_x)/(\zeta_t u_x)$ and M is the mean of the tidally averages of $|\zeta_t u_x|$ and $|u_t \zeta_x|$), in $x = 0$ km and $x = 41.5$ km.

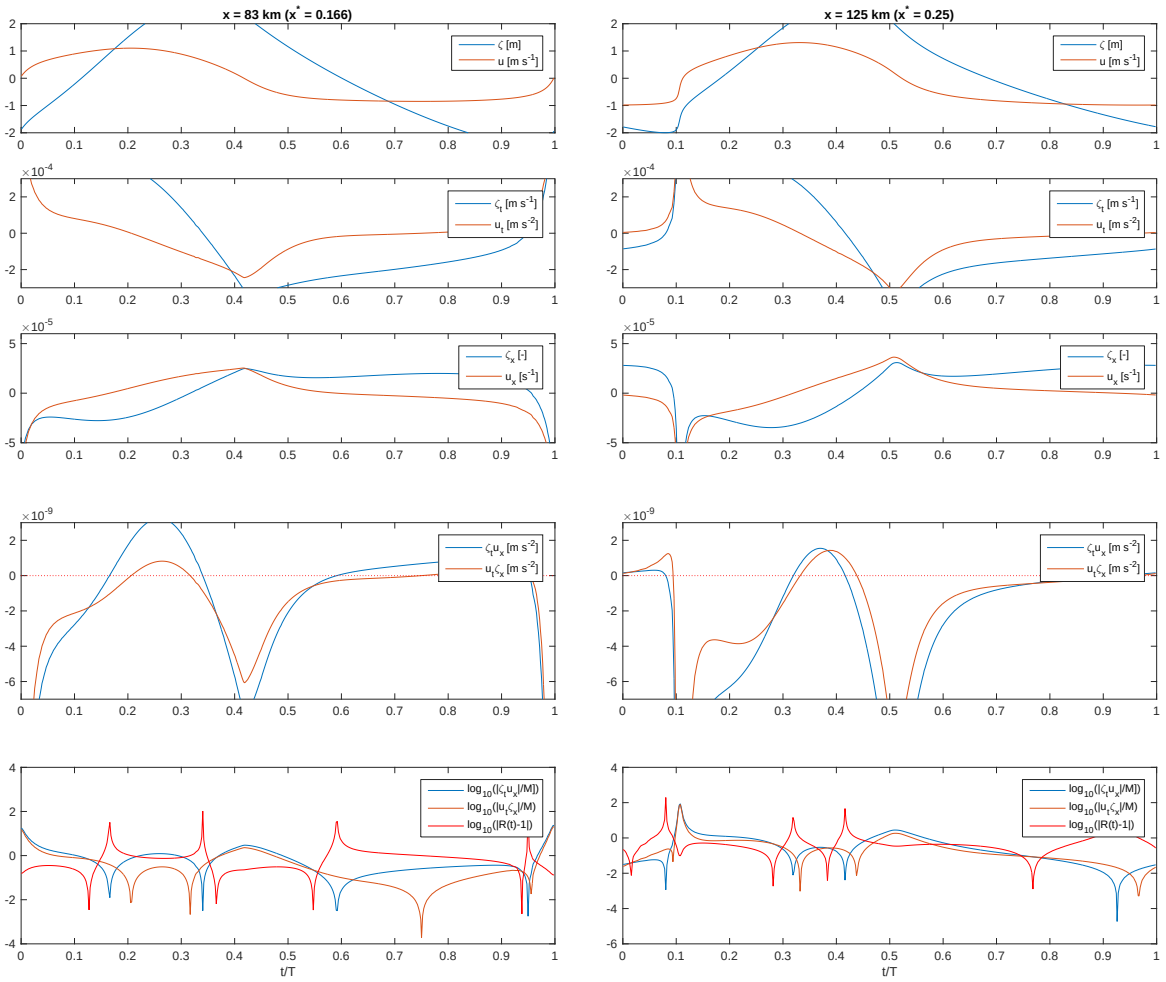

Figure 4: Temporal variation of ζ and u (first plot), ζ_t and u_t (second plot), ζ_x and u_x (third plot), $\zeta_t\, u_x$ and $u_t\, \zeta_x$ (fourth plot), and $\log_{10}(|\zeta_t u_x|/M])$, $\log_{10}(|u_t \zeta_x|/M)$, $\log_{10}(|R(t)-1|)$ (fifth plot, where $R(t) = (u_t\zeta_x)/(\zeta_t u_x)$ and M is the mean of the tidally averages of $|\zeta_t u_x|$ and $|u_t \zeta_x|$), in $x = 83$ km and $x = 125$ km.

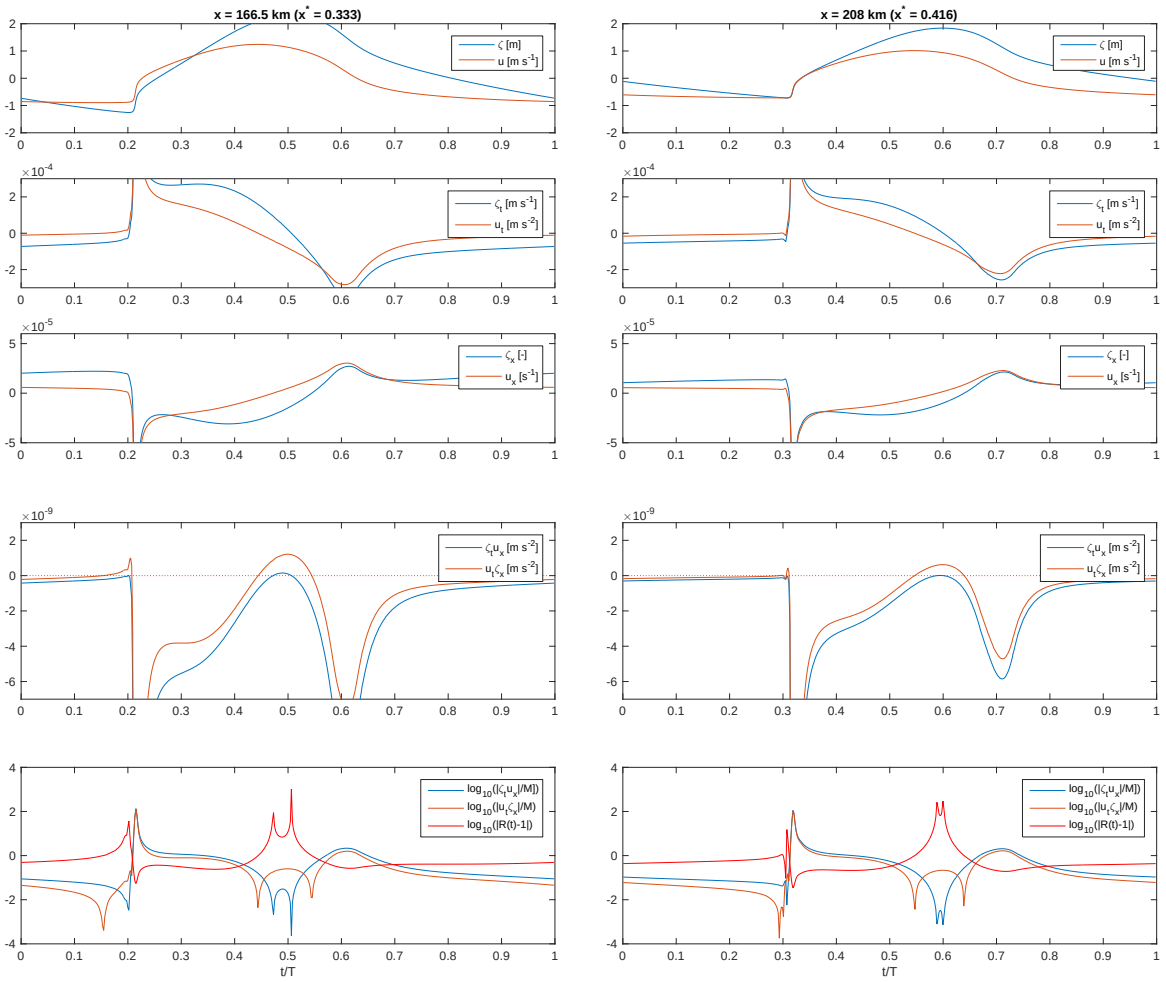

Figure 5: Temporal variation of ζ and u (first plot), ζ_t and u_t (second plot), ζ_x and u_x (third plot), $\zeta_t\, u_x$ and $u_t\, \zeta_x$ (fourth plot), and $\log_{10}(|\zeta_t u_x|/M])$, $\log_{10}(|u_t \zeta_x|/M)$, $\log_{10}(|R(t)-1|)$ (fifth plot, where $R(t) = (u_t\zeta_x)/(\zeta_t u_x)$ and M is the mean of the tidally averages of $|\zeta_t u_x|$ and $|u_t \zeta_x|$), in $x = 166.5$ km and $x = 208$ km.

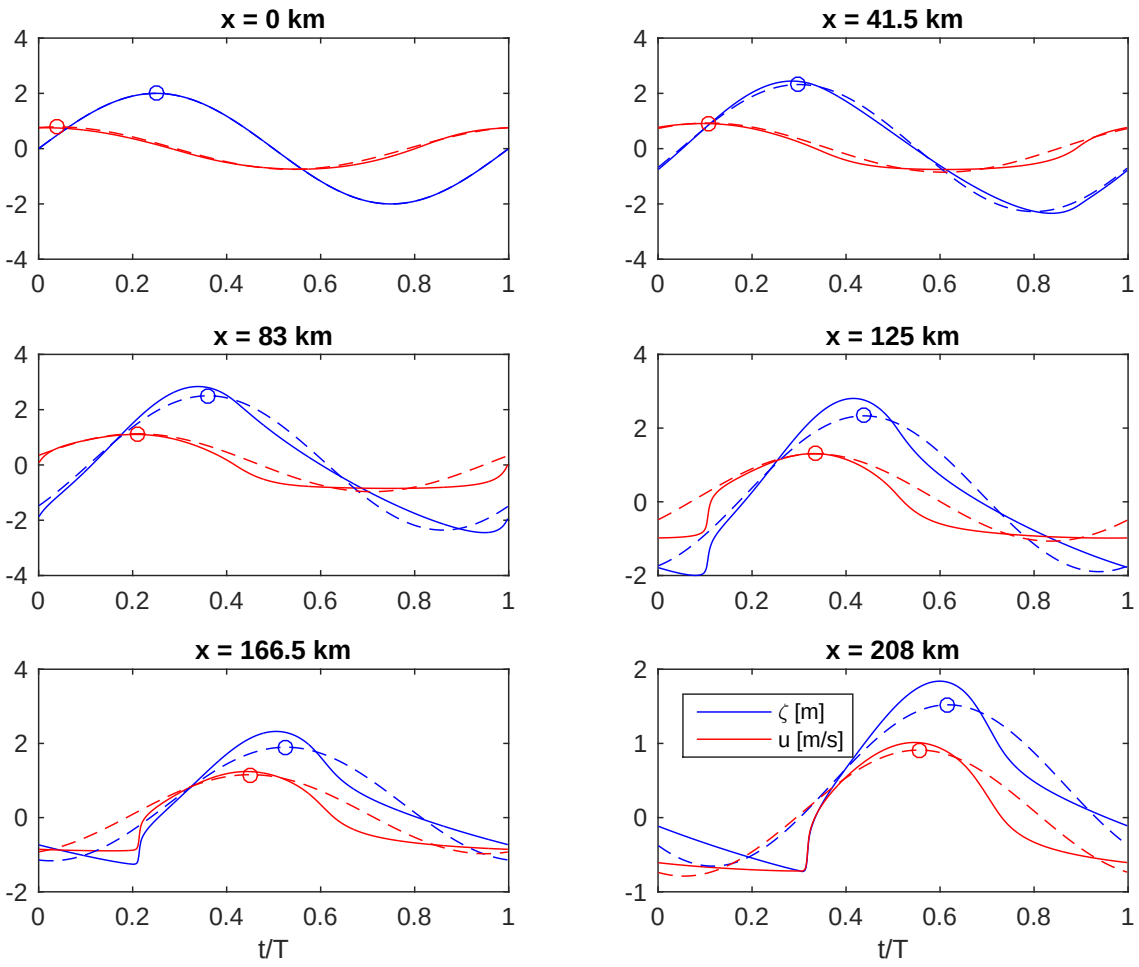

Figure 6: Tidal waves and Fourier series truncated at the first harmonic. Circles indicate the maxima of the dominant tidal component, from which it is possible to detect the phase lag u-ζ.

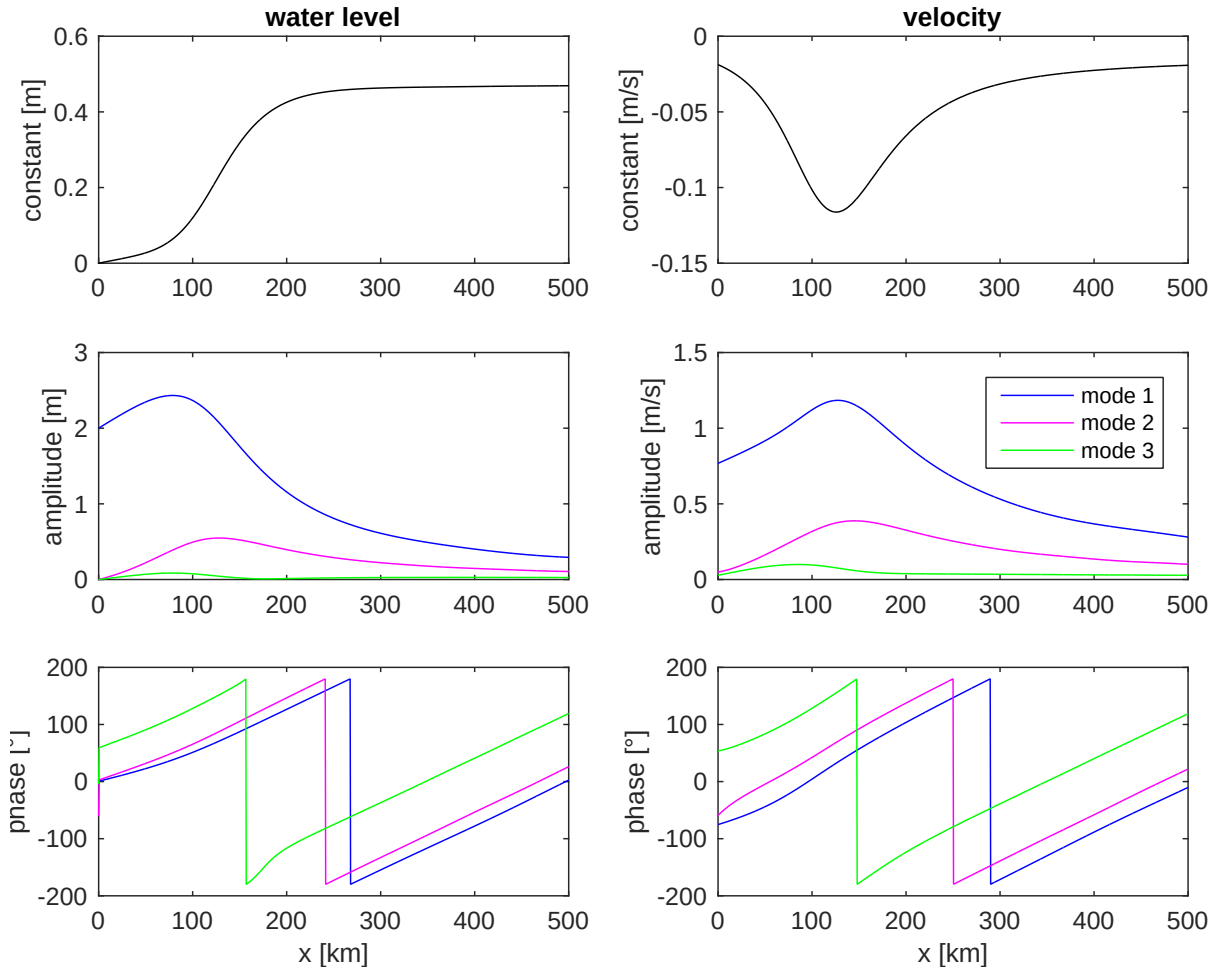

Figure 7: Fourier analysis of tidal wave. From top to bottom: constant term, amplitudes, phases of first three modes. Left column: water level ζ; right column: velocity u.

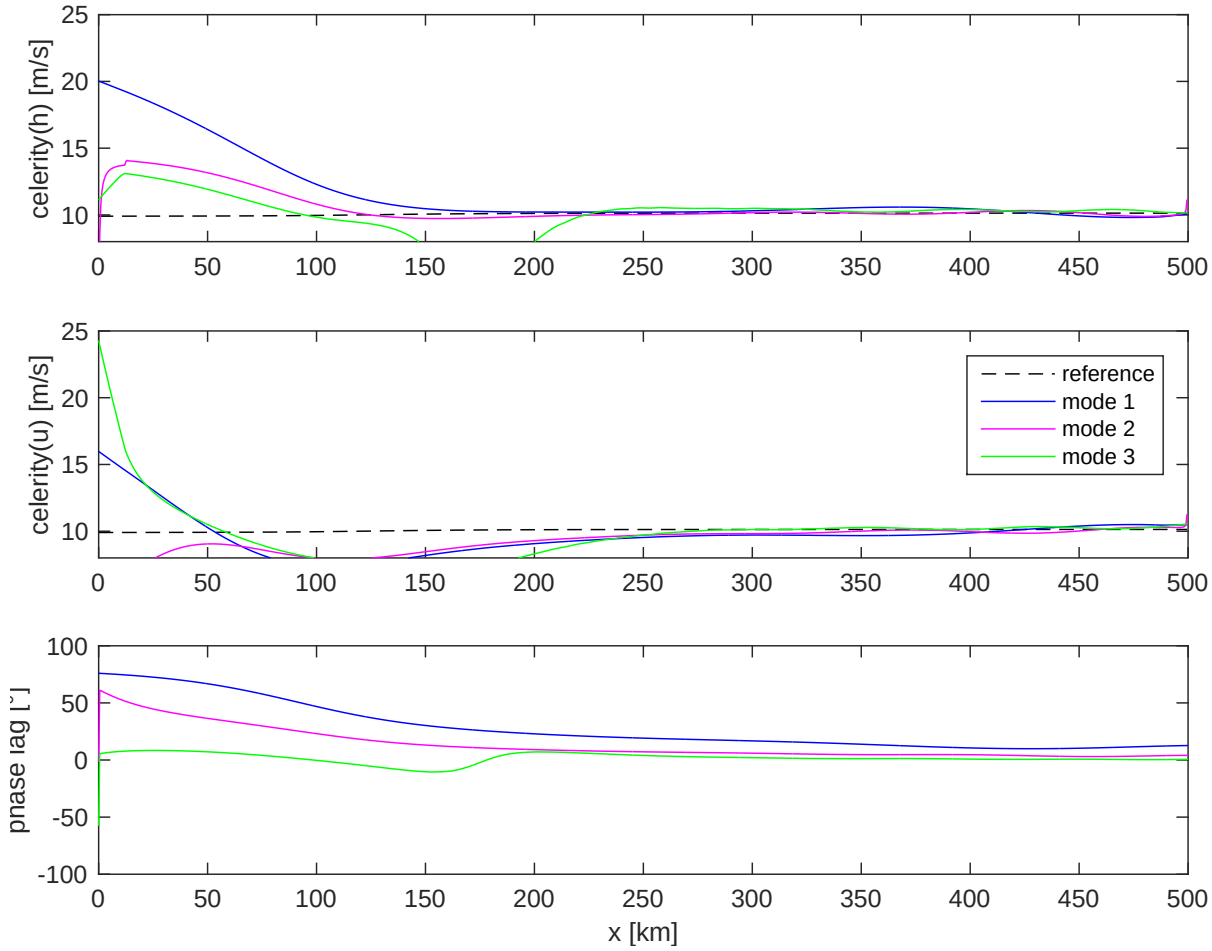

Figure 8: Wave celerity for water level ζ, for velocity u, phase lag u-ζ. Colors refer to the first three modes; black dashed line to wave celerity in a frictionless prismatic channel.

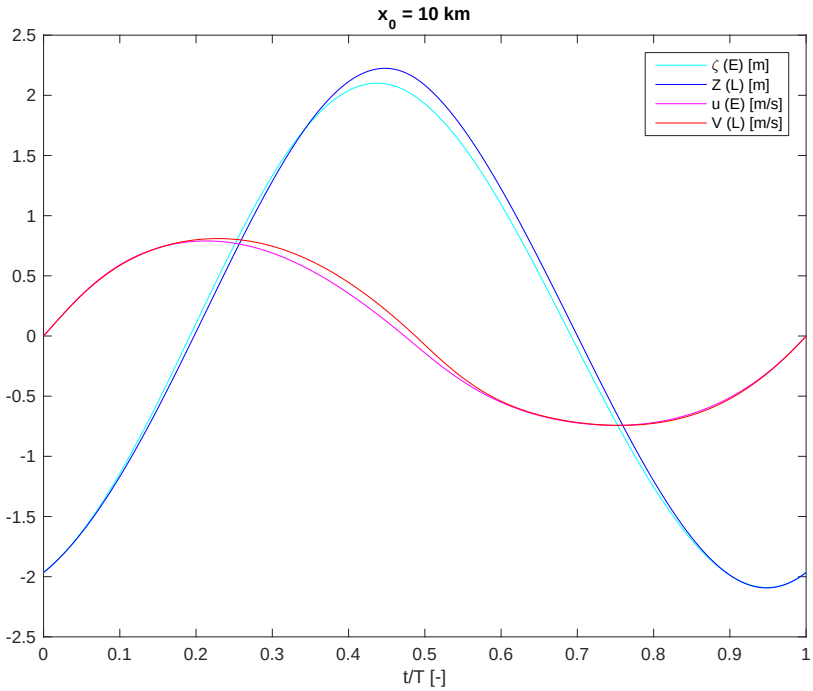

Figure 9: Lagrangean water level Z and velocity V compared with Eulerian values ζ and u, for $x_0 = 10$ km.

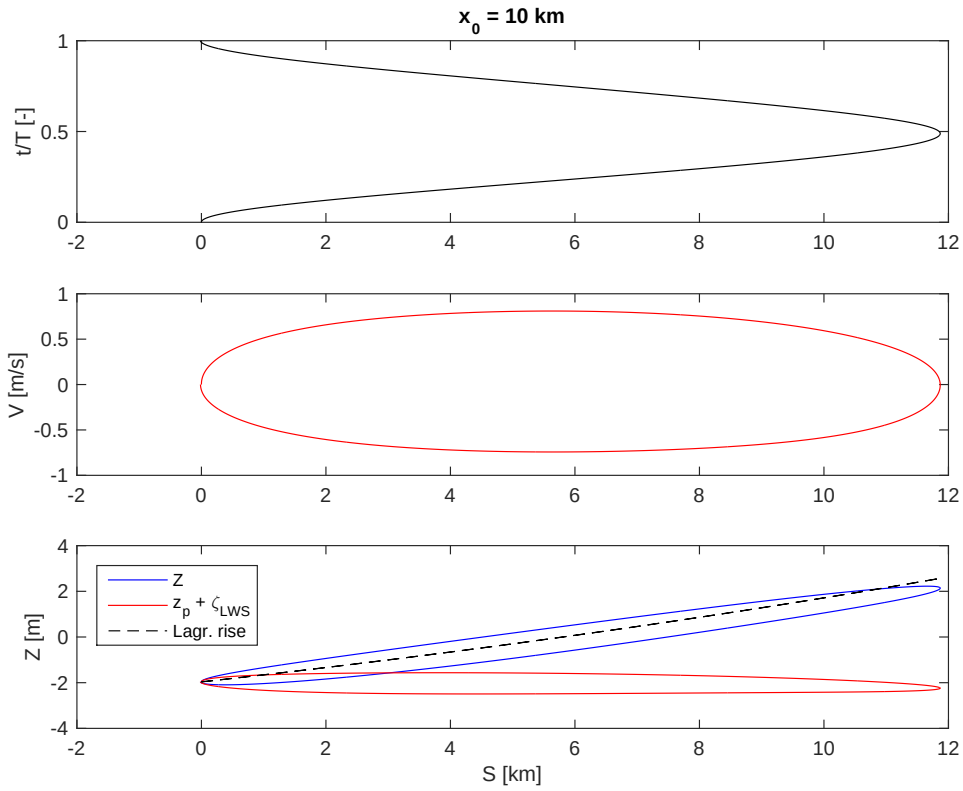

Figure 10: Lagrangean displacement S in time (first plot) and ellipses V-S (second plot) and Z-S (third plot), for $x_0 = 10$ km.

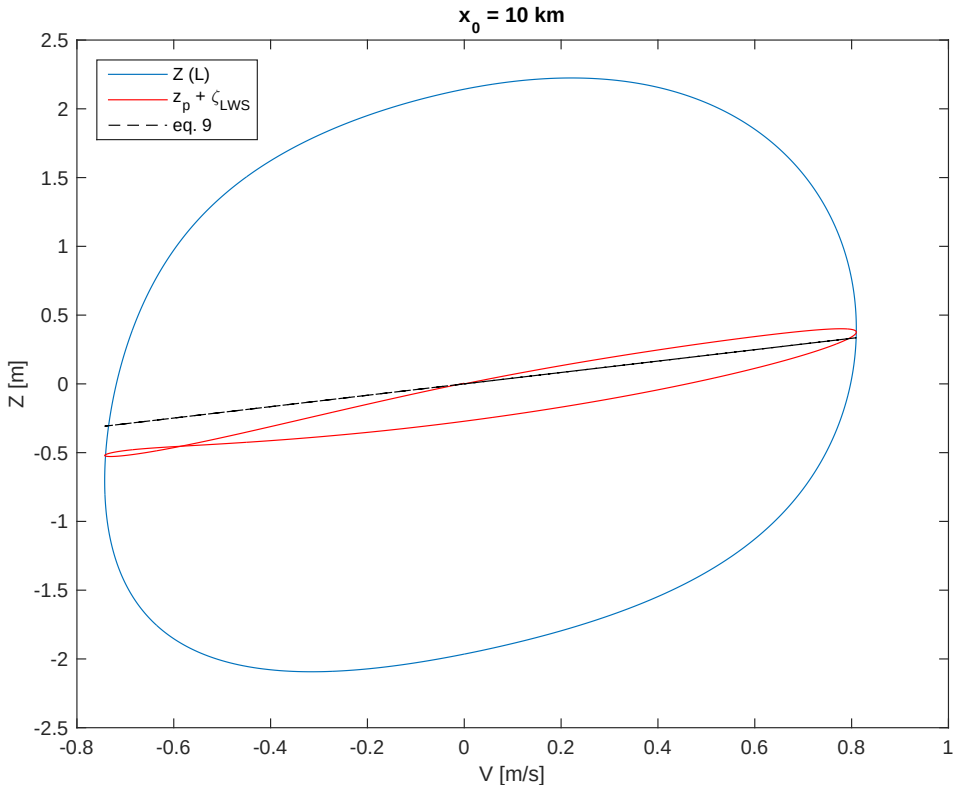

Figure 11: Lagrangean water level against velocity V: Z is the actual value, $z_p + \zeta_{LWS}$ is the transformed water level, for $x_0 = 10$ km. Black dashed lines: equation (9).